Studies of the Spatial Organization of Metabolism in *Shewanella oneidensis* and *Pseudomonas aeruginosa* Biofilms

Thesis by

Tracy K. Teal

In Partial Fulfillment of the Requirements

for the Degree of

Doctor of Philosophy

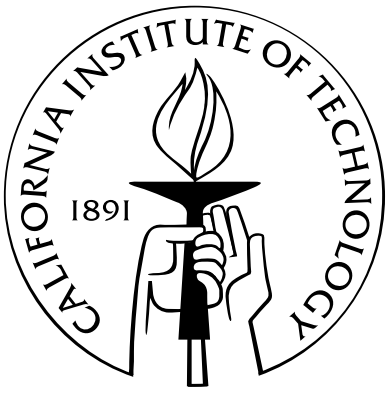

California Institute of Technology

Pasadena, California

2007

(Defended May 24, 2007)

Acknowledgements

I started Caltech as a member of the CNSY2K class and end a graduate student in a geomicrobiology lab. This journey could not have been made without the help and support of many people.

First, I would like to thank my advisors Dr. Dianne K. Newman and Dr. Barbara J. Wold. I have been extremely fortunate to have not one but two extraordinary mentors and role models throughout my graduate career. Their support and passion for science have kept me going through some of the more challenging times. Even in a different field, Barbara has always noted the essential points and suggested key experiments. Her attention to detail, yet broad vision has guided my work and inspired my thinking about all aspects of science. Dianne has an unending enthusiasm for science, and in her lab I have been able to learn more than I ever thought possible about microbiology, chemistry, bacterial physiology and so many other topics. She has always been available to discuss new ideas, offer a different perspective or work through the current experiment. I am so thankful to her for taking me as a student in her lab and offering encouragement and scientific acuity every step of the way.

I would like to thank the other members of my committee who guided me through my work and provided valuable feedback, Dr. Chris Adami, Dr. Erik Winfree and Dr. Mel Simon. In particular, Chris Adami introduced me to bacterial evolution and has been a constant source of support and valuable conversations. I wouldn't be here at Caltech or studying microbiology and computational biology without him.

I'm especially grateful to the scientists, postdocs and students who were there in the trenches everyday. Dr. Alexandre Tsapin at JPL first taught me how to culture bacteria and made me realize how amazing and diverse bacteria can be. Dr. Doug Lies taught me to know and love *Shewanella* and was there to help me through my first molecular biology forays. With his patience, insight and vast knowledge of everything microbiological, I truly enjoyed and learned from every discussion I had with him. Dr. Brian Williams in the Wold lab has always been willing to help whenever anyone needs it. He is a natural teacher and a generous person, and I appreciate all the time he spent helping me to set up and run microarray experiments. I am thankful to Dr. Lars Dietrich for including me in the sox project. Lars' scientific integrity and enthusiasm is an inspiration, and I am fortunate to have been able to work with him. Dr. Andreas Kappler not only organized our lab so that I could find the biofilm tubing, but he was a great source of support and advice in everything from chemistry to career planning.

Dr. Arash Komeili, Dr. Chad Saltikov, Dr. Anthea Lee, Dr. Jeff Gralnick, Dr. Lars Dietrich,

Dr. Nicky Caiazza, Dr. Yun Wang, Dr. Itzel Ramos-Solis and Dr. Soshanna Potter all made the lab a great place to be and showed me the tricks of the trade. Their contributions always made lab meetings interesting and exciting. Thank you to Anthea for getting me started on biofilms and to Chad for your attention to detail. Arash and Jeff held me to high standards, but were always willing to sit down and work through the details of a protocol. I would still be in the middle of thawing tubes and doing transformations if it weren't for them. Thank you to Nicky for the yeast cloning technique and especially for your encouragement and positive spirt. Itzel, it was great to have such a good partner in biofilms at the end. Yun, thank you for the chemistry help and the friendship and support. Thank you to Shanna for all our conversations about science and life.

The graduate students in the Newman lab have been the greatest compatriots I could ever hope for. Dr. Mariu Hernandez, Dr. Tanja Bosak and Dr. Laura Croal led the way and taught us how to be the senior graduate students in the lab and how to graduate with hard-work, brilliance and style. I always appreciated Dr. Yongqin Jiao's friendship, hard-work and ability to keep smiling. Thank you to Alexa Price-Whelan for showing me how to measure NADH anaerobically in the dark and for being able to answer any question I ever asked. And finally, Dr. Davin Malasarn, my partner in Team Miscellaneous, your positive outlook, scientific insight and friendship helped me through every aspect of graduate school both in the lab and in life.

A special thanks also to fellow CNSY2K classmates, Dirk Walther, Patricia Neil and Nathan Gray who were always there to provide coffee and company and let me know that we were all travelers together on this journey.

My greatest gratitude goes to my family, my mom, dad, and grandmother and my sister Jeremi and her husband Brian. They have always been my foundation, and I couldn't have made it through graduate school without their encouragement and unconditional support. You have been everything to me. Mom and Dad, you have taught me to live honesty and to go after my dreams, to pursue adventure and not be afraid to try. My courage can only come because I know that you are always there beside me on the mountain peaks and in the ocean's trenches. Whatever I accomplish, it's because you helped me get there.

Jeremi and Brian, you have been my balance, keeping me aware of the world outside the lab and showing such energy and enthusiasm for all aspects of life. Jeremi, we work in such different fields, but you have always showed such sincere interest in my work and given me confidence.

And last, but certainly not least, I thank my husband C. Titus Brown and his family who have taken me in as part of their family and offered me their support and friendship. Titus has always

been there to talk about programming or experiments or just read a book. He has shared my successes and my failures. He has given me strength I didn't know I had and believed in me even when I didn't. I am thankful every day to have such an amazing person and friend as my partner in life, and I look forward to all our adventures ahead.

And finally, I am very thankful for the little one who was with me at the end.

Abstract

Bacteria grow in the environment as surface-attached microbial communities. These communities are pervasive and resilient in the face of changing and challenging environmental conditions. Because of their community organization and three-dimensional structure, conditions within a biofilm are heterogenous, exposing the bacterial cells to individual microenvironments depending on their location in the biofilm and the biomass of the structure. Communities are therefore thought to be metabolically stratified. To understand how communities are organized with regard to growth activity and metabolic state and what role endogenous compounds might play in this organization, this thesis explores the spatiometabolic organization and dynamics of *Shewanella oneidensis* biofilms and the roles that acyl-homeserine lactones and phenazines might have in *Pseudomonas aeruginosa* communities.

Using unstable fluorescent reporters to measure growth activity and protein synthesis and conducting quantitative image analysis, domains of activity were determined for developing *S. oneidensis* biofilms. Biofilm structures reproducibly stratify with respect to growth activity and metabolism as a function of structure size. Within domains of growth-inactive cells, genes upregulated under anaerobic conditions are expressed demonstrating that cells in the nutrient-limited regions of the biofilm are not dead, but are capable of generating enough energy to persist.

To determine if these growth-inactive cells are able to respond dynamically to changes in environmental conditions and what types of nutrients affect growth activity profiles, *S. oneidensis* biofilms were exposed to increased concentrations of an electron acceptor and an electron donor. Cells in the growth-inactive regions were able to respond to nutrient changes, but were more affected by a change in electron acceptor than electron donor.

To investigate the role of small molecules in biofilm community organization, the degradation of acyl-homoserine lactone (AHL), was studied. This molecule is an important part of the quorum sensing signaling network in *P. aeruginosa* where the bacteria both produce and sense this molecule. When bacteria sense a specific concentration of the AHL, they are induced to form a biofilm or initiate a community wide response. To determine what role AHL degradation has on the community response, a mutant that constitutively degrades the compound was characterized and expression profiles for degradation were compared between this strain and wild type communities. Genes for AHL degradation were expressed in the middle of biofilm colonies suggesting that degradation may be an important part of the community response network. It was also shown that AHLs can be used as a substrate for growth, so nutrient-limited cells might also be able to use AHLs to generate energy.

Finally, to investigate whether endogenously produced redox-active small molecules could potentially play a role in energy maintenance in communities, the SoxR sensing system was studied. This system is typically thought to regulate the response to superoxide radicals. In *P. aeruginosa* and other organisms outside the class of enterics, however, recent evidence suggested that they may instead play a role in the sensing of redox-active small molecules produced under conditions of low nutrients and high cell density. To determine the ubiquity of this response mechanism, bioinformatic analyses were conducted to discover SoxR binding sites across all genomes containing SoxR. Predictions for binding sites and the mechanism of regulation, redox-active molecule induction, were confirmed in the Gram-positive bacterium *Streptomyces coelicolor*.

This work brings us closer to understanding how cells persist and retain the capacity to dynamically regulate their metabolism in biofilm communities. Using reporter assays and quantitative analyses, studies can be done to determine metabolic organization within communities and further investigate the role that endogenous small molecules can play in community organization.

Contents

List of Figures

List of Tables

Chapter 1

Introduction

> "One of the extraordinary things about life is the sort of places it's prepared to put up with living. Anywhere it can get some kind of a grip, whether its the intoxicating seas of Santraginus V, where the fish never seem to care whatever the heck kind of direction they swim in. the fire storms of Frastra, where, they say, life begins at 40,000 degrees, or just burrowing around in the lower intestine of a rat for the sheer unadulterated hell of it, life will always find a way of hanging on somewhere." - Douglas Adams, Mostly Harmless

Bacteria living in the environment face the challenge of living in communities under nutrient-limited conditions. Even areas we think of as being nutrient-rich such as our intestines, become nutrient-limiting when high numbers of bacteria are present, competing for resources. In particular, while it is often thought that bacteria live most of their lives as individual planktonic cells, it has recently been discovered that most bacteria live their lives in surface-attached microbial communities, or biofilms [31]. Biofilm communities have been shown to be prevalent in environments from hydrothermal vents and caves to the lungs of patients with cystic fibrosis [27, 36]. Because these bacteria aggregate together they are creating an environment where they are limiting themselves for nutrients [135]. Why this bacterial lifestyle would be preferred then is not understood. It is known however that bacteria living in biofilms are much more resistant to changes in environmental conditions, antibiotics and anti-microbial agents [123]. There must therefore be something to account for their ubiquity and persistence in the environment.

Because of the inherent nutrient limitation and heterogeneity in biofilm communities, the metabolic state of cells must be different than that of an exponentially growing cell in a nutrient replete environment. It has been suggested that sub-populations of cells within biofilms are actually dead, having sacrificed themselves for the community, invoking a type of hierarchical selection argument.

However, it is likely that while cells may not be able to generate enough energy to grow and divide, they are generating enough energy to maintain their lives. What processes must occur to generate this maintenance energy are not well understood. Small molecules have been reliably shown to be endogenously generated under such conditions of low-nutrients and high cell density [21]. Some of these small molecules have been shown to be involved in activating community wide responses, such as in quorum sensing [4], where bacteria produce and sense a small molecule that triggers bacteria to form biofilms at a given threshold concentration. Other redox-active compounds are known to act as both antibiotics and as molecules that can aid in the transport of nutrients, and the roles of many others remain unexplored. It is becoming apparent that these endogenously produced small molecules play multiple roles in bacterial survival, and may be extremely important factors in the maintenance of biofilm communities.

With these maintenance processes in bacterial communities largely not understood, I set out to explore the spatial organization and dynamics of metabolic states within bacterial biofilms and to further investigate what types of processes and compounds might be important for maintaining populations of cells in these environments. I proposed to address the following questions:

1. What is the spatial and temporal stratification of growth and metabolic states within a biofilm? In particular, can cells decouple metabolism from growth?

2. Does nutrient availability affect growth and metabolic stratification dynamically?

3. How are small molecules used differently within different regions of a biofilm?

4. Might redox-active small molecule production and sensing be a ubiquitous process that could be utilized for metabolism under biofilm conditions?

1.1 Overview

In this thesis I present our progress in answering these questions. **Chapter 2** reviews what we know about biofilm communities and the role of small molecules in bacterial metabolism and population signaling. This begins with a discussion of the pervasiveness and resilience of bacterial biofilms in the environment and the effects of biofilm communities on human health and industrial processes. This is followed by a review on biofilm formation, and it highlights what is known about how biofilm structures form, grow and detach. Next I focus on the heterogeneity within biofilm communities and discuss how diffusion and metabolism within biofilm structures has an effect on the microen-

vironments of cells within the bioflim. I review studies that have been conducted to explore the spatial organization of these communities with regards to their growth activity and some specific processes. I then discuss the role of endogenous small molecules, produced under conditions of low nutrients and high cell density, highlighting their role in biofilm formation and community response, as in quorum sensing, and the potential role of redox-active compounds in metabolic maintenance. Finally, I introduce two model organisms, *Shewanella oneidensis* and *Pseudomonas aeruginosa* and describe their merits as model organisms for the study of metabolic organization in biofilms and community response to endogenous small molecules. The chapter concludes with a brief summary focusing on what will be presented in this dissertation.

Chapter 3 presents our findings on the metabolic stratification of *Shewanella oneidensis* biofilms. We employed unstable fluorescent reporters to measure growth activity and protein synthesis *in vivo* over the course of *S. oneidensis* biofilm development and created a quantitative routine to compare domains of activity in independently grown biofilms. In these experiments we observed that biofilm structures reproducibly stratify with respect to growth activity and metabolism as a function of size. In order to determine if cells in the middle of a biofilm were dead as is often thought to be the case, we compared regions of growth activity with those of active protein synthesis under anaerobic conditions. Within domains of growth-inactive cells, genes typically upregulated under anaerobic conditions are expressed well after growth has ceased, indicating that cells in all regions of the biofilm are persisting and are able to turn on metabolic programs appropriate to their local microenvironment and developmental stage. This chapter was published in Applied and Environmental Microbiology 72(11): 7324-30.

In **Chapter 4** we characterize how nutrient availability affects *S. oneidensis* biofilm metabolic organization and whether previously growth inactive cells are able to respond dynamically to changing nutrient conditions. We measured oxygen levels, cell number and NADH/NAD+ ratios to correlate oxygen availability with metabolic state. We then determined whether the addition of an electron acceptor can affect the growth activity of stationary phase, oxygen-limited planktonic cells. Finally, we quantitatively characterized the growth activity profiles of *S. oneidensis* biofilms in response to an electron acceptor, fumarate, and an electron donor, lactate. We also determined the effect of fumarate on a *S. oneidensis* fumarate reductase mutant biofilm.

In **Chapter 5** we describe a variant of *Pseudomonas aeruginosa* $\text{PAO1}_{lagless}$, that constitutively degrades long chain acyl-homoserine lactones (AHL), the molecules used in quorum sensing. We compare long-chain AHL accumulation and growth on long chain AHLs in wild-type *P. aeruginosa*

and the variant PAO1$_{lagless}$. Using microarray analysis, we determine the genes differentially expressed in each strain. Finally, we examine the expression of PA1032, a gene required for AHL degradation, in wild-type *P. aeruginosa* and PAO1$_{lagless}$ under planktonic and biofilm conditions and determine the profiles of expression in biofilm conditions. This work was done in collaboration with Dr. Jean Huang and Dr. Jared Leadbetter.

In **Chapter 6**, we investigate whether SoxR may be regulated by redox-active small molecules endogenously produced under conditions of low-nutrients and high cell density, rather than by superoxides as the paradigm from *E. coli* would suggest. Using known binding sites for SoxR, we construct a position weight matrix (PWM) and use this PWM to find binding sites across all bacterial genomes. We then determine the specific genes that are being regulated by SoxR and categorize them according to function. To test our bioinformatics hypotheses, we determine the response of predicted SoxR regulated genes in *Streptomyces coelicolor* to actinorhodin, an endogenously produced redox-active compound. This work was done in collaboration with Dr. Lars E. P. Dietrich.

Chapter 7 contains a summary of the main findings of the work in this thesis, concluding remarks and potential directions for future work.

Two appendices are included. Appendix A describes the methods for growing *S. oneidensis* biofilms in more detail . Appendix B includes complete tables from Chapter 7.

Chapter 2

Background

2.1 Bacterial communities in the environment

Over the last decade our vision of microorganisms as cells swimming alone in the environment has shifted to the realization that most bacteria spend their lives as surface-attached microbial communities, or biofilms. These microbial biofilms are ubiquitous, resilient, responsive to their environment and able to communicate through chemical signalling [123]. Biofilms are generally described three-dimensional structures, often with pillar-like formations, consisting of bacterial cells and an extra-cellular matrix which holds the microcolonies together. Through the structure runs a network of open-water channels which can transport nutrients and waste products [99]. These complex differentiated communities are remarkably persistent in the face of changing environmental conditions and exposure to toxins [123]. Bacterial biofilms can be found in almost every environment. They have been characterized in regions as extreme as acidic hot springs, acid mine drainage and Antarctica to environments as mundane as shower curtains and the surfaces of our teeth [66, 71, 105, 142]. The presence of fossilized stromatolites suggests that the biofilm lifestyle is also an ancient one, having existed for thousands of years [47].

Biofilms are of particular importance in industrial systems and human health. Biofilms can contribute significantly to industrial processes such as waste water treatment, paper milling and potentially to biofuel production, or they can be destructive, clogging pipes and rusting surfaces [92]. In human health, biofilms of *Pseudomonas aeruginosa* form in the lungs of patients with cystic fibrosis [27, 87, 141]. (For a review of cystic fibrosis pathology see Boucher 2007 [14].) Plaque, leading to gingivitis, is a biofilm comprised of hundreds of species of bacteria [71]. Biofilms form on catheters and medical implants, on contact lenses and in wound infections [28]. Bacteria in these communities are up to one hundred times more resistant to antibiotics and other anti-microbial

agents than infections of planktonic cells.

It had been thought that the extracellular matrix that the cells produce was forming a diffusion barrier to toxins such as antibiotics and anti-microbial agents, but numerous studies have shown that this diffusion limitation alone cannot account for the remarkable resilience of these communities. An alternative factor that may account for the persistence of biofilms is that of the heterogeneity of the population and the potential for a subpopulation of cells in a less active metabolic state [13, 76, 123]. Nutrient diffusion, metabolism and microscale interactions create microenvironments within the community. Biofilm communities are therefore heterogeneous and spatially stratified, so that activity levels and biochemical processes occur differentially according to the location of a cell in the biofilm and overall mass of the biofilm structure [134]. Yet this metabolic heterogeneity is not well understood. In particular the spatial organization of growth and metabolic states and the dynamics of these states has not been well-characterized. In addition little is understood about the maintenance requirements or processes essential for growth of cells in these nutrient-limited communities. In order to understand the role of bacteria in the environment, i.e. how they affect nutrient cycling, trophic organization and other environmental processes, or to affect a biofilm community, for the purpose of using them in industrial processes or treating people with biofilm infections, it is important to understand the metabolic and maintenance processes being utilized and the organization of these processes within a community.

2.2 Biofilm formation

Biofilms formation proceeds much like a developmental process. As seen in Figure 2.1, bacteria attach to a surface and as more cells attach, they begin to form an extracellular matrix comprised of polysaccarides, extracellular DNA and other components [145]. In biofilms exhibiting the standard mushroom morphology seen in lab conditions and shown in Figure 2.1, the stalk of the mushroom is formed by cells on the surface continuing to grow and divide. The cap of the mushroom however forms as planktonic cells in the medium attach to the already growing structure, essentially pasting themselves to the outside of the colony and its extracellular polymeric substance (EPS) consisting of polysaccharides, extracellular DNA and other components [68]. Within the biofilm's structure, channels are formed around the macrocolonies that allow for nutrient and waste transport, creating a complex structure. When the colonies reach a certain size, cells in the middle of the structure begin to leave until finally the structure collapses.

Molecular genetic assays and proteomic studies have shown that particular sets of genes and

proteins are involved in specific steps along this pathway. For reviews see O'Toole 2003 [92], Ghigo 2003 [43], Stanley and Lazazzera 2004 [120] and Prüßet al [100]. While there are different pathways for making a biofilm, biofilm formation seems to be regulated at five main steps: surface attachment, microcolony formation, microcolony growth, depth of the mature biofilm and detachment. In attachment, both stable cell-surface interactions and specific environmental conditions are important. In many Gram-negative bacteria, flagella or pili are required for sensing contact with a surface and initiating surface adhesion [92]. In some non-motile Gram-positive strains however, only protein and polysaccharide adhesins have been shown to be required [48].

Microcolony formation and growth occurs when a community of bacterial cells a few layers deep develops on a surface and EPS is produced. In this process there is a transition from reversible to irreversible attachment. Initial characterization of this process in *P. aeruginosa* revealed that SadB, a protein of unknown function, mediates this transition [20].

In the maturation of biofilm structures, thick layers of cells are encased in EPS matrix. The structures can be homogenous mats of cells or complex structures composed of pillars and water channels. Much of the molecular characterization of biofilms has been done in *P. aeruginosa* where mutants have been identified that affect the depth or structure of biofilms within a given species. Similarly, different environmental conditions can have an effect on biofilm structure morphology. Catabolite repression and the transcription factor RpoS affect biofilm depth. Both mechanisms are used to report nutrient levels and therefore indicates that biofilm maturation is potentially regulated in response to nutrient levels in the environment [120]. Another mechanism important in biofilm maturation is a chemical cell-cell communication mechanism called quorum sensing, discussed in more detail below. During the maturation phase of biofilm develop, cells must be maintained in the structures. Rhamnolipid surfactant production is one component required for the maintenance of the pillar structures [30].

Because of the interest in eliminating biofilms in medical environments, attention has been paid to the process of cell detachment from a biofilm. It has been shown that this process is inducible by sudden carbon or oxygen limitation and that certain genetic pathways and cyclic dinucleotides are involved in this process [64, 132, 130].

These are some of the mechanisms in biofilm development that have been studied in more detail, but many proteomic and genomic studies have examined gene and protein expression at all stages of biofilm formation [111, 114, 113, 117, 146]. Progress continues in studying the role of some of these genes in biofilm development and maintenance.

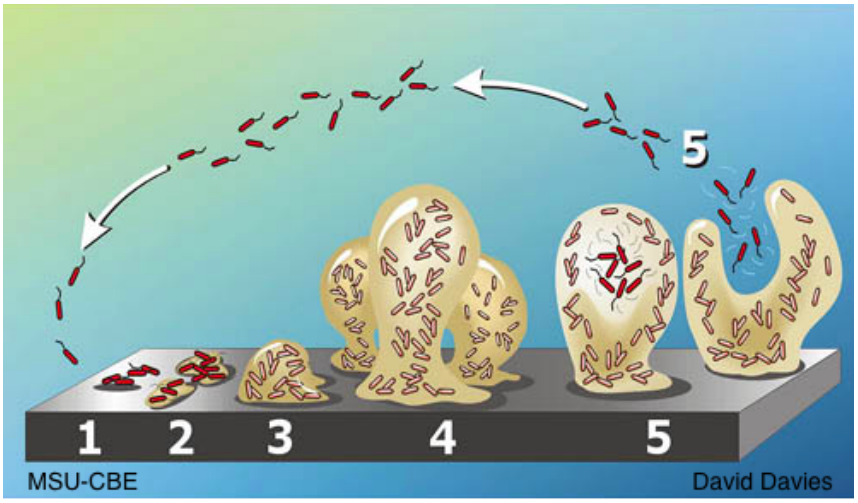

Figure 2.1: Stages of biofilm development.

2.3 Spatial organization of biofilm communities

While biofilm attachment, maturation and detachment have been well-studied, the metabolic states and organization of these states has been less well-characterized. In the complex structures that result from biofilm formation, each region has its own microenvironment due to diffusion and metabolism. Profiles of oxygen in aerobically grown biofilms show that oxygen is depleted approximately 30 μm into a *P. aeruginosa* biofilm structure [107]. Similiarly, in *S. oneidensis* lactate does not diffuse through the entire biofilm structure [82].

In laboratory based single species biofilms, several studies have investigated spatial patterns of cellular growth activity and metabolism using a variety of techniques. For a review see Tolker-Nielsen and Molin 2000 [135].

Growth activity has been monitored in *Klebsiella pneumoniae*, using an acridine orange dye [143], and by tracking alkaline phosphatase activity under phosphate starvation conditions [61]. In both of these studies, growth activity was limited to the outer edges of the biofilm, in the regions at the nutrient-biofilm interface. Numerous studies using Syto9 and propidium iodide in the Live/Dead stain as well as other methods have concluded that these cells in the middle of the biofilm are dead, or not actively synthesizing proteins [60, 80, 138], but the accuracy of the Live/Dead stain as a reporter of cell viability has been questioned [10]. A more direct measure is to make use of the link between growth rate and ribosomal synthesis. Direct *in situ* measurements of rRNA were used initially to determine ribosomal content [98]. Sternberg et al developed a fluorescent reporter assay to track ribosome synthesis. Fusing an unstable green fluorescent protein (*gfp*(AAV) to the

rrnB P1 promoter, which has been shown to correlate with ribosome synthesis and growth, growth acitivity could be tracked by monitoring green fluorescence levels [121]. Werner et al used this reporter in conjunction with an IPTG inducible green fluorescent protein (GFP) to track growth activity by ribosomal content as well as protein synthesis [144]. Additionally Werner et al tracked cells capable of elongation in a biofilm, treating colonies with carbenicillin to block cell division and then measuring individual cell length by transmission electron microscopy. Rani et al track growth activity and protein synthesis in Staphylococcal biofilms [106]. These studies demonstrate that cells display different amounts of growth activity correlated with the cell's location in the biofilm and the biofilm biomass. Growth activity was localized to the biofilm/bulk interface in both cases. It has been suggested that these profiles are determined by oxygen availability [148].

The use of these fluorescent reporters has greatly aided in the study of localization within biofilms. They have been used to track rhamnolipid synthesis [75] in *P. aeruginosa*, the virulence factor glucosyltansferases in *Streptococcus mutans* [150], multidrug efflux pumps [67] and other genes of interest [118]. These fluorescent protein reporters allow for real-time *in vivo* analysis of gene expression in a developing community and have the potential to elucidate the dynamics and distribution of gene expression within a developing biofilm. GFP requires oxygen to fold and fluoresce, but the lower limits required for folding, 0.1ppm dissolved oxygen, are likely to be present in biofilm conditions [49] and signals from GFP labelled cells have been shown to correlate with SYTO 60 nucleic acid staining [89].

These studies demonstrate that heterogeneity with regard to cellular activity and metabolism exists, and in particular, that biofilm communities show decreased growth activity near the center of the biofilm, where it is expected that cells are nutrient limited. Yet the specific localization of metabolic processes that occur in biofilms and how they might change over the course of biofilm development has remained largely unexplored. Questions remain as to whether growth inactive cells can decouple growth from metabolism so that they are still capable of generating energy for maintenance and responding to changes in environmental conditions.

2.4 The role of small molecules in biofilm development and maintenance

One mechanism that may be important in bacterial maintenance under these conditions is the generation of endogenous small molecules. Small molecule production has been show to occur under

conditions of nutrient-limitation and high cell-density, and these molecules are readily diffusible in biofilms [122]. Bacteria can use small molecules to control gene expression, as antibiotics, and as shuttles or redox active compounds to promote energy generation or iron acquisition. Because energy generation in low-nutrient regions of microbial communities is relatively unknown, the function of these small molecules is potentially of great importance for the ability of bacteria to sustain their metabolism [21].

2.4.1 Quorum sensing

One area of small molecule signaling that has received much recent attention, however, is that of quorum sensing. In many Gram-negative bacteria including *P. aeruginosa* and *Vibrio fisheri*, bacteria produce acyl-homoserine lactones that are sensed by other bacteria in a process known as quorum sensing [40]. In these species of bacteria, two sensing systems are in place, one that can recognize the AHLs of their own species and one that recognizes the signaling molecules of other organisms. The response of the bacteria is a threshold response, so that when the bacteria senses a specific concentration of its own species' AHL, it activates a genetic program in response [40]. In the case of *Vibrio fisheri*, this response is to generate light. In many other species however, this response is what activates biofilm formation and mutants in the genes that produce or sense the compound are unable to form biofilms. Through this system, bacteria are able to communicate information about the cell density in their environment. Recent evidence has also suggested that nutrient levels in the environment are another part of this sensing process, so that the bacteria are able to tune their threshold response based on the current nutritional environment [149].

While the generation and sensing of these compounds has received much study, the degradation of these compounds is not well understood. The degradation of AHL compounds may be as important a part of the signaling system as that of their production. AHLs in a biofilm may need to be degraded to activate programs responsible for dispersal from biofilms in the late stages of biofilm development. Another capability of AHLs may be important in community maintenance as well. Certain forms of AHLs may be able to be used as a carbon source, suggesting a role for AHLs in energy generation as well as in that of signaling. Understanding the lifecycle and potential uses of these compounds can help us understand all aspects of their roles in biofilm communities.

2.4.2 Redox active compounds

While quorum sensing has received much of the recent focus, small molecules may be essential in many other processes involved in community response and metabolic maintenance. Redox-active compounds are usually implicated primarily for their role in virulence. However, recent evidence is suggesting that these compounds may play other roles in redox homeostasis, iron-chelation and metabolic maintenance as well as acting as signals to regulate community wide responses. It has been shown that the phenazine pyocyanin, a redox-active compound produced by *P. aeruginosa* is used as an additional signaling factor in quorum sensing [34]. This same compound can be used to promote mineral reduction [53] or may be used to regulate redox state through NADH pools (Price-Whelan et al 2007, in press). The *P. aeruginosa* quinolone signal involved in quorum sensing also has an iron-chelating effect [16]. Because these small molecules are produced under conditions of low-nutrients and high cell-density, it is possible that they are playing an important role in biofilm physiology.

It is not clear how pervasive the production, degradation and response mechanisms of these molecules is however. In order to establish their role in metabolism and biofilm physiology, we must first determine how widespread these compounds are and the types of effects these compounds have on bacteria.

2.4.3 *Shewanella oneidensis* as a model organism for the study of metabolic organization in biofilms

Shewanella oneidensis MR-1 is a facultatively anaerobic Gram-negative bacterium with remarkable respiratory versatility found mainly in sediment environments [139]. Under anaerobic conditions, *S. oneidensis* can use many oxidized metals such as Mn(III), Mn(IV), Fe(III), Cr(VI), and U(VI) as well as thiosulfate, fumarate, sulfite, elemental sulfur, and nitrate as terminal electron acceptors. *S. oneidensis* can use lactate, succinate, pyruvate, and D-galactose as carbon sources [116, 133]. The bacterium is rod-shaped and non-spore forming. Individual cells are 2-3 μm long and 0.5 - 0.6 μm in diameter. The cells are motile with a single unsheathed polar flagella. Colonies are pinkish in color and circular with 1-4 mm diameters. *Shewanella oneidensis* can form biofilms under batch and flow conditions on a variety of surfacea [131, 139]. The genome of *S. oneidensis* has been sequenced and annotated, and it is relatively easy to manipulate genetically. [52]

As well as being able to utilize a variety of substrates for growth, *Shewanella oneidensis* can reduce electron acceptors, such as Fe(III) at a distance, raising the possibility that cells not directly

associated with an electron acceptor may still be able to generate energy from its reduction [77].

Because of its versatile respiratory capabilities, *S. oneidensis* is of interest in bioremediation processes [133] and in energy generation using fuel cells [11, 24, 108], and as such its response to various environmental conditions has been studied extensively. Genome-wide examinations of *S. oneidensis*'s response to acidic and alkaline pH [74], elevated salt conditions [79], ionizing radiation [101], UV radiation [102] and strong magnetic fields [41], as well as studies of growth on Cr(VI), Vanadium(V), and U(VI) have been conducted [7, 22]. Microarray and proteomic analyses have characterized the regulons under anaerobic and aerobic conditions, such that genes regulated under specific oxygen conditions have been determined [6, 5, 44].

Additionally, the central metabolic pathways of *S. oneidensis* under a variety of oxygen conditions have also been examined in the Keasling laboratory. Tracking cellular metabolites and the products of carbon metabolism, they were able to construct a metabolic pathway model to quantify the central metabolic flux distributions [127, 125, 126]. In these studies they also find that cells can continue to grow well at low dissolved oxygen levels [127].

Because of *S. oneidensis*'s versatile respiration, ability to form biofilms, well-characterized metabolism and response to different environmental conditions, as well as its potential to use redox-active compounds to promote energy generation, it is an ideal experimental system in which to explore domains of metabolism within a biofilm.

2.4.4 *Pseudomonas aeruginosa* as a model organism for the study of community response to endogenous small molecules

Pseudomonas aeruginosa is a Gram-negative bacterium measuring approximately 0.5 μm by 2.0 μm. It is an aerobic bacterium found commonly in water and soils, but is renowned as a opportunistic pathogen, causing infections in wounds, burns and those who are immunocompromised. *P. aeruginosa* infects the lungs of patients with cystic fibrosis, forming biofilm-like microcolonies encased in the thick mucous layer associated with the pathology of this disease. These infections caused by *P. aeruginosa* biofilms are extremely resistant to antibiotics.

Quorum sensing has been well-established for *P. aeruginosa* and is controlled in part by the the lasI/R, rhlI/R, which synthesize and detect specific AHLs [65] and also by the psq system [83]. Also, because of the interest in *P. aeruginosa* biofilms in infection, the development and genetic pathways involved in biofilm production are the most well-characterized of any microbe.

P. aeruginosa produces several redox active small molecules that are used as antibiotics, signals

in co-ordinating community responses and potentially facilitating extracellular electron transfer [34, 53]. One class of these compounds, phenazines, are heterocyclic redox-active compounds that are produced endogenously [73]. They are excreted from cells in stationary phase and have antibiotic effects on other microbes and eukaryotes. While the effects of phenazines as antibiotics has received much attention, the primary function of phenazines in the producing organism is still unknown.

Because *P. aeruginosa* has been well-established as a model organism in biofilm development and quorum sensing and endogenously produces AHLs and phenazine compounds under low-nutrient and high-cell density conditions, it is an ideal organism with which to study the effects of small molecules on cell physiology and to elucidate what their role might be in metabolism and signaling in biofilm communities.

2.5 Summary

Bacterial biofilms are prevalent in the environment, but their resilience is not well understood. Due to diffusion, metabolism and microscale interactions, biofilm communities are spatially stratified such that cells in different regions of the biofilm experience different microenvironments. Within these microenvironments, activity levels and biochemical processes occur differentially according to the location of a cell in the biofilm and the biofilm structure's biomass. The heterogeneous nature of these communities is likely a key factor in the community's ability to survive in the face of challenging environmental conditions, yet the metabolic organization and dynamics within a biofilm community are not well-understood. In this dissertation, a study of the metabolic organization of biofilms and an exploration of possible roles for small molecules in maintaining energy generation within the community is presented.

Chapter 3

Spatiometabolic stratification of *Shewanella oneidensis* biofilms

This chapter includes sections from Teal, T.K., D. Lies, B. J. Wold, D. K. Newman. 2006. Spatiometabolic stratification of *Shewanella oneidensis* biofilms. Applied and Environmental Microbiology 72(11): 7324-30.

3.1 Abstract

Biofilms, or surface-attached microbial communities, are both ubiquitous and resilient in the environment. Although much is known about how biofilms form, develop, and detach, very little is understood about how these events are related to metabolism and its dynamics. It is commonly thought that large subpopulations of cells within biofilms are not actively producing proteins or generating energy and are therefore dead. An alternative hypothesis is that within the growth-inactive domains of biofilms, significant populations of living cells persist and retain the capacity to dynamically regulate their metabolism. To test this, we employed unstable fluorescent reporters to measure growth activity and protein synthesis in vivo over the course of biofilm development and created a quantitative routine to compare domains of activity in independently grown biofilms. Here we report that *Shewanella oneidensis* biofilm structures reproducibly stratify with respect to growth activity and metabolism as a function of size. Within domains of growth-inactive cells, genes typically upregulated under anaerobic conditions are expressed well after growth has ceased. These findings reveal that, far from being dead, the majority of cells in mature *S. oneidensis* biofilms have actively turned-on metabolic programs appropriate to their local microenvironment and developmental stage.

3.2 Introduction

Many bacteria in the environment are thought to grow as surface-attached microbial communities, or biofilms, and it has been suggested that this biofilm lifestyle may account for the remarkable persistence of bacterial populations in the face of changing environmental conditions [31]. Biofilms are composed of many hundreds of cells, each of which experiences it own microenvironment due to strong chemical gradients that are established by metabolism and diffusion. Biofilm communities are therefore heterogeneous and spatially stratified, so that activity levels and biochemical processes occur differentially according to the location of a cell in the biofilm and the biofilm structures biomass [135]. Previous studies have investigated the spatial organization of microbial biofilm communities. In mixed species biofilms, using measurements of metabolites, fluorescent in situ hybridization, and community analysis by PCR, it has been shown that species stratification occurs [26, 50, 85, 91]. In laboratory based single species biofilms, several studies have investigated spatial patterns of cellular growth activity and metabolism using a variety of techniques [32, 62, 61, 75, 82, 90, 98, 121, 143, 144, 148, 150]. These studies demonstrate that heterogeneity with regard to cellular activity and metabolism exists, and in particular, that biofilm communities show decreased growth activity near the center of the biofilm, where it is expected that cells are nutrient limited. To our knowledge, however, no systematic studies have been done to characterize the specific metabolic processes that occur in biofilms and how they might change over the course of biofilm development. As a first step towards this end, we set out to create a system where we could quantitatively and reproducibly measure spatiometabolic patterning in biofilms. In particular we wanted to address the question of whether biofilm cells could decouple growth from metabolism. Numerous studies using the LIVE/DEAD stain and other methods have concluded that cells in the middle of the biofilm are dead, or not actively synthesizing proteins [60, 80, 138], but it is not clear how accurately these reporters reflect cell viability in a biofilm. To explore the spatiometabolic stratification of developing and mature biofilms, we selected *Shewanella oneidensis* strain MR-1, a biofilm-forming, facultative anaerobe with remarkable metabolic versatility. *S. oneidensis* can use oxygen and many other lower potential substrates, including metals, as electron acceptors in respiration, making it an attractive experimental system in which to explore domains of metabolism within a biofilm [52, 131, 132, 139].

3.3 Materials and Methods

3.3.0.1 Bacterial strains, plasmids and media.

Shewanella oneidensis strain MR-1 was grown planktonically using LML medium [pH 7.4, containing 0.2 g/L yeast extract, 0.1 g/L peptone, 2.5 g/L Na HEPES and 0.243 mL/L 60% lactate syrup (5 mM lactate)]. Planktonic cells were grown shaking at 250 rpm at 30°C. When required, antibiotics were added at final concentrations of 15μg/mL tetracycline or 50μg/mL kanamycin.

S. oneidensis MR-1 constitutively expressing the GFPmut3* (green) or ECFP (cyan) fluorescent protein were generated using mini-Tn7-KSGFP or mini-Tn7-KSCFP to insert the gfpmut3* or ecfp gene at the unique attTn7 site in the MR-1 genome, creating strains DKN308 and DKN309 respectively. (The mini-Tn7 system in Supplemental Methods [2, 25, 29, 46, 70, 88, 140]) To allow detection of growth activity in *S. oneidensis* the reporter system described by Sternberg et al. was used [121]. The NotI fragment of pSM1606 [121] containing the growth-rate regulated E. coli *rrnB* P1 promoter [3] fused to the *gfp*(AAV) gene encoding an unstable green fluorescent protein (GFP) was cloned into the highly stable broad host range plasmid pME6031 [51] to create the plasmid pTK4. GFP(AAV) is unstable because it has a specific C-terminal oligopeptide extension that makes it susceptible to relatively fast degradation by intracellular tail-specific proteases thereby enabling real-time expression imaging [1]. pTK4 was transferred by conjugation into the ECFP-expressing strain *S. oneidensis* DKN309, to yield strain DKN310. The *mtrB* reporter strain, DKN311, was made via homologous recombination. Primers were designed to amplify flanking 1kb regions up and downstream of the end of the *mtrB* gene from *S. oneidensis* MR-1 (upstream region primers 5 CGGGATCCGCGGCCGCATAATACCCAAGTAGAAGAA and 3 ATCAATCAACTAGTTCTAGAGCGATTAGAGTTTGTAACTCATGCT; downstream region primers 5 GCAGCAGTTTAATGCTAGCGAACATTTGCCTCATATGCTCAAAAG and 3 ATAAGAATGCGGCCGCTGTTGAATTGAATCCCCTGTT) and insert *eyfp*(AAV) between them. *eyfp*(AAV) encodes an unstable yellow fluorescent protein and was constructed by amplifying *eyfp* from pMP4658 [12] using primers that included the AAV tail [1] to fuse the AAV to *eyfp*. Using NotI restriction sites, the upstream region, the sequence for *eyfp*(AAV) and the downstream region were inserted into the kanamycin-resistance suicide plasmid pSMV10, such that *eyfp*(AAV) was in between the upstream and downstream regions of the end of the *mtrB* gene. This plasmid was cloned into E. coli WM3064 [110] and mated with *S. oneidensis* MR-1, selecting for strains with kanamycin resistance. Such transconjugants were plated on LB/5% sucrose plates to select for secondary recombinants lacking the integrated plasmid, which encodes sucrose sensitivity. Colonies

from these plates were tested via PCR for the presence of the *eyfp*(AAV) gene. P_{lac}-ecfp from miniTn7(Gm)PA1/04/03 ecfp-a [72] was inserted into pME6031 using KpnI and MluI to create constitutively-expressing ecfp on plasmid, pTK5. This plasmid was introduced into the MR-1 *mtrB-yfp*(AAV) strain DKN311 by conjugation to create strain DKN312 that constitutively expresses ECFP and expresses EYFP(AAV) from the end of the *mtr* operon.

3.3.0.2 Plasmid stability determination.

To assay the stability of pTK4 and pTK5 in *S. oneidensis* MR-1 biofilms, *S. oneidensis* with pTK4 was grown for 5 days in 96 well polyvinyl chloride plates at 30°C in LML medium. As biofilm cells were attached to the walls of the well, the medium was exchanged every day to eliminate planktonic cells. After 5 days, the biofilm cells that were still attached to the well walls were removed and resuspended. Dilutions were plated on LB plates and incubated at 30°C overnight. 309 colonies from the plates were picked and each colony was streaked on LB and LB + tetracycline plates that were incubated at 30°C overnight. 308 of the 309 colonies grew on both plates, indicating that 99.7% of MR-1 cells were tetracycline resistant and therefore contained pTK4.

3.3.0.3 GFP expression and stability measurements.

Cells were grown overnight in LML medium and allowed to reach stationary phase. Cells were then diluted into fresh medium to an OD_{600} of 0.0143 and grown aerobically for 20 hours with samples taken for growth and fluorescence measurements using a Bio-Tek Synergy HT. For measuring growth, optical density at an absorbance of 600nm was used. For green fluorescence, measurements were taken using a 485/20 excitation filter and a 528/20 emission filter.

3.3.0.4 Determination of respiration rates.

S. oneidensis overnight cultures were diluted into fresh LML medium and allowed to reach stationary phase. Cells were then transferred to a stoppered bottle where no oxygen could be introduced. Oxygen concentrations were measured over time using an oxygen microelectrode until concentrations reached zero. The slope of this data was calculated, and this was determined to be the oxygen consumption rate for the number of cells in the flask. Colony forming unit counts were done for each flask, and the slope value was divided by the number of cells in the flask to determine the oxygen consumption rate per cell.

3.3.0.5 Biofilm experiments.

A flow cell system was constructed such that biofilms could be grown under constant conditions and imaged over time. Flow cells have 4 channels machined from polyurethane with coverslips attached via epoxy. Each channel is 40.6 mm long, 11.4 mm wide and 0.203 mm deep. A 0.5 mM lactate LML medium [pH 7.4, 0.2 g/L yeast extract, 0.1 g/L peptone, 2.5 g/L Na HEPES and 0.043 mL 60% lactate syrup] is run through the flow cell system. The flow cell is inoculated with 300 μL of a culture in exponential phase, at an OD_{600} of approximately 0.075, using a sterile syringe. Flow is not started immediately in order to allow cells to attach to the surface. After 1 hour the flow is started at a rate of 4.1μ/sec, 1.5 rpm on a Watson-Marlow peristaltic pump. The flow continues at this rate for the length of the experiment. Using this technique, biofilms were grown for up to 7 days. Confocal fluorescence microscopy was used to image bacterial biofilms grown in the flow cells. A Zeiss LSM 510 inverted microscope with a 63x Achroplan water immersion lens at the Caltech Beckman Institute Biological Imaging Center was used. Z-series images were acquired for multiple fields of view at multiple time points during the experiment. For imaging egfp or eyfp, the excitation was 488nm and the emission filter used was a BP500-550. For imaging ecfp the excitation was 420nm and the emission filter used was a BP465-485. Images were processed using the Imaris software.

3.3.0.6 LIVE/DEAD stain.

S. oneidensis biofilms were grown in flow cells. At an end time point, flow was stopped and 1.5 μL of Propidium Iodide and 1.5 μL of Syto 9 from the Molecular Probes BacLight LIVE/DEAD stain kit L7012, in 1 mL 0.5mm lactate LML, was injected into the tubing upstream of the biofilm. Flow was started briefly to deliver the stain to the biofilm. Flow was then stopped for 1 minute to allow staining to occur, and was resumed to wash away residual stain. Imaging was done using 488 nm excitation and the emission filter BP500-550 for the green fluorescence. Excitation was 543 nm and the emission filter was LP605 to image the red fluorescence.

3.3.0.7 *mtrB* expression with varying oxygen levels.

LB medium containing 20 mM lactate was prepared. 10 mL of media was added to 250 mL anaerobic Balch tubes. The tubes were stoppered and flushed with the appropriate oxygen concentration. 0%, 2% and 10% oxygen tanks consisted of the appropriate concentration of oxygen and the remainder nitrogen. Tubes containing 21% oxygen were flushed with filtered air. 20 mM fumarate was added to 0% oxygen cultures. Cells were grown overnight in aerobic cultures. Cells were then diluted 1:1000

into each tube to an OD_{600} of 0.075 at each oxygen concentration in duplicate. Cells were allowed to grow for 2 hours or less to an OD_{600} of 0.150. Cells were then collected and treated with Qiagen RNA protect, and the RNA was immediately extracted using the Qiagen RNAqueous Micro kit. The RNA was DNase treated using the Qiagen DNase I treatment and DNase inactivation protocol. To synthesize cDNA, reverse transcriptase PCR (RT-PCR) was done using the Applied Biosystems TaqMan kit in a 50 μL reaction. To quantitate the cDNA, Quantitative RT-PCR was performed. Twenty-one base pair primers flanking a 100 base pair region for genes *mtrB, gfp, envZ and recA* were diluted to 5 pmol/μL. For each reaction, 1 μL cDNA from the RT-PCR reaction, 6.5 μL DEPC water, 10 μL 2x SybrGreen mix and 2.5 μL of a primer pair mix were added to one well of a 96 well QPCR plate. A no cDNA control was also run for each primer set. Q-RT-PCR analysis was done using an Applied Biosystems Gene Amp 7500 Sequence Detector machine. A fluorescence level of 0.5 on a log scale was selected as the threshold for comparison of cycle numbers. The genes *envZ* and *recA* were used for normalization.

3.3.0.8 Quantitative analysis of biofilm images.

Biofilms were imaged at multiple time points in multiple fields of view. For each image, the fluorescence intensity profile for the reporter was mapped through the center x-axis of the structure using NIH ImageJ. These fluorescence values were exported as a text file of x-coordinates and fluorescence intensity for each pixel. We wrote an analysis program to analyze and process this data. The brightest pixel was defined as 100% fluorescence and all fluorescence values were determined relative to that value. To automatically determine the edges of a structure, an edge detection algorithm was used where the region of greatest contrast between the empty space surrounding the biofilm structure and the fluorescence of the structure was defined to be the edge. Using the defined edges, the center could then be specified. Then, the intensity of each nine-pixel bin was determined in relationship to its distance from the center of the structure, and a plot of fluorescence intensity versus distance from the center of the structure was constructed automatically for each image. This analysis generated a profile of fluorescence for each image. Twelve biofilms from the growth reporter strain, DKN310 and eight from the anaerobic reporter strain, DKN312, representing images from all stages in biofilm development were analyzed in this way, determining the size of the structure and its fluorescence profile. Biofilms were binned into representative sizes, and the average fluorescence profile across all the structures of that size, with a minimum of six in each category, was calculated

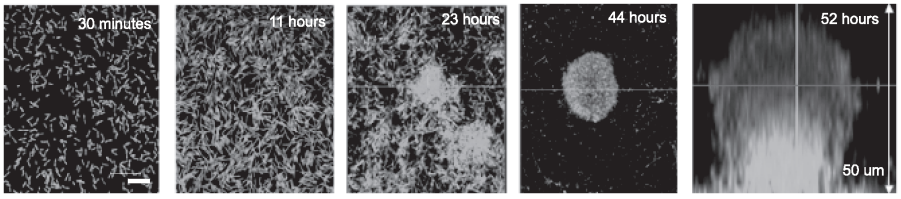

Figure 3.1: Time course of *S. oneidensis* biofilm development. Cells are expressing a constitutive GFP. The first four panels are x-y slices at the base of the developing biofilm structure. The final panel is a z-profile through the structure. Scale bar is 10 μm.

3.4 Results

3.4.0.9 Development of *S. oneidensis* biofilms

S. oneidensis was labeled with a constitutively expressing GFP from a lac basal promoter. Cells were grown in a flow cell system with a 0.5 mM lactate LML medium and imaged using confocal laser scanning microscopy. As shown in Figure 3.1, *S. oneidensis* first forms a monolayer; after 23 hours, the first structures become 3-dimensional mounds; at about 44 hours, these structures begin to become mushroom-like with a distinct stalk and cap. This basic mushroom morphology is then maintained until approximately 100 hours when the biofilms begin to dissolve at both cap and stalk. Although *S. oneidensis* forms single-layer biofilms under some conditions [132], in our flow cell system biofilms develop as mushroom-shaped structures very similar to those described for other bacteria, including *Pseudomonas aeruginosa*, *Pseudomonas fluorescens* and *Escherichia coli* [115].

3.4.0.10 LIVE/DEAD stain for *S. oneidensis* biofilms

To establish the live/dead patterns within a *S. oneidensis* biofilm, as typically reported by the Molecular Probes® LIVE/DEAD®BacLight stain, biofilms grown in the flow cell system were stained with the LIVE/DEAD® reagent at developmental time points (Figure 3.2). At early time points, or in structures with little biomass, the entire biofilm stains as live. As biofilms increase in biomass, cells throughout the structure stain dead, until structures reach their maximum biomass when almost all cells in the middle of the structure stain dead. These patterns match the live and dead profiles reported for similar biofilms [37, 80]. Yet some studies have seen a discrepancy between LIVE/DEAD® staining and other viability measures indicating that there may be a potential for bias with this method [103]. The LIVE/DEAD® stain uses two fluorescent nucleic acid stains, Syto9 and propidium iodide. Syto9 is used to quantify live cells because it can permeate cells under all conditions; propidium iodide is used to quantify dead cells because, as a highly charged molecule,

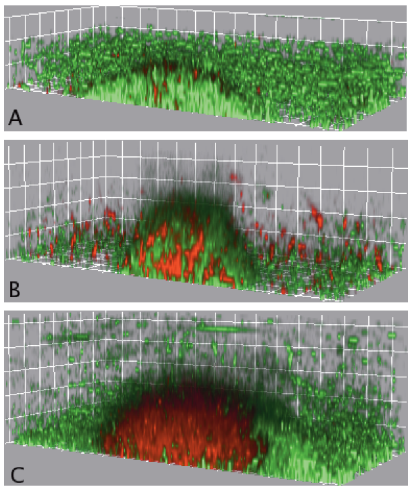

Figure 3.2: LIVE/DEAD staining in *S. oneidensis* biofilms. Green is the live stain, Syto9, and red is the dead stain, propidium iodide. Grid marks are 10 μm. (A) At 60 μm in diameter most cells continue to stain as live. (B) At $\sim$80 μm in diameter cells throughout the biofilm start to stain dead. (C) At $\sim$140 μm in diameter almost all cells in the middle of the biofilm are stained as dead.

it is unable to permeate cells with a strong electrochemical gradient across their membrane (i.e. the chemiosmotic potential). Although the LIVE/DEAD® stain typically correlates with growth assays in liquid or solid nutrient medium, as described in the Molecular Probes® manual, little is understood about how the membrane properties of cells in biofilms might change with time. Given this uncertainty, and that the LIVE/DEAD® stain is a terminal assay, we reasoned that an in vivo method for assessing growth might give a more accurate representation of the metabolic state of the biofilm.

3.4.0.11 Patterns of growth activity in biofilms using the *rrnB* P1 reporter

Strains of *S. oneidensis* MR-1 with in vivo fluorescent reporters of growth activity were constructed to spatially monitor cell growth in situ over the development and maturation of a biofilm. The growth reporter plasmid, pTK4, was made using the system designed by Sternberg et al. [121], in which GFP is expressed from the E. coli *rrnB* P1 ribosomal promoter, the activity of which correlates with ribosome production [3]. *S. oneidensis* MR-1 containing pTK4 fluoresces green with an unstable GFP, GFP(AAV), when cells are producing ribosomes, a process associated with growth and protein synthesis capacity. To determine if this reporter would function as a good indicator of growth state in *S. oneidensis* time course experiments were performed with well-characterized planktonic cultures. As seen in Figure 3.3, for both the constitutively green fluorescent strain, DKN308, and the strain containing the ribosomal green fluorescent reporter, DKN310, fluorescence increased with

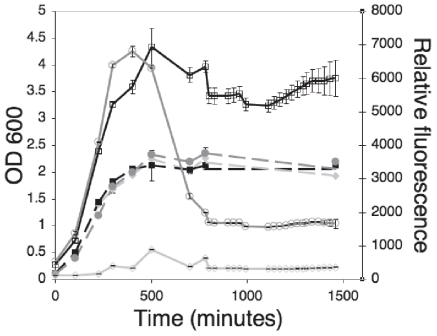

Figure 3.3: Fluorescence levels and absorbance at OD_{600} for *S. oneidensis* MR-1 (diamonds), *S. oneidensis* DKN308 constitutively expressing GFP (squares), and *S. oneidensis* DKN310 expressing GFP(AAV) from a ribosomal promoter, representing growth activity (circles). OD_600 is indicated by dashed lines, and fluorescence by solid lines. As cells grow through exponential phase, fluorescence levels increase, but when stationary phase is reached, fluorescence levels from the constitutively expressing GFP remain high whereas fluorescence from the growth active version decreases rapidly. Error bars represent standard deviations of triplicate cultures; in some cases the error is smaller than the size of the symbol.

OD_{600} until the culture reached 1.2 x108 cells/mL where the OD_{600} plateaued. Fluorescence then stayed high in strain DKN308 but decreased in strain DKN310, reaching zero 240 minutes after the cell density stopped increasing. Green fluorescence from the ribosomal reporter increased during exponential phase, as expected for a marker of growth, and then decreased due to the combined effects of RNA downregulation and prompt protein turnover during stationary phase. These results verify that this GFP reporter is a sensitive, time-resolved indicator of growth activity in *S. oneidensis*.

To monitor growth activity relative to the entire developing biofilm over time, pTK4 was used as one part of a dual color fluorescent system imaged by confocal microscopy. The pTK4 plasmid was introduced into *S. oneidensis* DKN309, a strain of *S. oneidensis* that also expresses ECFP constitutively from a basal lac promoter. The resulting new strain, DKN310, fluoresces cyan at all times to mark cellularity and also fluoresces green to mark cells actively engaged in growth, as indicated by active synthesis of the ribosomal machinery. To learn if there is a defined developmental progression, and to ask what parameters (size, shape, age, etc.) correlate most directly with growth activity, *S. oneidensis* DKN310 biofilms were grown in flow cells for up to 100 hours. Individual biofilms were imaged longitudinally, at multiple time points and in multiple fields of view, using dual-channel fluorescence imaging of cyan and green on a Zeiss 510 confocal laser scanning microscope. A representative developmental course is shown in Figures 3.4A-E. Growth activity, indicated by pTK4 reporter fluorescence, was uniform throughout the biofilm at early stages in development, in

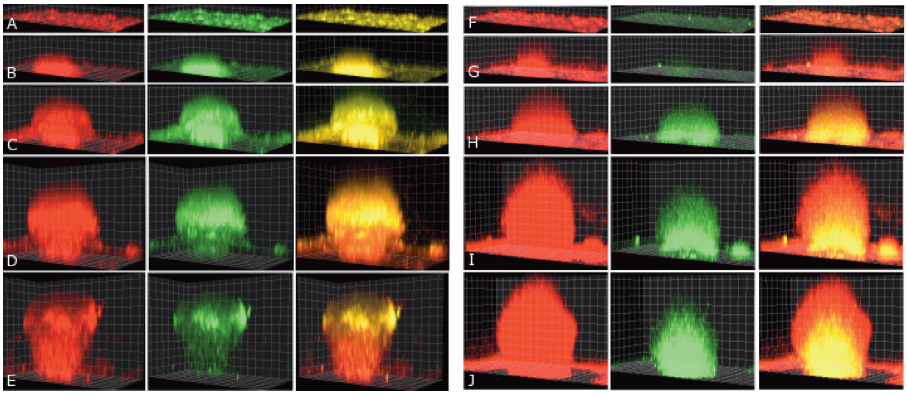

Figure 3.4: Development of a mushroom structure in a *S. oneidensis* biofilm with a ribosomal (growth) reporter (DKN310, panels A-E) and an anaerobic reporter mtrB (DKN312, panels F-J). Grid squares are 10 μm x 10 μm. In the first column cells are constitutively expressing ecfp and fluorescence from it is false colored red. In the second column of panels A-E, cells expressing the growth active GFP(AAV) appear as green. In the second column of panels F-J, cells expressing the *mtrB* reporter are green. The third column is an overlay of red and green channels. (A) 18 hours, height 8 μm (B) 28 hours, height 18 μm (C) 41 hours, height 52 μm (D) 65 hours, height 92 μm (E) 77 hours, height 112 μm. (F) 17 hours, height 8 μm (G) 29 hours, height 31 μm (H) 47 hours, height 58 μm (I) 71 hours, height 104 μm (J) 85 hours, height 118 μm

structures up to 60 μm in height that do not have a mushroom cap. When the structures develop a mushroom cap, structures can then get up to 120 μm in height and still be growth active in all regions of the biofilm. As structures get larger and reach their final mature state, up to 140 μm in height, growth activity in the cap is maintained, but growth activity in the stalk is only maintained in the outer approximately 25 μm.

3.4.0.12 Patterns of metabolism under anaerobic conditions in biofilms using the *mtrB* reporter

To determine if metabolism (i.e. protein synthesis and energy generation) might occur in regions where cells are not actively growing, a reporter that is expressed under these conditions was required. It is known that as biofilms increase in biomass, molecular oxygen (O_2) levels in the inner regions become more limited [107, 122], and these might correspond to domains where the *rrnB* P1 growth reporter is not active. To test whether this might be relevant for our system, we measured the O_2 consumption rate for stationary phase *S. oneidensis* cells in LML medium. Using this rate (5.53mg O_2/L*s) and applying a biofilm diffusion model, as described by Stewart [122], we estimate that the concentration of O_2 required to sustain growth will be depleted approximately 30 μm into the biofilm. This is consistent with O_2 profiles measured in many other biofilm systems [26, 107, 122]. Therefore, if cells are still capable of actively metabolizing in regions of low growth activity, it is

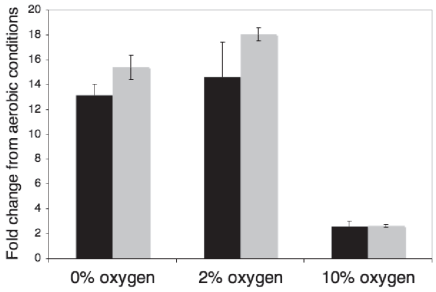

Figure 3.5: Fold change in expression, as measured by Q-RT-PCR, of *mtrB* and *eyfp* in *S. oneidensis* DKN312 relative to aerobic (21% O2) conditions. Black bars represent *mtrB* and gray bars *eyfp*. *mtrB* and *eyfp* expression is upregulated under anaerobic and microaerobic conditions. Error bars represent the range of duplicate cultures.

expected that genes expressed under low O_2 conditions would most likely be upregulated in these regions. Previous work from our lab and those of others suggested that *mtrB* might be such a gene: *mtrB* is expressed under low O2 conditions by Shewanella, and its product, an outer membrane β-barrel protein, facilitates electron transfer under anaerobic conditions [6, 77]. Therefore, a reporter construct for *mtrB* was made, and an unstable YFP, *eyfp*(AAV), was inserted into the chromosome after the mtr operon, creating strain DKN311. To establish whether YFP fluorescence from the mtr operon in DKN311 is an accurate indicator of metabolism under anaerobic conditions, DKN311 was grown under aerobic, microaerobic, and anaerobic conditions. Quantitative real-time PCR experiments conducted with different O_2 concentrations (0%, 2%, 10% and 21%, or air) showed that *mtrB* and *eyfp* expressed from the *mtr* operon were 12-fold upregulated only under 0% and 2% O_2 concentrations (Figure 3.5), validating that *eyfp*(AAV) expression in the *mtr* operon can be used as a marker of new metabolism in low oxygen domains. DKN312, the reporter strain used for imaging, was created by inserting the pTK5 plasmid that constitutively expresses ECFP from the lac promoter, into strain DKN311; DKN312 constitutively expresses ECFP and expresses EYFP only under anaerobic or microaerobic conditions. Because EYFP and ECFP have an absolute requirement for O_2 to fold properly, fluorescence of either color implies the presence of at least trace amounts of oxygen in the biofilm [49]. Biofilms of *S. oneidensis* DKN312 were grown exactly as described for the growth activity reporter strain, DKN310. Figures 3.4F-J show that *mtrB* is not expressed at early stages of biofilm development, consistent with full O_2 availability in structures less than 60 μm in diameter. *mtrB* expression only appeared in the interior spatial domains of biofilms at late developmental stages, in structures greater than 100 μm in diameter, when the interior cells were likely O_2-limited.

3.4.0.13 Quantitative analysis of expression patterns

To assess the reproducibility of these results across multiple individual biofilms and through replicate experiments, we developed a quantitative analysis system to map reporter expression profiles across multiple biofilms. Using this system a plot of fluorescence intensity versus distance from the center of the structure was constructed automatically for each image. For the different biofilm developmental stages, averages for the *S. oneidensis* DKN310, or growth activity, strain and the *S. oneidensis* DKN312, or *mtrB*, strain were calculated. The patterns of the reporters were remarkably consistent relative to structure size and shape. The most important factor in determining these patterns was not the time that the biofilm had developed, but its size, which is a far better and more consistent correlate of reporter gene domain of activity. This quantitative analysis also reveals that *mtrB* expression profiles are the inverse of those for the growth activity GFP marker (Figure 3.6).

3.5 Discussion

Although various single-species biofilms have been well studied with respect to what controls their physical development, far less attention has been paid to their metabolic dynamics. From the LIVE/DEAD® stains (Figure **??**), it might be predicted that large sub-populations of cells within mature biofilms are not actively generating energy and are therefore dead. However, our *in vivo* metabolic activity reporter system does not support this interpretation. Although patterns of cell viability at early stages in biofilm development (diameter < 60 μm) correlate with the results from the LIVE/DEAD® stain, beginning in the middle developmental stages (60 μm $<$ diameter $<$ 140 μm), the patterns of metabolic activity diverge from the LIVE/DEAD® stain. Larger regions of growth activity (as measured by the *rrnB* P1 reporter) are observed, and subpopulations where metabolism decouples from growth (as measured by the *mtrB* reporter) also appear. In mature biofilms (diameter $>$ 140 μm), although growth activity is restricted to the outer $\sim$25 μm, strong fluorescent signatures of *mtrB* expression dominate the interior; this is in sharp contrast to what is seen in the LIVE/DEAD® stain, where all cells in the interior stain as dead. These patterns, of both growth activity and *mtrB* expression, are remarkably consistent and correlate specifically with the size of the biofilm structure. This demonstrates that growth-inactive regions of the biofilm are, nevertheless, metabolically active. At a minimum, they generate sufficient energy to synthesize recently induced new proteins. The involvement of the mtr operon further implies competence for key cellular metabolism including electron transport and anaerobic metabolism that is enabled

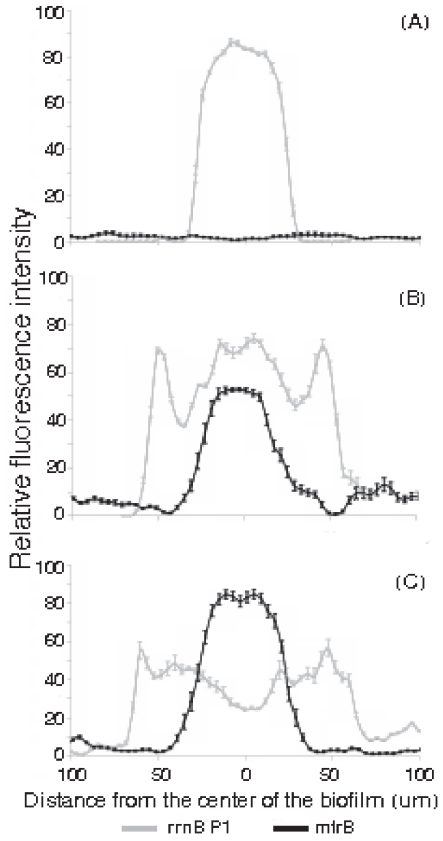

Figure 3.6: Quantitative analysis of patterns of growth activity and metabolism in *S. oneidensis* biofilms. Gray lines are strain DKN310 (*rrnB* P1) showing growth activity profiles and black lines are strain DKN312 showing *mtrB* expression. (A) Biofilm structures approximately 60 μm in diameter. (B) Structures approximately 110 μm in diameter. (C) Structures approximately 140 μm in diameter. Each line represents an average of a minimum of six different structures. Error bars are the standard deviation of the binned pixel intensity values across all the images included in the plot. In panels (B) and (C), local minima at the edge of the colonies are regions with no cells, thought to be EPS. Patterns of expression relative to the size of the biofilm structure are remarkably consistent across multiple structures, and *mtrB* continues to be expressed in regions where growth activity has decreased.

by mtr gene products. Thus, there appear to be major interior domains of biofilms where cells generate energy although they are not actively growing. The state of these interior cells may be akin to the stationary phase of planktonic cultures or might represent a biofilm-specific state of metabolism. What is strikingly clear from these time-resolved imaging studies is that the vast majority of cells in all regions of a biofilm are physiologically active, even though they are eventually running dramatically different programs of activity. In conclusion, we have observed remarkably reproducible spatiometabolic stratification in *S. oneidensis* biofilms. These findings are leading us to rethink previous interpretations of what it means to be a dead cell in a biofilm and has implications for understanding how cells in a biofilm react to antibiotics, toxins or other changes in environmental conditions. Cells that are maintained in a non-growing state, yet are still capable of synthesizing proteins, may be responding to introduced agents in unexpected ways and have the ability to act as a reservoir of survival. Indeed, in many natural systems where microorganisms exist at high cell densities, such as infections, microbial mats, as well as in engineered bioreactors, it is likely that a significant fraction of the population is not actively growing [31, 135]. A better understanding of what defines and controls the capabilities and activities of this growth-inactive state is not only essential for understanding basic aspects of biofilm biology, but is also extremely relevant for applications that aim to exploit the metabolic activity of biofilms for energy conversion and other purposes [59, 104].

3.6 Acknowledgements

We thank William Berelson for help with O_2 respiration measurements, Søren Molin for plasmids and the Caltech Biological Imaging Center for use of the facility. This work was supported by grants from the Office of Naval Research, Packard Foundation and Howard Hughes Medical Institute to D.K.N.

3.7 Supplemental methods

3.7.0.14 Mini-Tn7 Derivative Construction and Characterization.

Mini-Tn7 derivatives for constitutive expression of fluorescent proteins in *S. oneidensis* were constructed as follows. The EcoRI-XbaI mini-Tn7KmΛSm1 fragment from pBK-miniTn7-KmΛSm1 [70] was cloned into the EcoRI site of the small mobilizeable R6K-based plasmid pUX66 (D. Lies and G. Roberts, unpublished), after the digested plasmid and insert fragment were treated with

Klenow DNA polymerase to generate blunt ends, to create plasmid pURR21. The NotI fragment from pBK-miniTn7-gfp3 [70] containing the *gfpmut3** gene expressed from the lac PA1/04/03 promoter derivative was cloned into the NotI site of pURR21 to generate the transposon mini-Tn7-KSGFP and the plasmid pURR25. Mini-Tn7-KSGFP contains the NotI fragment after the Λ cassette in the transposon while mini-Tn7gfp3 has the NotI fragment between the cassette and the kanamycin resistance cassette. An ECFP expression cassette was constructed by cloning the pURR25 NotI fragment onto a version of pOK12 [140] lacking SphI and HindIII sites and replacing the gfpmut3* gene from this fragment with an *ecfp* gene amplified by PCR from pMP4641 [12] using ECFPN (5-GACCGCATGCTGAGCAAGGGCGAGGAGCTG-3) and ECFPC (5-GGTGAAGCTTACTTGTACAGCTCGTCCATGCC-3) primers. This ECFP expression cassette was cloned as a NotI fragment into pURR21 to generate the transposon mini-Tn7-KSCFP and the plasmid pURR27. The plasmid pURR21 and its derivatives were constructed to provide mini-Tn7 and fluorescent protein gene delivery vehicles with a plasmid R6K-based origin of replication. We examined the utility of these plasmids in *S. oneidensis* using a donor strain containing pURR25 in comparison with the pMB1-based plasmid pBK-miniTn7-gfp2, which was previously used as a mini-Tn7 donor to produce GFPmut3* expression in *S. oneidensis* MR-1 [131]. The E. coli donor strain WM3064 [110] carrying either plasmid was mated with *S. oneidensis* MR-1 using a 1:5 donor:recipient ratio and incubated for 5h at 30°C on LB agar plates containing 300 ?M diaminopimelic acid, in the presence or absence of WM3064 containing the transposition helper plasmid pUX-BF13 [2]. In the absence of pUX-BF13, matings between WM3064(pBK-miniTn7-gfp2) and MR-1 yielded *S. oneidensis* transconjugants resistant to 15 μg/ml gentamicin at frequencies of 10-5 per recipient. Plasmid extractions from 12 of these transcojugants all contained plasmid DNA of the same size as pBK-miniTn7-gfp2. Similar matings in the presence of pUX-BF13 yielded the same frequency of transconjugants and these transconjugants also contained plasmid DNA of the same size as pBK-miniTn7-gfp2. Matings performed with WM3064(pURR25) and *S. oneidensis* MR-1 in the absence of pUX-BF13 yielded transconjugants resistant to 50 μg/ml kanamycin at frequencies of 10-9 per recipient. Matings between WM3064(pURR25), WM3064(pUX-BF13) and *S. oneidensis* MR-1 yielded kanamycin-resistant transconjugants at frequencies of 10-5 per recipient. No new plasmid DNA was detected in plasmid extractions from two transconjugants from matings lacking pUX-BF13 or from five transconjugants from matings in the presence of pUX-BF13. These results indicate that, unlike pURR25, pBK-miniTn7-gfp2 replicates in *S. oneidensis* MR-1 and cannot easily be used for delivery of mini-Tn7 derivatives at single copy into the genome of MR-1. We have

confirmed this observation with seven other derivatives of this group of mini-Tn7 delivery plasmids reported by [72] and have demonstrated that the plasmid pRK2013 is also maintained in *S. oneidensis* MR-1. Thus, contrary to a previous report [88] but consistent with a more recent report [46], we find that pMB1- and ColE1-based plasmids replicate in MR-1. Plasmid R6K-based derivatives such as those constructed here and reported elsewhere [25] are more useful vehicles for chromosomal delivery of mini-Tn7 derivatives. Tn7 inserts in most Gram-negative bacteria in a site- and orientation-specific manner downstream of the glmS gene [25, 29]. We analyzed 20 MR-1 transconjugants containing mini-Tn7-KSGFP by PCR using transposon-specific primers (Tn7aphAUp: GCCAGTTTAGTCTGACCATCTC and Tn7catEndDown: TGTCGGCAGAATGCTTAATGA) and primers targeting *glmS* and the downstream gene *menB* from MR-1 (MR1glmSDown: CGCCACTGATTTACACTATCCC and MR1menBUp: CGATCAAGACTTCTCAGCCTTC). Specific PCR products for all 20 transconjugants could be obtained with the primer pairs MR1glmSDown-Tn7catEndDown and Tn7aphAUp-MR1menBUp but not with other combinations of these primers. Only the MR1glmSDown-MR1menBUp primer pair yielded a specific PCR product from wild-type MR-1 DNA, which was absent in the transconjugants presumably because of the large size of the inserted transposon. These results indicate that Tn7 inserts between *glmS* and *menB* in *S. oneidensis* MR-1, oriented with the Tn7R end near glmS and the Tn7L end near *menB*. We sequenced the specific upstream and downstream PCR products from five of the mini-Tn7-KSGFP transconjugants to determine the specific insertion site for the transposon in MR-1. In all five of the transconjugants, mini-Tn7-KSGFP inserted following base pair (bp) 4951342 of the MR-1 genome sequence (NCBI accession number AE014299.1) and duplicated the six-bp sequence GCCAGT (bp 4951347-4951342 of the MR-1 genome). This sequence is part of an imperfect 42 bp inverted repeat presumably capable of forming a stem-and-loop structure and putatively serving as the rho-independent transcriptional terminator of *glmS*, which would be interrupted by insertion of the transposon.

Chapter 4

Metabolic dynamics and heterogeneity in *Shewanella oneidensis* biofilms

4.1 Abstract

Bacteria in biofilm communities are resilient to changes in environmental conditions and resistant to toxins and antibiotics. The communities are spatially stratified and metabolically heterogenous, suggesting that the communities may respond differentially to environmental changes. Some regions within the community are not growth-active, but are still persisting and are capable of generating energy for maintenance. To determine whether these growth-inactive regions are able to dynamically respond to nutrient changes and how growth-activity profiles might be affected by these changes, we modified the nutrient environments of mature *Shewanella oneidensis* biofilms and tracked *in vivo* expression of a growth activity reporter. Using a quantitative analysis, we determined regions of growth activity and how these profiles changed under different conditions. We found that cells previously growth-inactive could become active with the addition of an electron acceptor and that profiles of growth activity match those expected for the diffusion and reaction of the acceptor. However, the addition of an electron donor had little effect on biofilm metabolic profiles. These findings suggest that metabolic organization of *S. oneidensis* biofilms is dynamic and influenced primarily by the availability of an electron acceptor.

4.2 Introduction

Bacteria grow in the environment as surface-attached microbial communities that are heterogeneous and spatially stratified [31, 135]. It has been shown that while not all regions of the biofilm are actively growing, much of the community is still alive and capable of generating energy to persist [128]. Some studies have shown that growth activity profiles can be modified when media conditions are changed, but these studies have focused on early stages of biofilm development when the community may not have been as differentiated as in mature structures [121]. In mature biofilms studies have been conducted to trigger cell dispersal and in these cases a subset of the population responds and detaches from the community [132]. Often these changes in environmental conditions are very dramatic. It is not known however, how growth and metabolic profiles might be modified in response to changes in nutrient availability or what substrates might have an effect on growth profiles. Gaining an understanding of how biofilm growth and metabolic profiles are affected can give us insight into how biofilms live in the environments and how responsive or terminally differentiated they might be.

To explore whether growth activity patterns of mature biofilms are dynamically responsive to changes in nutrient availability and how these patterns might be affected by different nutrients and concentrations, we chose to work with *Shewanella oneidensis*. *S. oneidensis* can form biofilms, has versatile respiratory capabilities and its metabolism has been well-characterized, making it an ideal organism for investigating metabolic responsiveness and heterogeneity.

4.3 Material and Methods

4.3.1 Bacterial strains, plasmids and media.

Shewanella oneidensis strains were grown planktonically using LB (Sigma) or LML (0.2 g/L yeast extract, 0.1 g/L peptone, 2.5 g/L sodium HEPES, and 0.243 mL/L 60% lactate syrup (20mM), pH 8.0). When required tetracycline was added at the final concentration 15 μg/mL. For cultures grown with fumarate 20mM or 2mM Disodium fumaric acid was added to the basal media. For biofilm experiments LML with 0.5mM lactate was used.

S. oneidensis derivative DKN310 expressing an ECFP from a lac promoter and an unstable gfp (*gfpAAV*), from a ribosomal reporter, *rrnB* P1, were constructed as described [128]. The *lac-ecfp* fusion was inserted into the chromosome using a mini-Tn7 system. The *rrnB* P1-*gfpAAV* fusion was inserted into plasmid pME6031, creating plasmid pTK4. *S. oneidensis* strain DKN580 is strain

MR-1 with the pTK4 plasmid.

S. oneidensis DSP10 is a spontaneous rifampicin resistant mutant of MR-1, created by Doug Lies [129]. No differences in growth aerobically or anaerobically on any alternative electron acceptor have been observed between DSP10 and MR-1. A non-polar mutant in the fumarate reductase flavoprotein subunit precursor, SO_0970, was made by deleting a portion of the gene using the native PstI sites in the gene in *S. oneidensis* DSP10, creating strain NP-FC-1 [78]. This deletion was confirmed to be in frame by sequencing. Plasmid pTK4 was added to strains DSP10 and NP-FC-1 creating strains DSP10 pTK4 and NP-FC-1 pTK4. NP-FC-1 is unable to reduce fumarate, but could still grow on and reduce TMAO and thiosulfate under anaerobic conditions [78]. The pTK4 plasmid was added to DSP10 and NP-FC-1 creating strains *S. oneidensis* DSP10 pTK4 (DKN578) and *S. oneidensis* NP-FC-1 pTK4 (DKN579) respectively.

Anaerobic cultures were grown using LML media and adding 20mM fumarate as the electron acceptor. Media was prepared, dispensed into Balch tubes, stoppered and autoclaved. Immediately after autoclaving, media was flushed with mixed gas for 30 seconds.

4.3.2 Measurements of growth and fluorescence

Growth and fluorescence measurements were taken using a Bio-Tek Synergy HT. For measuring growth, optical density at an absorbance of 600nm was used. For green fluorescence, measurements were taken using a 485/20 excitation filter and a 528/20 emission filter.

4.3.3 Fermentor experiments

Cultures were grown in a New Brunswick Scientific BIOFLO 110 Fermentor/Bioreactor to supply oxygen at a constant rate and measure dissolved oxygen concentrations. Oxygen was supplied to the culture by attaching a standard air line, presumably containing 21% oxygen, to the fermentor and regulating the inflow pressure to 2 lpm. The fermentor was calibrated to measure oxygen values by throughly oxygenated the medium using the air inflow line and setting this value to 100%. or 1.0. As per the instructions for the fermentor, the dissolved oxygen sensor was disconnected from the machine and when the readout settled, this value was set to 0.0. Oxygen values were then recorded as the readout from the dissolved oxygen sensor. Samples were taken from the fermentor at various time points using the sampling port. Samples were measured for OD_{600}.

4.3.4 NADH and NAD+ measurments

Measurements of NADH and NAD+ were obtained as described [112]. Briefly, two 1mL aliquots of culture were collected in two separate ependorph tubes and centrifuged at 14,000 for 1 minute. The supernatant was removed and one pellet was resuspended in 300 μL of 0.2M NADH for the NADH measurement and the other pellet was resuspended in 300 μL of 0.2M HCl for the NAD+ measurement. Samples are incubated at 50°C for 10 minutes and then incubated on ice for 20 minutes, or until they reached 0°. Then 150 μL of 0.1M HCl (for the NADH sample) or 0.1M NaOH (for the NAD+ sample) is added to the lysate and vortexed. An additional 150 μL of the same reagent is added to the lysate and vortexed. Samples are centrifuged for 3 minutes at 14,000 rpm. The supernatant is then extracted to a fresh tube and stored at -80°C. To measure NADH and NAD+ concentrations in the samples, a reagent mix of 8x H_2O, 1x 2.0M Bicine, 2x 100% EtOH, 1x 80mM EDTA, 2x 4.2 mM MTT and 4x 16.6 mM PES is prepared under anaerobic conditions. The reagent mix is allowed to warm up to 30°C. 90 μL of the reagent mix is pipetted to wells of a 96 well plate. 5 μL of the NADH or NAD+ sample is then added to the well, and the plate is kept anaerobic. On the benchtop 3mg Alcohol Dehydrogenase (ADH II) is added to 3 mL 0.1M Bicine and dispensed into a boat. The plate is transferred to the benchtop where 5 μL ADHII mix is quickly added to each well. The plate is transferred to a Bio-Tek Synergy HT plate reader held at a temperature of 30°C, and kinetic measurements are taken at 570nm at intervals of 53 seconds for 20 minutes. Before each read the plate is shaken for 1 second at an intensity of 1. For each well the data is plotted and the slope of the line is determined. The slope of the line is what indicates how much NADH and NAD+ is in the sample. This data is also obtained for known concentrations of NADH and NAD+. Using the slopes of the lines from the NADH and NAD+ standard curves, the concentrations of NADH and NAD+ for each sample can be determined.

4.3.5 Growth activity response to the addition of fumarate

10 mL LB with 20mM lactate was added to 25 mL tubes. 4 tubes contained LB with 20mM lactate. 2 tubes contained LB with 20mM lactate and 100mM fumarate. *S. oneidensis* pTK4 was innoculated into the tubes to an OD_{600} of 0.01. Cultures were grown shaking at 250rpm and 30°C and time points for OD_{600} and green fluorescence were taken every 60 minutes for 720 minutes. At 420 minutes, when cells had entered stationary phase, the four cultures not containing fumarate were spun down at 7500rpm for 2 minutes. Cells from two samples were resuspended in the same media: LB with 20mM lactate. The two other samples were resuspended in LB with 20mM lactate

and 100mM fumarate, effectively spiking the culture with an addition of 100mM fumarate. Cultures continued to grow shaking at 30°C, and growth and fluorescence were measured every hour.

4.3.6 Growth activity of *S. oneidensis* DSP10 and *S. oneidensis* NP-FC-1 in aerobic and anaerobic conditions

Strains *S. oneidensis* DSP10 pTK4 and *S. oneidensis* NP-FC-1 pTK4 were grown aerobically and anaerobically. Aerobic cultures were grown in 3mL LML in 25mL tubes at 30°C shaking. Anaerobic cultures were grown at 30°C in Balch tubes in LML with 20mM fumarate. Cultures were grown for 1320 minutes. At each time point OD_{600} and green fluorescence were measured.

4.3.7 Biofilm experiments

A flow cell system was constructed as described such that biofilms could be grown under constant conditions and imaged over time [128]. A 0.5 mM lactate LML medium [pH 8.0, 0.2 g/L yeast extract, 0.1 g/L peptone, 2.5 g/L Na HEPES and 0.043 mL 60% lactate syrup] was used as the basal media. For experiments with fumarate, 20mM or 2mM Disodium fumaric acid was added to the media. For experiments with increased lactate concentrations, 20mM lactate was added to the media. The flow cell is inoculated with 300 μL of a culture in exponential phase, at an OD600 of approximately 0.075, using a sterile syringe. Flow is not started immediately in order to allow cells to attach to the surface. After 1 hour the flow is started at a rate of 4.1μL/sec, 1.5 rpm on a Watson-Marlow peristaltic pump. The flow continues at this rate for the length of the experiment. Using this technique, biofilms were grown for up to 4 days. If media conditions were changed bottles of the original media were exchanged for new media, and the new media flowed through the system at the same rate. Confocal fluorescence microscopy was used to image bacterial biofilms grown in the flow cells. A Zeiss LSM 510 inverted microscope with a 40x C-Apochromat 1.2W corr water immersion lens at the Caltech Beckman Institute Biological Imaging Center was used. Z-series images were acquired for multiple fields of view at multiple time points during the experiment. For imaging EGFP or EYFP, the excitation was 488nm and the emission filter used was a BP500-550. For imaging ECFP the excitation was 420nm and the emission filter used was a BP465-485. Images were processed using the Imaris software.

4.3.8 Quantitative image analysis

Fluorescence profiles and colony sizes were quantitated as described [128]. To determine colony size an x-axis cross-section through the largest part of the colony was taken. An edge detection algorithm was used to determine the region of greatest contrast between the empty space around the colony and the colony. In this way, the edge of each side of the colony was found, and the distance between the two edges was taken to be the size of the colony.

4.4 Results

4.4.1 Growth and growth activity of *S. oneidensis* DSP10 and *S. oneidensis* NP-FC-1 in aerobic and anaerobic conditions

Shewanella oneidensis contains one gene required for required for fumarate reduction, SO_0970 [81, 137]. When a mutant is made in this gene, *S. oneidensis* can no longer grow on fumarate under anaerobic conditions. We tested the ability of our mutant strain, NP-FC-1 to grow aerobically and anaerobically on fumarate. Aerobically NP-FC-1 grew the same as wild-type DSP10 (Figure 1.1). To determine growth activity, we used the pTK4 plasmid, where GFP is expressed from the *E. coli rrnB* P1 ribosomal reporter, whose activity correlates with ribosome production. This growth activity, as measured by fluorescence, increased during exponential phase, but decreased during stationary phase, as expected since the cells are producing less ribosomes and less growth active. However, when grown in anaerobic conditions on fumarate strain NP-FC-1 is not able to grow, while strain DSP10 pTK4 can. The growth activity profile is shifted so that growth activity decreases later in stationary phase than under aerobic conditions, but growth activity still is high during exponential phase and drops off through stationary phase. Both DSP10 and NP-FC-1 behave as wild-type MR-1 when grown aerobically in both their growth curve and growth activity profiles, but NP-FC-1 is not able to grow anaerobically on fumarate as we expected.

4.4.2 Fermentor measurements of growth, dissolved oxygen and NADH/NAD+ ratios

To determine the correlation between growth state, oxygen concentration and NADH/NAD+ levels, cultures of *S. oneidensis* MR-1 were grown in a fermentor where dissolved oxygen levels could be monitored. LB medium was added to the fermentor at the beginning of the experiment and was not

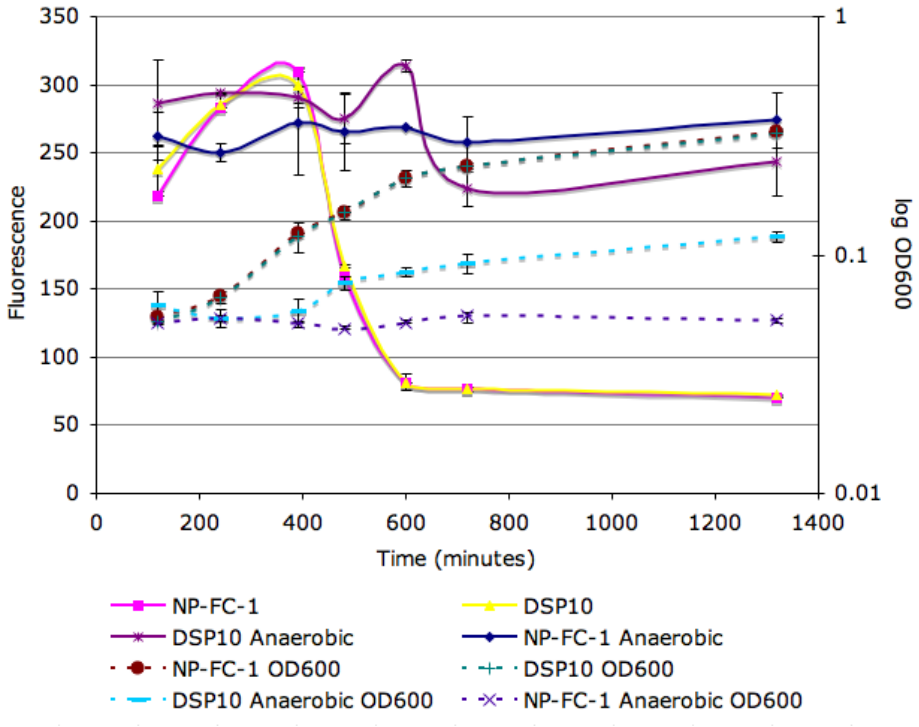

Figure 4.1: Fluorescence levels and OD_{600} for *S. oneidensis* DSP10 pTK4 and *S. oneidensis* NP-FC-1 pTK4 grown aerobically and anaerobically on fumarate. OD_{600} is indicated by dashed lines and fluorescence by solid lines.

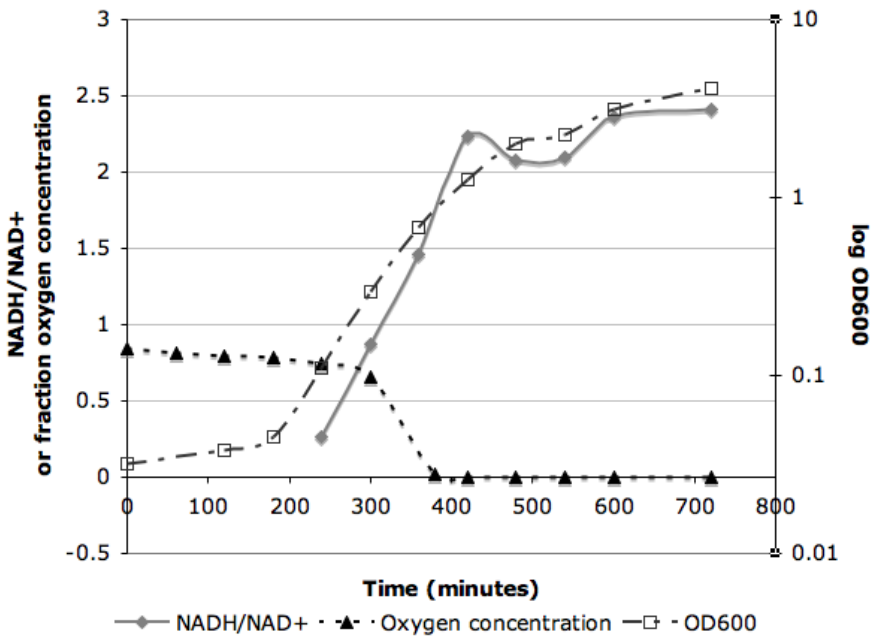

Figure 4.2: Representative curve of growth, dissolved oxygen concentration and NADH/NAD+ ratios for *S. oneidensis* MR-1 cultures grown in a chemostat. The solid gray line is NADH/NAD+ ratio. The dashed black line with the solid black triangles is dissolved oxygen concentration, where 1.0 represents the maximum concentration in air, 21% oxygen. The dashed black line with the open squares is growth as measured by OD_{600}. Oxygen concentrations decrease as cell density increases, and there is a brief drop in the NADH/NAD+ ratios during this transition in cell density and oxygen concentration.

exchanged. Air was added to the fermentor at a constant flow rate of 2 lpm and the culture was well-mixed. Oxygen levels stayed high through lag and early exponential phase, but as the cells entered exponential phase, dissolved oxygen concentrations decreased until they were being measured as zero in early stationary phase (Figure 1.2). A dissolved oxygen concentration of zero does not mean that there is no oxygen in the system, only that cells are consuming the oxygen as quickly as it enters the system. The decrease in oxygen concentrations and entrance into stationary phase also correlates with a brief drop in the NADH/NAD+ ratio. This brief decrease in the NADH/NAD+ ratio is observed in flask cultures as well (data not shown). This suggests that the cells may be switching systems utilized to keep NADH/NAD+ ratios, and the redox state, constant under electron acceptor limited or stationary phase conditions.

4.4.3 Growth activity response to the addition of fumarate

To determine if the addition of alternative electron acceptor could influence the growth activity of *S. oneidensis* MR-1, we grew MR-1 aerobically in media without fumarate, with fumarate and with

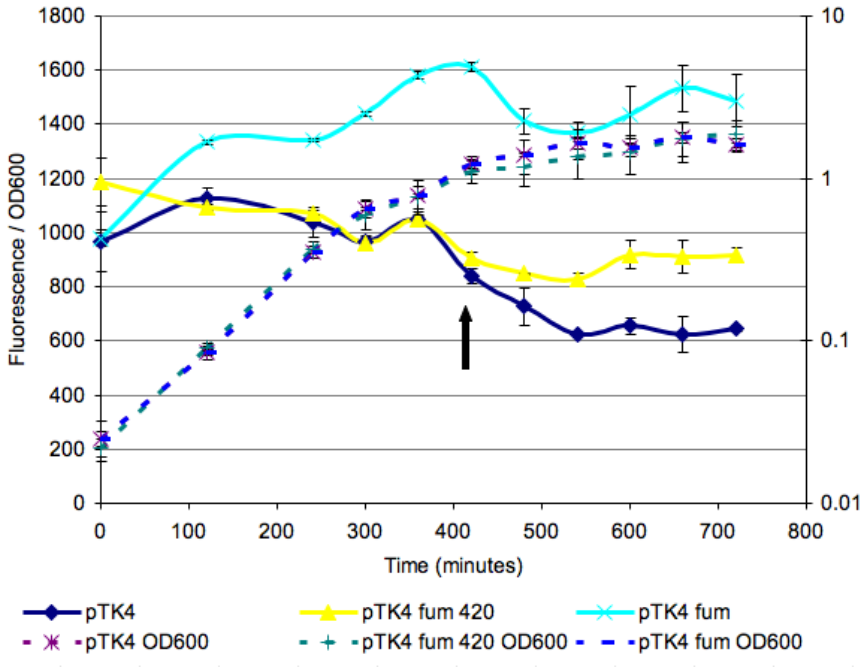

Figure 4.3: Fluorescence levels and OD_{600} for *S. oneidensis* MR-1 pTK4 grown aerobically with and without fumarate. OD_{600} is indicated by dashed lines and fluorescence by solid lines. pTK4 fum 420 cultures were switched to media containing fumarate at 420 minutes, indicated by the arrow on the graph. pTK4 fum cultures were grown in media containing fumarate through the whole experiment.

fumarate added in early stationary phase when cultures became oxygen limited. Cultures without fumarate were grown in LB plus 20mM lactate. Cultures with fumarate were grown in LB plus 20mM lactate and 100mM fumarate. From chemostat measurements where growth and dissolved oxygen concentrations were measured, we were able to determine that oxygen levels quickly dropped to zero when cells reached early stationary phase. Therefore, when cells reached early stationary phase and were limited for oxygen as an electron acceptor we switched the cells to media amended with 100mM fumarate. As seen in Figure 1.3 cells grown with fumarate through the whole experiment maintained a high growth activity even when cells were oxygen limited in stationary phase. In cultures where fumarate was added, growth activity stopped decreasing through stationary phase in contrast to cultures not amended with fumarate that continued to show decreased growth activity. This demonstrates that the addition of an alternative electron acceptor when cells are electron acceptor limited can influence the cells and allow them to be more growth active. Interestingly, the addition of fumarate did not change the amount of growth in the cultures. It may be that the addition of 100mM fumarate, as a less favorable electron acceptor than oxygen, is enough to affect ribosome synthesis, but cannot generate enough energy to appreciably affect cell number.

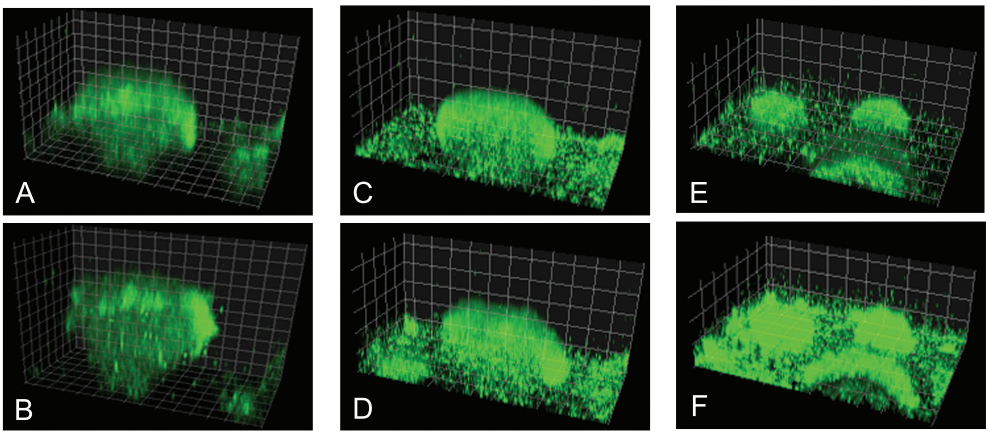

Figure 4.4: Representative images of *S. oneidensis* MR-1 pTK4 biofilms with no change in media (A and B), with the addition of 2mM fumarate (C and D) or with the addition of 20mM fumarate (E and F). Images A, C and F are the biofilms at 48 hours before a change in conditions. Images B, D and F are 56 hours, 6 hours after the media change. Green fluorescence is fluorescence from the ribosomal reporter pTK4 and indicates regions of growth activity. In panels A and B, no change in the media is made and there is a slight decrease in fluorescence intensity at 56 hours. In panels C and D, there is a slight increase in the intensity and region of fluorescence at 56 hours when the biofilm has been exposed to 2mM fumarate. In panels E and F there is a greater increase in the intensity and region of fluorescence after exposure to 20mM fumarate.

4.4.4 Biofilm growth activity profiles with the addition of fumarate or lactate.

Biofilms were grown for approximately 48 hours and imaged in multiple fields of view for each sample. At approximately 50 hours the media was switched to media amended with 2mM fumarate, 20mM fumarate, 20mM lactate or left the same. Biofilms were allowed to grow in this new media for approximately 6 hours and the same colonies were re-imaged. In biofilms where conditions were switched to media containing fumarate the regions of growth activity increased. The increase was more significant in the biofilms amended with 20mM fumarate than with 2mM fumarate (Figure 1.4). In biofilms where 20mM lactate was added, there was no significant change in the growth activity profiles.

Quantifying the regions of growth activity for a minimum of 6 colonies under each condition, regions of growth activity increase from 30 μm in no fumarate biofilms to 37 μm in biofilms grown with 2mM fumarate and 46 μm in biofilms grown with 20mM fumarate. There was no significant change in the colony size under each condition, indicating that regions of growth activity were increasing and not that new cells were attaching to the structure.

Meshulam-Simon et al measured fumarate and succinate levels in *S. oneidensis* MR-1 cultures

grown anaerobically on pyruvate and fumarate [84]. While the electron donor is different than in our medium, a rate of fumarate respiration can be calculated from this data that should be comparable to reduction rates under our conditions. Calculating the rate through the linear sections of the curve, the rate of fumarate reduction is 60.8 μmols/hour. Using this value, we can then calculate how far we would expect 20mM and 2mM fumarate to diffuse into the biofilm. Using the equation from Stewart 2003, we predict that 20mM fumarate will diffuse approximately 11 μm into the biofilm [122]. This value is made assuming that all cells are consuming fumarate. However, since the fumarate reduction requires proteins expressed only under oxygen-limiting conditions, it is likely that cells on the outer edges that are exposed to oxygen are not consuming fumarate. If we instead add the region where we predict oxygen to be available (30 μm) [128] and the region of predicted fumarate diffusion, we find that an electron acceptor should be available approximately 33 μm into the biofilm in the presence of 2mM fumarate and approximately 41 μm into the biofilm with 20mM fumarate. This matches well with our results where we observe that growth activity occurs 37 μm into the biofilm with 20mM fumarate and 46 μm into the biofilm with 2mM fumarate.

4.4.5 Profiles of growth activity in biofilms of the *S. oneidensis* fumarate reductase mutant, NP-FC-1

Biofilms of *S. oneidensis* NP-FC-1 develop the same as wild type *S. oneidensis* MR-1 using 0.5mM LML media. However, when *S. oneidensis* NP-FC-1 biofilms are switched to a media containing 20mM fumarate, the colony size decreases dramatically. Average colony size in biofilms with media with no fumarate are 110 μm and the average colony size in fumarate amended biofilms is 68 μm (Figure 1.5). Growth activity remains high in these smaller colonies, but it appears that cells are leaving the biofilms. This phenotype is similar to that seen when pH is decreased dramatically or high concentrations of DMSO are added to the media (data not shown). It is possible that without a functioning fumarate reductase, fumarate is not able to be metabolized by the cells and is having a toxic effect. This issue remains to be explored.

4.5 Discussion

Although hypotheses about biofilm resilience and the heterogeneous nature of biofilm communities would predict that regions within the biofilm are able to respond differentially to changes in nutrient conditions, it has been yet to be demonstrated conclusively. We have shown that when the availability

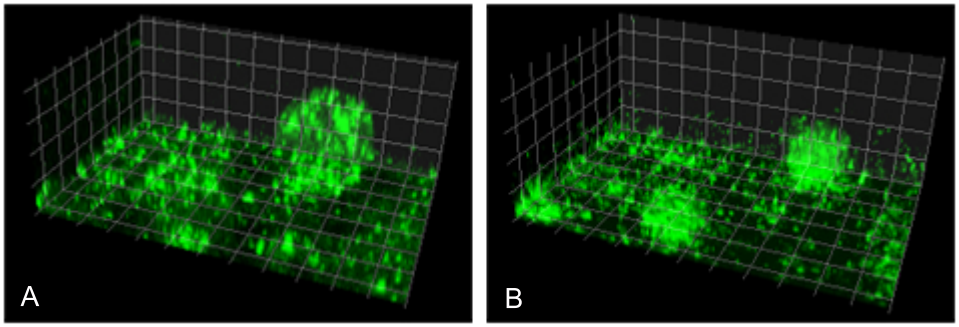

Figure 4.5: Representative images of the fumarate reductase mutant, *S. oneidensis* NP-FC-1 pTK4, biofilms before and after the addition of 20mM fumarate to the media. Panel A is 48 hours and panel B is at 56 hours, 6 hours after the addition of fumarate. Green fluorescence is fluorescence from the ribosomal reporter pTK4 and indicates regions of growth activity. After the addition of fumarate, colonies of *S. oneidensis* NP-FC-1 pTK4 maintain their growth activity, but significantly decrease in size.

of the electron acceptor, fumarate, is increased, growth activity profiles expand. In particular, regions that were not growth active and were instead in a more dormant metabolic state, responded to the electron acceptor availability and were activated.

These regions of growth activity correspond with predictions for fumarate diffusion into a biofilm if different regions or different cells were primarily using one electron acceptor. Since the fumarate reductase of *S. oneidensis* is only upregulated under microaerobic or anaerobic conditions, cells sensing and respiring on higher levels of oxygen are not likely to be able to respire on fumarate as well, validating this prediction. If individual cells are primarily using one electron acceptor, it indicates the the biofilm community is metabolically differentiated, giving credence to the idea that metabolic heterogeneity may be contributing to the persistence of biofilms.

S. oneidensis is able to use fumarate as a part of its citric acid cycle. In order to differentiate the effects of fumarate as an electron acceptor versus its potential role in the the electron donor pathway, we determined the response of the biofilm community to the addition of an electron donor, lactate. When lactate was added there was no significant effect on colony morphology or growth activity profiles. This result is interesting, since we might predict that given the low concentration of electron donor in the basal media, 0.5mM lactate, the cells would be electron donor limited. While electron acceptor concentrations are low, at the biofilm-bulk interface at least, oxygen should be readily available. However, these low lactate conditions are required for biofilm formation [131], and it may be that under these conditions the bacteria utilize another carbon source such as EPS components, extracellular DNA or endogenously produced compounds. It may also be that under biofilm conditions, the requirements for electron donor are extremely low or that the primary limiting

resource is the electron acceptor.

When a strain is not able to reduce fumarate for growth, in the presence of increased fumarate concentrations, biofilm colonies get smaller while maintaining high growth activity. We expected to see only that growth activity profiles would not be affected by the addition of an electron acceptor that the bacteria could not utilize. Instead this dispersal suggests that fumarate has some toxic effects on *S. oneidensis* when it is unable to reduce it, or that the redox balance may somehow be skewed. While many studies have characterized *S. oneidensis* growth and molecular mechanisms of fumarate respiration under anaerobic conditions, to our knowledge no one has investigated the potential effects of fumarate on a fumarate reductase mutant. Since the fumarate reductase is required for growth on fumarate, it is potentially difficult to decouple an inability to grow with a toxic effect. It may also be that this phenotype is unique to cells grown in biofilm conditions, where the bacteria may be particularly sensitive to changes in redox balance.

In this paper, we have shown that the metabolic organization of a *S. oneidensis* biofilm community is dynamic and responsive to changes in electron acceptor availability. The response of biofilm communities to antibiotics and other exogenous compounds has received much focus, but a better knowledge of how bacteria in biofilms can respond to changes in nutrient availability and redox balance is important for the understanding of how bacteria live in biofilms and are so resilient in the environment.

Chapter 5

Expression studies of the AHL acylase QuiP of *Pseudomonas aeruginosa* PAO1 by wild type and by an AHL signal degrading variant of PAO1

5.1 Abstract

Pseudomonas aeruginosa PAO1 uses acyl-homoserine lactone (AHL) signaling molecules to engage in cell to cell communication and to regulate the production of numerous genes and virulence factors. PAO1 has the ability to degrade and utilize long chain, but not short chain signaling molecules. Two genes of *P. aeruginosa*, PA2385 (*pvdQ*) and PA1032 (*quiP*), were previously found sufficient for the degradation of long chain AHL, with only the PA1032 gene necessary for AHL degradation. This study examines the expression of PA1032 in *P. aeruginosa* PAO1 and in a variant of *P. aeruginosa*, $PAO1_{lagless}$, which constitutively degrades AHL. We compare the phenotypes, transcriptomes and expression of PA1032 in PAO1 and $PAO1_{lagless}$ strains and find that while $PAO1_{lagless}$ expresses the PA1032 AHL acylase all of the time, PAO1 wild type expresses this gene for long chain AHL degradation in the center of microcolonies during the biofilm growth state.

5.2 Introduction

The acyl-homoserine lactones (AHLs) are signaling molecules used by some gram negative bacteria in cell-to-cell communication known as quorum sensing (19). In this process, bacteria couple their

gene transcription to changes in cell population density. The opportunistic pathogen *Pseudomonas aeruginosa* PAO1 has two AHL mediated quorum sensing systems, the lasI/R and rhlI/R systems which involve the production and response to two main AHLs: 3OC12HSL and C4HSL respectively (38, 51, 61). The two systems are connected and behave in a hierarchy where, after a critical concentration of the long chain signal 3OC12HSL is accumulated, rhlR, the response regulator for C4HSL is transcribed (34, 49). The AHL mediated quorum sensing systems of PAO1 control distinct gene regulons and also interact to regulate the expression of genes for numerous virulence factors, exoenzymes, nutrient acquisition and certain aspects of biofilm formation (reviewed in (30, 48, 51, 58)). This AHL quorum sensing system is estimated to regulate approximately 6%-9% of the PAO1 genome (48, 56, 58). Multiple global regulators of the AHL quorum sensing system of PAO1 have been identified (17, 24, 45, 48) indicating that quorum regulated genes are subject to regulation and cues from the environment (65).

P. aeruginosa has the ability to degrade long chain AHL, but not short chain AHL (28). Two enzymes sufficient for AHL degradation have been identified: PvdQ, encoded by the gene PA2385 and QuiP, encoded by the gene PA1032 (27, 28, 50). PvdQ is not necessary for degradation of long chain AHL, whereas *quiP* is necessary and its transcript and protein product are present during degradation of long chain signal when AHL is the sole carbon source (27). To determine when *P. aeruginosa* may use this signal degrading ability, the expression and regulation of PA1032 in *P. aeruginosa* PAO1 and in PAO1$_{lagless}$, a variant that constitutively degrades long chain AHL, were studied.

5.3 Material and Methods

5.3.1 Strains and culture conditions

The bacterial strains used in this study are listed in Table 5.1. All cultures were maintained in LB (Lysogen Broth) amended with antibiotics when appropriate. Antibiotic concentrations used for *Pseudomonas aeruginosa* were: 60μg/ml tetracycline, 50μg/ml gentamycin and 250μg/ml carbenicillin, and for *E. coli*, 100μg/ml ampicillin, 15μg/ml gentamycin and 10μg/ml tetracycline. A defined freshwater medium buffered at pH 5.5 with 5mM 2-(N-morpholino)-ethanesulfonic acid (MES) was used for studies with growth on defined carbon sources (35).

A variant of PAO1 was obtained from six serial transfers of PAO1 that was growing exponentially on long chain AHL signal to identical fresh medium with 1mM C10HSL as the sole carbon source.

Table 5.1: Bacterial strains and plasmids

Strain	Relevant characteristics	Source
P. aeruginosa		
$PAO1_{wt}$	wild type	Laboratory stock (originally from B. Iglewski)
$PAO1_{lagless}$	constitutive expression of PA1032, long chain AHL degrader	this study
$PAO1_{lagless2}$	long chain AHL degrader	this study
P. aeruginosa wild type and *P. aeruginosa* lagless mutants		
ΔmvfR	PA1003::Gm	this study
ΔvqsR	PA2591::Gm	this study
ΔlasR	PA1430::Gm	this study
ΔqscR	PA1898::Gm	this study
ΔlasR ΔqscR	ΔPA1430, PA1898::Gm	this study
PAO1 YFP	ΔPA1032::YFP, Gm	this study
$PAO1_{lagless}$ YFP	ΔPA1032::YFP, Gm	this study
PAO1 YFP_att_CFP	ΔPA1032::YFP, attTn7::miniTn7T-Gm-PA1033_32, pMP4641 (eCFP)	this study
$PAO1_{lagless}$ YFP_att_CFP	ΔPA1032::YFP, attTn7::miniTn7T-Gm-PA1033_32, Gmr, pMP4641 (eCFP), Tetr	this study
E.coli		
TOP10	Electrocompetent cells for cloning	Invitrogen (Carlsbad, CA)
Plasmids		
pCM351	allelic exchange vector, Gmr, Ampr, Tetr	(39)
pCM157	Ampr, Cre - expressing plasmid	(39)
pFUNR	plasmid containing YFP	(Sidney Cox, Caltech, unpublished)
pMW312	PQF50 plasmid, lacZ with rsaL(PA1431) promoter	(63)
pUC18TminiTN7T-Gm	Gmr Amr plasmid for neutral site integration	(8)
pTNS1	helper plasmid for pUC18TminiTN7T-Gm	(8)
pMP4641	Tetr, constitutive eCFP expression from Plac	(3)

Primers
Primer1: AAAGGTACCTGCTTTGGTGGAGCGC
Primer2: GTCGTTGGCCATCAGGCTCTT
Primer3: CCTGATGGCCAACGACAAAATAAGGAGG
Primer4: AAAAAAGCGGCCGCTTATTTATACAGTTCGTCCATA
PA1032_MCS2_F: AAAACCGGTCAAGCGGCTGACGCTCAC
PA1032_MCS2_R: AAAGAGCTCAGCAGCTCAACCTGCGCC
PA1033_32_Tn7_F: AAGGATCCACCCTTCGCACGCGCC
PA1033_32_Tn7_R. AAAAAGCTTTCAGCGAGCGGGAGTGAGCGTCA

The resulting variant strain, $PAO1_{lagless}$, constitutively degraded long chain AHL without lag. Another lagless strain, $PAO1_{lagless2}$, was obtained from a separate experiment in which selection repeated a second time starting with wild type PAO1. $PAO1_{lagless2}$ also constitutively degraded long-chain AHLs without lag.

5.3.2 Construction of ΔPA1032::YFP transcriptional fusion strains and mutants

ΔPA1032::YFP reporter strains were constructed by homologous recombination. A 1 kb fragment that included 855 bp upstream of PA1032 was amplified using primer 1 (KpnI site underlined) and primer 2. Promoterless YFP, which was designed from Venus YFP (41) and Citrine YFP (22) with a monomeric A206K mutation (Sidney Cox, Caltech), was amplified from the plasmid pFUNR

(Sidney Cox, Caltech, unpublished) using primers 3 and 4 (NotI site underlined). Two additional basepairs were added in primer 3 to amplify YFP, which was amplified with its own ribosome binding site from pFUNR, out of frame for a transcriptional fusion within PA1032. The resulting deletion within PA1032 was in frame minimizing potential polar effects. The PCR product from PA1032 was fused to the YFP fragment with PCR using primers 1 and 4. This fragment was sequenced to verify the PCR sewed product. The product was cloned into pCM351 (39) by digestion with KpnI and NotI enzymes and ligation. In the second multi cloning site of pCM351, a 1kb DNA fragment downstream of PA1032, which included 31bp from the end of the gene, was amplified using primers PA1032_MCS2_F (AgeI site underlined) and PA1032_MCS2_R (SacI site underlined) and cloned into pCM351 using restriction enzymes AgeI and SacI followed by ligation. The resulting plasmid was transformed into wild type PAO1, PAO1$_{lagless}$ and PAO1$_{lagless2}$ via electroporation (7). Double recombinants were selected based on resistance to gentamycin (50μL/ml) and sensitivity to tetracycline (55 μg/ml). Putative double recombinants were confirmed by sequencing. The Gm resistance gene was removed using a cre-lox system (39). The plasmid pCM157 was transformed into strains with ΔPA1032::YFP. Colonies that were sensitive to gentamycin, which indicated successful cre-mediated excision of the gm resistance gene, were picked. The pCM157 plasmid was lost after two rounds of growth in LB without antibiotic selection. The resulting strains were used for PA1032 transcriptional reporting and phenotype tests. To produce cells that constitutively express CFP, the plasmid pMP4641(3) was transformed into PAO1 cells and tetracycline selection and microscopy were used as criteria for positive transformants.

5.3.3 Complementation of the ΔPA1032::YFP mutants

A fragment that contained the putative operon PA1032 and PA1033 and promoter, 122 bp upstream of PA1033 (Supplemental materials), was amplified from PAO1 gDNA using primers: PA1033_32_F (BamHI site underlined) and PA1033_32_R (HindIII site underlined) primers. This fragment was inserted into a neutral site downstream of the *glmS* gene of PAO1 using a mini Tn7 transposon containing plasmid (8). The BamHI and HindIII digested PCR product was ligated into the plasmid pUC18TminiTN7T-Gm (8) and sequence fidelity verified by sequencing. The resulting plasmid, pUC18TminiTN7T-Gm_PA1033_32, was electroporated into the wild type, PAO1$_{lagless}$ and PAO1$_{lagless2}$ strains that contained ΔPA1032::YFP reporter constructs with the aid of the helper plasmid pTNS1 (8). Putative transformants were selected based on resistance to gentamycin and insertion of the PA1033_32 genes into the correct site was verified by PCR using the primers glmS_Up

and glmS_down (8). The ability for the complemented mutants to degrade signal was tested by providing strains with AHL as the sole carbon source in minimal medium as described previously (35). The amount of long chain AHL accumulated by the $PAO1_{wt}$ and $PAO1_{lagless}$ with ΔPA1032::YFP and these strains complemented with PA1032 in a neutral site, was measured from cultures grown in 50mM MOPS buffered LB. 5 ml aliquots of culture were removed at late log phase at an OD_{600}nm of approximately 2.5 and the AHL extracted using acidified ethyl acetate. The amount of signal was quantified in comparison to standards of known concentration, using a Hewlett-Packard 1100 series LC/APCI MS as described previously (28).

5.3.4 YFP transcriptional reporter activity in cells grown in batch culture

YFP reporter activity from $PAO1_{wt}$ and $PAO1_{lagless}$ strains with the YFP transcriptional fusion in the PA1032 gene was followed in cells grown in batch culture. Cells were grown in 5 ml cultures in 1/10 LB medium at 37°C shaking at 250rpm. Over time samples were taken for optical density at 600nm, and fluorescence of YFP determined with excitation of 485/520nm and emission 525/540nm using a Synergy HT multi-detection microplate reader (Bio-Tek Instruments) and KC4 software. This experiment was repeated for ΔPA1032::YFP strains complemented with PA1032 and its promoter in a neutral site downstream of the glmS gene.

5.3.5 Biofilm experiments

Biofilm formation of the $PAO1_{wt}$ and $PAO1_{lagless}$ strains in a once flow through system (54) were analyzed. 1/10 LB medium was pumped through Tygon silicone tubing with an internal diameter of 1/16, an outer diameter of 1/8 and wall of 1/32 by a Watson-Marlow peristaltic pump with a flow rate of .8 rpm. A biofilm flow chamber (Stovall, Greensboro, NC) was added to each line of silicone tubing. Cultures of $PAO1_{wt}$, the $PAO1_{wt}$ strain with a ΔPA1032::YFP reporter and expressing CFP from a plasmid, and $PAO1_{lagless}$ with the same constructs were grown in 1/10 LB. Exponentially growing cell cultures with an optical density of 600nm of approximately 0.4 were inoculated into the silicone tubing upstream of biofilm flow chambers and flow was re-started after an hour of still incubation. The biofilms that grew within the chambers were analyzed imaged using a Zeiss Axiovert 100M inverted confocal microscope with a 40X Achroplan water immersion lens and LSM5 Pascal software V 3.2 (Carl Zeiss) at the Caltech Beckman Institute Biological Imaging Center. Images were analyzed using the Imaris program (Bitplane). Additionally, from each strain, eight colonies approximately 40 μm across, imaged at approximately 70 hours, were selected for quantitative image

analysis. The YFP and the CFP channels were separated and analyzed separately. Intensity profiles were obtained and analyzed for both channels for each image as previously described (55). The average fluorescence profiles for CFP and YFP for each strain was then calculated and plotted as fluorescence intensity versus distance from the center of the colony.

5.3.6 Microarray experiments

The transcriptomes of PAO1$_{wt}$ and PAO1$_{lagless}$ strains were compared using microarray analysis. Strains were grown from freezer stock on LB agar and single colonies that developed were picked and grown in MES pH 5.5 minimal medium (35) with 5mM succinate as the sole carbon source overnight at 37°C. 1 mL of overnight cell culture was inoculated into flasks containing 15 ml of sterile MES pH 5.5 medium that contained 8 mM sodium succinate and grown at 37°C and shaking at 250 rpm. 10 ml of cell culture were harvested at optical density 600nm of 0.4 and RNA was stabilized immediately with RNA Protect Bacterial Reagent (Qiagen) and processed according to manufacturers protocol. Total RNA was extracted from cultures using the RNeasy kit (Qiagen) and prepared for hybridization to *P. aeruginosa* GeneChips (Affymetrix) as previously described (44, 48). Hybridization, washing and scanning of Affymetrix GeneChips was performed at the University of Iowa Genome Center using an Affymetrix fluidics station. Genechip analysis were performed in duplicate and data analyzed using Microarray Suite software. We report gene activity changes showing greater than 2.5-fold up or down regulation. Microarray data were verified by RT PCR and comparison of expression of *rsaL*, a gene differentially expressed by PAO1$_{wt}$ and PAO1$_{lagless}$, using beta-galactosidase assays of the plasmid pMW312, which contained promoterless lacZ driven by the *rsaL* promoter (62).

5.4 Results

5.4.1 Characteristics of PAO1$_{lagless}$ strains

A variant of PAO1 that, unlike the wildtype, degrades long chain AHL constitutively, was selected by successive transfers of PAO1 into minimal medium with long chain AHL as the sole carbon source. PAO1$_{lagless}$ degrades AHL even in the presence of a preferred carbon source such as succinate (data not shown). When grown at 37°C on rich medium such as LB, the lagless strain produces significantly more blue pigment, indicating pyocyanin production, than wild type strains in plates and in liquid culture. The wild type and lagless strains have similar growth rates in LB medium, but the lagless

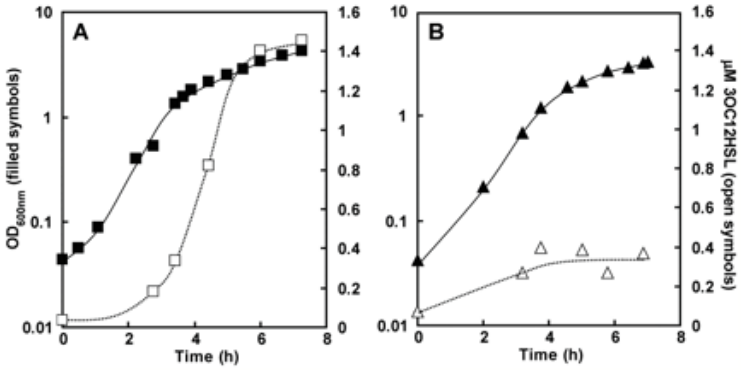

Figure 5.1: Growth and accumulation of naturally produced 3OC12HSL by PAO1$_{wt}$ and PAO1$_{lagless}$ strains. Growth of cultures in pH 7 buffered LB was measured using optical density 600nm, and the 3OC12HSL accumulated was determined using LC/MS of culture samples extracted with acidified ethyl acetate. (A) PAO1$_{wt}$ (B) PAO1$_{lagless}$ strain.

strain accumulated about a fourth of the amount of signal as wild type (Figure 5.1). A second lagless strain, obtained through a second selection of PAO1 grown successively on signal, behaved similarly to the original PAO1$_{lagless}$ strain in that it overproduced blue pigment and constitutively degraded long chain AHL (data not shown).

5.4.2 Differential gene expression of PAO1$_{wt}$ and PAO1$_{lagless}$ grown in succinate

Several genes were significantly up-regulated and a few down regulated in PAO1$_{lagless}$ relative to PAO1$_{wt}$ when both strains were grown with succinate as the carbon source (Figure 5.2). Notably, the genes differentially expressed in PAO1$_{lagless}$ relative to PAO1$_{wt}$ were genes previously found to be quorum regulated. PA1032 was significantly up-regulated in PAO1$_{lagless}$ relative to PAO1$_{wt}$. Knock out mutants in transcriptional regulators that were significantly up-regulated in the PAO1$_{lagless}$ strain relative to wild type: PA1003 (*mvfR*), PA2591 (*vqsR*) and PA1431 (*rsaL*), did not affect the ability for the wild type or lagless strains to degrade AHL (Supplemental material Table 2). Additionally, knock out mutations in PA1430 (*lasR*) and PA1898 (qscR) and a double mutant in the PAO1$_{wt}$ and PAO1$_{lagless}$ strain backgrounds did not affect the ability for strains to degrade AHL (data not shown).

Up-regulated:

ORF	Gene	Gene product	Fold change[a]
*PA0996	pqsA	probable coenzyme A ligase	4.3
*PA0997	pqsB	homologous to acyl-carrier protein synthase	3.2
*PA0998	pqsC	homologous to acyl-carrier protein synthase	4.4
*PA0999	pqsD	3-oxoacyl-[acyl-carrier-protein] synthase III	3.1
+*PA1003	mvfR	transcriptional regulator MvfR	2.5
+ PA1032	quiP	Probable penicillin amidase	4.4
*PA1250	aprI	alkaline proteinase inhibitor AprI	2.9
+*PA1431	rsaL	Regulatory protein RsaL	7.0
*PA1432	lasI	autoinducer synthesis protein LasI	5.9
*PA1657		Conserved hypothetical protein	3.4
*PA1659		hypothetical protein	2.7
*PA1869		probable acyl carrier protein	3.3
*PA1897		hypothetical protein	3.8
PA2065	pcoA	copper resistance protein A precursor	3.3
*PA2193	hcnA	hydrogen cyanide synthase HcnA	4.7
*PA2194	hcnB	hydrogen cyanide synthase HcnB	4.1
*PA2195	hcnC	hydrogen cyanide synthase HcnC	4.3
*PA2305		probable non-ribosomal peptide synthetase	5.2
+*PA2591	vqsR	probable transcriptional regulator	3.1
*PA3328		probable FAD-dependent monooxygenase	2.8
*PA3329		hypothetical protein	3.5
*PA3330		probable short chain dehydrogenase	3.5
*PA3331		cytochrome P450	3.9
*PA3332		Conserved hypothetical protein	2.4
*PA3334		probable acyl carrier protein	3.4
PA3874	narH	Respiratory nitrate reductase beta chain	2.8
PA3875	narG	Respiratory nitrate reductase alpha chain	3.3
PA3876	narK2	nitrite extrusion protein 2	2.6
PA3877	narK1	nitrite extrusion protein 1	2.5
*PA3904		hypothetical protein	4.9
*PA3905		hypothetical protein	5.5
*PA3906		hypothetical protein	5.5
*PA3907		hypothetical protein	3.0
*PA3908		hypothetical protein	4.6
PA3915	moaB1	moaB1	3.1
*PA4130		probable sulfite or nitrite reductase	2.8
*PA4131		probable iron-sulfur protein	3.4
*PA4133		cytochrome c oxidase subunit (cbb3-type)	2.7
*PA5391		hypothetical protein	3.1
Intergenic		PA1030 and PA1031, 1087095-1087843, (-) strand	2.7

Down-regulated:

ORF	Gene	Gene product	Fold change[a]
*PA1320	cyoD	cytochrome o ubiquinol oxidase subunit IV	-3.4
PA3581	glpF	glycerol uptake facilitator protein	-4.3
PA3584	glpD	glycerol-3-phosphate dehydrogenase	-3.3

Table 5.2: Genes significantly up or down-regulated in $PAO1_{lagless}$ compared to $PAO1_{wt}$ grown in minimal medium with succinate as the carbon source. mRNA extracted from cultures grown in duplicate were analyzed using a *P. aeruginosa* GeneChip microarray (Affymetrix). Starred genes have been found to be quorum regulated (48, 58, 63). [a] Genes with a ¿ 2.5 fold change in expression are shown. + indicates that knock out mutations in $PAO1_{wt}$ and $PAO1_{lagless}$ were made in these genes

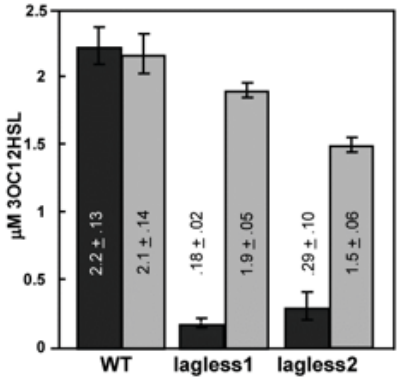

Figure 5.2: Accumulation of 3OC12HSL by PAO1$_{wt}$ and PAO1$_{lagless}$ parent strains (black bars) and strains with ΔPA1032::YFP transcriptional fusions (grey bars). All cultures were grown in pH 7 buffered LB and 3OC12HSL was measured using LC/MS.

5.4.3 PAO1$_{lagless}$ accumulated less 3OC12HSL than wild type in batch culture

PAO1$_{wt}$ and PAO1$_{wt}$ with ΔPA1032::YFP accumulated similar amounts of 3OC12HSL signal when grown in batch culture in rich medium (Figure 5.2). The lagless strains accumulated significantly less 3OC12HSL long chain signal than the wild type in batch culture (Figure 5.2). The ΔPA1032 mutation in the lagless strain accumulated up to 88% of long chain AHL accumulated by the wild type strain (Figure 5.2). The signal degradation phenotype of the lagless strain was lost in ΔPA0132 mutants, but was restored by the addition of a single copy of the PA1032 gene and its promoter at a neutral site in the chromosome (Supplemental Figure 5.8.2).

5.4.4 Studies of PA1032 expression in batch culture

The PAO1$_{wt}$ and PAO1$_{lagless}$ strains with the ΔPA1032::YFP transcriptional fusions and these strains complemented with the PA1032 gene grew similarly in 1/10 LB (Figure 5.3). In PAO1$_{l}$*agless*, both the transcriptional fusion strain and the strains with PA1032 complementation expressed the YFP reporter across all growth phases with similar ratios of YFP fluorescence/OD. This ratio showed two - fold variance over time of growth. The ΔPA1032::YFP reporter gene was not expressed significantly by the wild type during any phase of growth in batch culture (Figure 5.3)

5.4.5 PA1032 expression by PAO1$_{lagless}$ and PAO1$_{wt}$ growing in biofilms

PAO1$_{lagless}$ expressed the ΔPA1032::YFP reporter gene throughout biofilm formation from initial attachment to formation of mushroom structures (Figure 5.4 D-F). The expression of the YFP

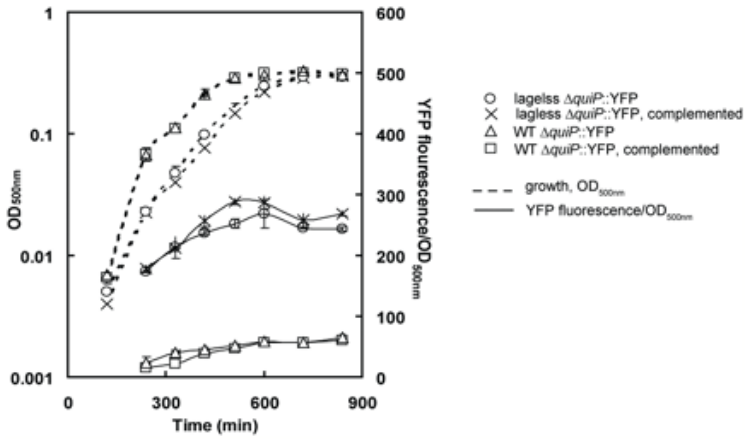

Figure 5.3: Growth and YFP expression by PAO1$_{wt}$ and PAO1$_{lagless}$ strains with ΔPA1032::YFP transcriptional fusions and by the strains complemented with PA1032 in a neutral site (att). Cells were grown in batch culture in 1/10 LB. Growth of strains was measured by optical density at 500nm and YFP fluorescence by excitation at 485/520nm and emission at 525/540nm.

reporter by the lagless strain closely followed the expression of CFP expressed constitutively by all cells from a plasmid (Figure 5.5 F-J). PAO1$_{wt}$ with the PA1032::YFP transcriptional fusion did not express YFP during the initial attachment to the surface (Figure 5.4 A), but after microcolonies formed, the center regions showed expression of the YFP gene (Figure 5.4B, C). The wild type showed expression of CFP in regions outside of the YFP expression, indicating that only a subset of the cells were expressing PA1032 (Figure 5.5 C-E). The transcriptional fusion strains complemented with a functional copy of the PA1032 gene and its promoter in a neutral site showed similar patterns of YFP expression as the respective parent strains (Figure 5.4 D, H).

5.5 Discussion

PA1032 (QuiP) of *P. aeruginosa* was previously found necessary and sufficient for degradation of long chain AHL that was provided as a carbon source (27). These studies examine the role of *quiP* and its expression in *P. aeruginosa* wild type and a variant of P. aeruginosa, PAO1$_{lagless}$, which constitutively degrades long chain AHL. The experiments described were performed to understand how AHL signal degradation by the PA1032 gene may be regulated and when quorum signal degradation may occur by PAO1.

The PAO1$_{lagless}$ strain is defective in the regulation of the PA1032 gene, such that PA1032 is constitutively expressed and long-chain AHLs constantly degraded. A knock out mutation in PA1032, in which the gene was replaced with a YFP reporter gene, eliminated the ability for the

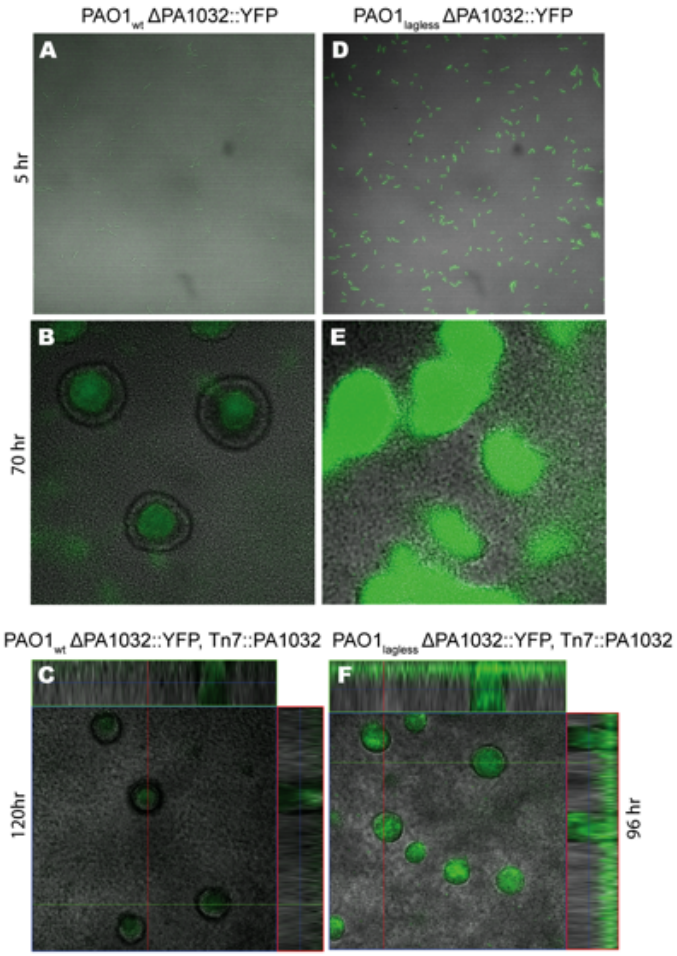

Figure 5.4: Confocal microscopy of biofilms formed by $PAO1_{wt}$ and $PAO1_{lagless}$ strains containing ΔPA1032::YFP transcriptional fusions. Strains were grown in a once-flow though biofilm system and imaged using filters for YFP and phase microscopy at 40X. (A)-(B) $PAO1_{wt}$ ΔPA1032::YFP. (C) $PAO1_{wt}$ ΔPA1032::YFP complemented with PA1032 at a neutral site, ortho view. (D)-(E) $PAO1_{lagless}$ ΔPA1032::YFP. (F) $PAO1_{lagless}$ ΔPA1032::YFP complemented with PA1032, ortho view.

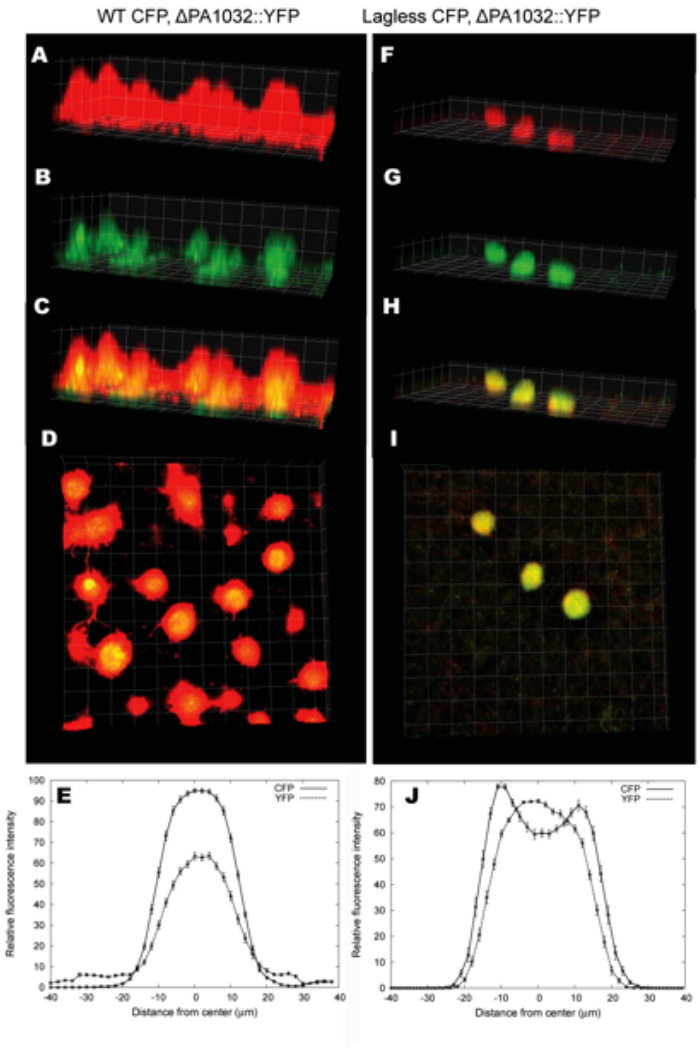

Figure 5.5: Confocal microscopy of biofilms formed by PAO1$_{wt}$ and PAO1$_{lagless}$ strains expressing CFP from a plasmid and with a ΔPA1032::YFP transcriptional reporter. A-E PAO1$_{wt}$ at 96 hrs. (A) CFP biofilm image; (B) YFP biofilm image; (C) merged fluorescence channels with overlap of CFP and YFP in yellow; (D) cross section through the biofilm; (E) quantification of expression profiles of CFP and YFP for PA01wt. (F-J) PAO1$_{lagless}$ strain at 120hr. (F) CFP image of the biofilm; (G) YFP image; (H) merged fluorescence channels with overlap of CFP and YFP in yellow; (I) cross section through the biofilm; (J) quantification of expression profiles of CFP and YFP for PA01$_{l}agless$. Images were visualized using Imaris software. Biofilm images were quantified by averaging intensity profiles across 8 colonies approximately 40 μm in size for each strain. Error bars indicate the standard deviations of the binned pixel intensity values for all the images included in the plot. The double peaks in the PAO1$_{lagless}$ CFP channel are the result of increased cell numbers, and therefore increased fluorescence, at the edges of the colonies.

lagless strain to degrade signal as a carbon source and restored the accumulation of nearly wild type levels of naturally produced 3OC12HSL (Figure 5.2). The signal degradation phenotype could be regained by a single copy of PA1032 with its promoter present in a neutral site in the chromosome (Supplemental Figure 5.8.2). There were no differences between the putative PA1032 promoter regions in $PAO1_{wt}$ and $PAO1_{lagless}$ (data not shown). The PA1032 gene was also necessary for long chain AHL degradation in a second lagless strain and the PA1032 mutation in this strain background restored significant accumulation of long chain AHL (Figure 5.2). These results indicate that the reduced accumulation of long chain signal in both lagless strains is not due to defects in long chain signal synthesis, but to constitutive degradation of signal produced. The PA1032 mutation in wild type *P. aeruginosa* did not influence the accumulation of long chain signal (Figure 5.2), which is consistent with lack of expression of this gene during batch growth conditions (Figure 5.3).

The $PAO1_{lagless}$ strain differentially expressed several genes relative to the wild type strain during growth on succinate as shown by microarray analysis. The over-expression of PA1032 by lagless is consistent with its ability to degrade long chain signal without lag and accumulate less naturally produced 3OC12HSL (Figure 5.2). Several quorum regulated genes were also upregulated in the lagless strain relative to the wild type (Table 5.2). It is surprising that the lagless strain expresses quorum regulated genes (Table 5.2) when it accumulates only a fraction of the long chain signal as the wild type (Figure 5.1 and Figure 5.2). It is not known if the genes differentially expressed by the lagless strain share a common regulator that is broken in this strain or if and how PA1032 is related to them.

Knock out mutations were made in the lagless and wild type strains in transcriptional regulator encoding genes: *rsaL* (PA1431), *mvfR* (PA1003), and *vqsR* (PA1003) that were differentially expressed in the lagless strain relative to wild type, and in the known response regulators for long chain AHL in PAO1: *lasR* and *qscR*. Examination of these genes cast a wide net to find out what circuits might intersect with the regulation of signal degradation. *rsaL* was 7 fold up-regulated in the lagless strain and was previously reported to influence the production of 3OC12HSL by encoding a protein that is a negative regulator of *lasI* (14). The significant up-regulation of this gene in the lagless strain despite the decreased accumulation of 3OC12HSL signal suggests that there could be another regulator for the rsaL gene that has aberrant expression in the lagless strain. *mvfR* encodes a transcriptional regulator that affects multiple quorum regulated genes and is required for pyocyanin production and synthesis of *Pseudomonas* quinolone signal (16, 20, 57, 64). The lagless strain with the mutation in *mvfR* no longer produced blue pigment and this is consistent with studies that

show *mvfR* is a key regulator of pyocyanin synthesis (6, 20). *vqsR* encodes a LuxR family regulator that that is known to control multiple quorum regulated genes (30, 56). None of the mutations in these genes affected the ability for the lagless strains to degrade signal without lag or precluded the ability for the wild type to eventually degrade signal when it was provided as a carbon source (Supplemental Figure 5.8.2). This indicates that PA1032 is not regulated by these transcriptional regulators and the aberrant regulation in the lagless strain is potentially upstream of these genes and the PA1032 gene.

Knock out mutations in *lasR*, which encodes the response regulator protein for 3OC12HSL, and *qscR*, a LuxR homolog that does not have a corresponding signal synthase gene, but has been shown encode a protein responsive to 3OC12HSL (9, 36, 37) as well as knock out mutations in both of these loci were made in the wild type and lagless stains. Mutations in these genes also did not influence signal degradation by the lagless or wild type strains (Supplemental Figure 5.8.2) indicating that degradation of long chain signal is not dependent on perception of long chain signal by these known response regulators. If PAO1 has a genetic program to degrade AHL, the cue may be other than the signal itself and the lagless strain may have a mutation that is a short circuit to signal degradation.

The ΔPA1032::YFP transcriptional reporter in the wild type background did not show significant expression during any phase of growth whereas the lagless strain expressed PA1032 throughout growth (Figure 5.3). The lagless YFP reporter strain complemented with PA1032 in a single copy in the chromosome showed similar ratios of YFP fluorescence/optical density indicating that PA1032 expression is not influenced by feedback from the gene itself. The differential expression of PA1032 by the lagless and wild type is consistent with microarray studies which show that the lagless strain over-expresses this gene in comparison to the wild type (Table 5.2) and accumulates less 3OC12HSL that the wild type due to constitutive degradation (Figure 5.2).

The stages of PAO1 biofilm formation have been well described and consist of attachment to a surface, microcolony formation, maturation to mature mushroom structures and dispersion, where sessile cells return to planktonic growth (12, 32, 46, 53). Though the lagless strain accumulated a fraction of the 3OC12HSL as the wild type (Figure 5.2), there were not significant structural differences in biofilms formed by the two strains over time. The amount of long chain signal that was accumulated by $PAO1_{lagless}$ may have been sufficient to activate genes involved in biofilm formation, or the conditions under which the biofilms were formed may not have been selective for a phenotype in the lagless strain. Previous reports have shown that the production and detection of long chain AHL signal, but not short chain AHL is important for the formation of biofilm architecture in *P.*

aeruginosa (13). In other studies the differences were not as striking (15, 25, 43) and the structure of biofilms has been found to be influenced by experimental conditions such as the carbon source used for growth (33) and hydrodynamics (43). It would be interesting to compare biofilms formed by PAO1$_{lagless}$ under such different conditions.

PAO1$_{wt}$ and PAO1$_{lagless}$ differentially expressed PA1032 in biofilms. Cells of the lagless strain with the ΔPA1032::YFP reporter fusion attached and colonized the surface similarly as the wild type strain, but PAO1$_{lagless}$ clearly expressed the YFP fusion whereas the wild type strain did not (Figure 5.4 A and D). Within 3 days, both strains formed macrocolonies that appeared similar in size and structure, but differed in expression of the YFP reporter for PA1032 expression (Figure 5.4 E, J). PAO1$_{wt}$ showed local expression of YFP in the center regions of the biofilm (Figure 5.4 B-C, Figure 5.5 B-E). The PAO1$_{lagless}$ strain expressed CFP and YFP in all areas throughout the mushroom structure (Figure 5.4 E-F, Figure 5.5 G-J). These observations are consistent with constitutive expression of PA1032 by the lagless strain under all conditions tested so far (Figure 5.2, Figure 5.3). The biofilms formed by wild type and lagless YFP reporter strains that were complemented with PA1032 showed similar biofilm structure and patterns of YFP expression within the microcolonies as the parent strains that contained ΔPA1032::YFP (Figure 5.4 C and F).

The differential expression of the PA1032 gene in the lagless and wild type strains within biofilms is the first report of PA1032 expression under standard laboratory conditions as it has only been previously identified as the gene necessary for degradation of long chain AHL when it is provided as a carbon source (27). The center of microcolonies in biofilms is also the location of multiple activities which could give clues as to how this signal degradation process is related to the rest of *P. aeruginosa* physiology. Biofilm detachment by seeding dispersal, where cells vacate the center of microcolonies, has been shown to originate from the center where cells become highly motile, increase expression of flagella and decrease expression of pillus genes and produce the surfactant rhamnolipid (4, 29, 42, 47). Cells in the biofilms are differentiated from free-living, planktonic bacteria (60) and in the dispersal process cells transition from sessile growth within biofilms to planktonic growth (31). The long term survival of bacteria that form biofilms is thought to be dependent on the ability for bacteria to leave sessile growth and re-colonize new areas (52). In some biofilms we observed wild type cells expressing the ΔPA1032::YFP transcriptional fusion that appeared to be leaving the center of the microcolony (Figure 5.4 B). It is possible that signal degradation could be part of the switch to prepare bacteria for growth in less population dense areas, and this could potentially include a re-setting of AHL mediated quorum sensing by degrading signals in the local environment.

Rhamnolipid surfactant produced in the center of microcolonies in dispersion state of growth could potentially mediate the degradation of the fatty acid hydrocarbon (2), which could potentially aid in long chain AHL degradation. The environmental cues and molecular mechanisms that trigger cells to enter planktonic growth are not well known (42). Nutrient availability has been found to promote detachment (21, 29, 47) and recently NO was identified to promote dispersal (1). Understanding biofilm dispersal has implications for treatment infections caused by bioiflms (1, 4). It is not known if degradation of AHL signal is related to the cell dispersal process, but it would be interesting to investigate the timing of PA1032 expression relative to known dispersal processes such as up-regulation of flagella or rhamnolipid production. Another possibility is that cells in the middle of the biofilm are using AHLs as a carbon source and using it to produce energy for maintenance.

It is not clear what environmental cues *P. aeruginosa* may be using to regulate the expression of PA1032 within biofilms. The data suggest a cue or integration of multiple cues from within the center of biofilm microcolonies for the expression of PA1032. Biofilms are heterogenous environments with microniches (11), and there is also diversification of cells in this growth state that is thought to be beneficial for nutrient utilization and survival within the biofilm (5). The center of microcolonies in particular is where there are the most intense gradients of oxygen (38), nutrients (10) and where signaling molecules may be concentrated according to modeling studies of biofilms (26). The sessile microbial cells in the biofilm themselves can produce gradients of microbial metabolic products (1). The cues for PA1032 expression could therefore be complex, and this may explain why the expression of this gene has not been seen under any conditions in batch culture (Figure 5.3). Expression of PA1032 has not been identified in any previous microarray studies in batch culture (48, 58) or biofilms (23, 59), but it is unclear whether localized gene expression could be captured using this method. Expression of an AHL acylase in the center of microcolonies could be a phenotype that serves to prepare bacteria for conditions outside of the biofilm and return to growth in the planktonic state.

5.6 Acknowledgements

We thank Marvin Whiteley and Ashley Peterson from The University of Oklahoma Health Sciences Center for working with us on with microarray experiments, Nathan Dalleska at the Caltech Environmental Analysis Center for assistance with LC/MS, Sidney Cox at Caltech for use of the pFUNR plasmid containing YFP, and Chris Waters at the Caltech Beckman Imagining Center for help with confocal imaging studies.

This work was done in collaboration with Dr. Jean Huang and Dr. Jared Leadbetter. As lead author, Jean constructed all the strains and conducted phenotypic characterization, microarray and 3OC12HSL measurement experiments.

5.7 Bibliography

1. Barraud, N., D.J. Hassett, S.H. Hwang, S.A. Rice, S. Kjelleberg, and J. S. Webb. 2006. Involvement of nitric oxide in biofilm dispersal of Pseudomonas aeruginosa. J. Bacteriol. 188:7344-53.

2. Beal, R. R., and W. B. Betts. 2000. Role of rhamnolipid biosurfactants in the uptake and mineralization of hexadecane in Pseudomonas aeruginosa. J. Appl. Microbiol. 89:158-68.

3. Bloemberg, G. V., A.H. Wijfjes, G.E. Lamers, N.N. Stuurman, and B. J. Lugtenberg. 2000. Simultaneous imaging of Pseudomonas fluorescens WCS365 populations expressing three different autofluorescent proteins in the rhizosphere: new perspectives for studying microbial communities. Mol. Plant Microbe In 13:1170-6.

4. Boles, B. R., M. Thoendel, and P. K. Singh. 2005. Rhamnolipids mediate detachment of *Pseudomonas aeruginosa* from biofilms. Mol. Microbiol. 57:1210-23.

5. Boles, B. R., M. Thoendel, and P. K. Singh. 2004. Self-generated diversity produces "insurance effects" in biofilm communities. Proc. Natl. Acad. Sci. 101:16630-5.

6. Cao, H. K., G., Goumnerov, B., Tsongalis, J., Tompkins R., Rahme, L.G. 2001. A quorum sensing-associated virulence gene of *Pseudomonas aeruginosa* encodes a LysR-like transcription regulator with a unique self-regulatory mechanism. Proc. Natl. Acad. Sci. USA 98:14613.

7. Choi, K. H., A. Kumar, and H. P. Schweizer. 2006. A 10-min method for preparation of highly electrocompetent *Pseudomonas aeruginosa* cells: application for DNA fragment transfer between chromosomes and plasmid transformation. J. Microbiol. Meth. 64:391-7.

8. Choi, K. H., J.B. Gaynor, K.G. White, C. Lopez, C.M. Bosio, R.R. Karkhoff-Schweizer, and H. P. Schweizer. 2005. A Tn7-based broad-range bacterial cloning and expression system. Nat. Methods 2:443-8.

9. Chugani, S. A., M. Whiteley, K.M. Lee, D. D'Argenio, C. Manoil, and E. P. Greenberg. 2001. QscR, a modulator of quorum-sensing signal synthesis and virulence in Pseudomonas aeruginosa. Proc. Natl. Acad. Sci. 98:2752-2757.

10. Costerton J.W., Z. L., D.E. Caldwell, D.R. Korber, H.M. Lappin-Scott. 1995. Microbial biofilms. Annu. Rev. Microbiol. 49:711-45.

11. Costerton, J. W., Z. Lewandowski, D. DeBeer, D. Caldwell, D. Korber, and G. James. 1994.

Biofilms, the customized microniche. J. Bacteriol. 176:2137-42.

12. Davey, M. E., and G. A. O'Toole. 2000. Microbial biofilms: from ecology to molecular genetics. Microbiol. Mol. Biol. R. 64:847-67.

13. Davies, D. G., M. R. Parsek, J. P. Pearson, B. H. Iglewski, J. W. Costerton, and E. P. Greenberg. 1998. The involvement of cell-to-cell signals in the development of a bacterial biofilm. Science 280:295-298.

14. De Kievit, T., P.C. Seed, J. Nezezon, L. Passador, and B. H. Iglewski. 1999. RsaL, a novel repressor of virulence gene expression in Pseudomonas aeruginosa. J. Bacteriol. 181:2175-2184.

15. De Kievit, T. R., R. Gillis, S. Marx, C. Brown, and B. H. Iglewski. 2001. Quorum-sensing genes in *Pseudomonas aeruginosa* biofilms: Their role and expression patterns. Appl. Environ. Microbiol. 67:1865-1873.

16. Dziel, E., S. Gopalan, A.P. Tampakaki, F. Lpine, K.E. Padfield, M. Saucier, and L. G. R. G. Xiao. 2005. The contribution of MvfR to *Pseudomonas aeruginosa* pathogenesis and quorum sensing circuitry regulation: multiple quorum sensing-regulated genes are modulated without affecting lasRI, rhlRI or the production of N-acyl-L-homoserine lactones. Mol. Microbiol. 55:998-1014.

17. Diggle, S. P., K. Winzer, A. Lazdunski, P. Williams, and M. Cmara. 2002. Advancing the quorum in Pseudomonas aeruginosa: MvaT and the regulation of N-acylhomoserine lactone production and virulence gene expression. J. Bacteriol. 184:2576-86.

18. Farinha, M. A., and A. M. Kropinski. 1990. Construction of broad-host-range plasmid vectors for easy visible selection and analysis of promoters. J. Bacteriol. 172:3496-3499.

19. Fuqua, W. C., S. C. Winans, and E. P. Greenberg. 1994. Quorum sensing in bacteria - the LuxR-LuxI family of cell density-responsive transcriptional regulators. J. Bacteriol. 176:269-275.

20. Gallagher, L. A., S.L. McKnight, M.S. Kuznetsova, E.C. Pesci, and C. Manoil. 2002. Functions required for extracellular quinolone signaling by Pseudomonas aeruginosa. J. Bacteriol. 184:6472-80.

21. Gjermansen, M., P. Ragas, C. Sternberg, S. Molin, and T. Tolker-Nielsen. 2005. Characterization of starvation-induced dispersion in Pseudomonas putida biofilms. Environ. Microbiol. 7:894-906.

22. Heikal, A. A., S. T. Hess, G. S. Baird, R. Y. Tsien, and W. W. Webb. 2000. Molecular spectroscopy and dynamics of intrinsically fluorescent proteins: coral red (dsRed) and yellow (Citrine). Proc. Natl. Acad. Sci. USA 97:11996-2001.

23. Hentzer, M., L. Eberl, M. Givskov. 2005. Transcriptome analysis of *Pseudomonas aeruginosa*

biofilm development: anaerobic respiration and iron limitation. Biofilms 2:37-61.

24. Heurlier, K., V. Dnervaud, G. Pessi, C. Reimmann, and D. Haas. 2003. Negative control of quorum sensing by RpoN (sigma54) in *Pseudomonas aeruginosa* PAO1. J. Bacteriol. 185:2227-35.

25. Heydorn, A., B. Ersbll, J. Kato, M. Hentzer, M.R. Parsek, T. Tolker-Nielsen, M. Givskov, and S. Molin. 2002. Statistical analysis of *Pseudomonas aeruginosa* biofilm development: impact of mutations in genes involved in twitching motility, cell-to-cell signaling, and stationary-phase sigma factor expression. Appl. Environ. Microbiol. 68:2008-17.

26. Horswill, A. R., P. Stoodley, P.S. Stewart, and M. R. Parsek. 2007. The effect of the chemical, biological, and physical environment on quorum sensing in structured microbial communities. Anal. Bioanal. Chem. 387:371-80.

27. Huang, J. J., A. Petersen, M. Whiteley, and J. R. Leadbetter. 2006. Identification of QuiP, the product of gene PA1032, as the second acyl-homoserine lactone acylase of *Pseudomonas aeruginosa* PAO1. Appl. Environ. Microbiol. 72:1190-1197.

28. Huang, J. J., J.I. Han, L.H. Zhang, and J. R. Leadbetter. 2003. Utilization of acyl-homoserine lactone quorum signals for growth by a soil pseudomonad and *Pseudomonas aeruginosa* PAO1. Appl. Environ. Microbiol. 69:5941-5949.

29. Hunt, S. M., E.M. Werner,, B. Huang, M.A. Hamilton, and P. S. Stewart. 2004. Hypothesis for the role of nutrient starvation in biofilm detachment. Appl. Environ. Microbiol. 70:7418-25.

30. Juhas, M., L. Eberl, and B. Tummler. 2005. Quorum sensing: the power of cooperation in the world of Pseudomonas. Environ. Microbiol. 7:459-471.

31. Klausen, M., A. Aaes-Jrgensen, S. Molin, and T. Tolker-Nielsen. 2003. Involvement of bacterial migration in the development of complex multicellular structures in *Pseudomonas aeruginosa* biofilms. Mol. Microbiol. 50:61-8.

32. Klausen, M., M. Gjermansen, J.U. Kreft, and T. Tolker-Nielsen. 2006. Dynamics of development and dispersal in sessile microbial communities: examples from *Pseudomonas aeruginosa* and Pseudomonas putida model biofilms. FEMS Microbiol. Lett. 261:1-11.

33. Klausen, M. M., A. A. Heydorn, P. P. Ragas, L. L. Lambertsen, A. A. Aaes-Jrgensen, S. S. Molin, and T. T. Tolker-Nielsen. 2003. Biofilm formation by *Pseudomonas aeruginosa* wild type, flagella and type IV pili mutants. Molecular microbiology 48:1511-24.

34. Latifi, A., M. Foglino, K. Tanaka, P. Williams, and A. Lazdunski. 1996. A hierarchical quorum-sensing cascade in *Pseudomonas aeruginosa* links the transcriptional activators LasR and RhIR (VsmR) to expression of the stationary-phase sigma factor RpoS. Mol. Microbiol. 21:1137-1146.

35. Leadbetter, J. R., and E. P. Greenberg. 2000. Metabolism of acyl-homoserine lactone quorum-sensing signals by Variovorax paradoxus. J. Bacteriol. 182:6921-6926.

36. Lee, J. H., Y. Lequette, and E. P. Greenberg. 2006. Activity of purified QscR, a *Pseudomonas aeruginosa* orphan quorum-sensing transcription factor. Mol. Microbiol. 59:602-9.

37. Lequette, Y., J.H. Lee, F. Ledgham, A. Lazdunski, and E. P. Greenberg. 2006. A distinct QscR regulon in the *Pseudomonas aeruginosa* quorum-sensing circuit. J. Bacteriol. 188:3365-70.

38. Lewandowski, Z., and P. Stoodley. 1995. Flow induced vibrations, drag force, and pressure drop in conduits covered with biofilm. Water Sci. Technol. 32:19-26.

39. Marx, C. J., and M. E. Lidstrom. 2002. Broad-host-range cre-lox system for antibiotic marker recycling in gram-negative bacteria. Biotechniques 33:1062-7.

40. Miller, J. H. 1972. Experiments in molecular genetics. Cold Spring Harbor Laboratory, Cold Spring Harbor, N.Y.

41. Nagai, T., K. Ibata, E. S. Park, M. Kubota, K. Mikoshiba, and A. Miyawaki. 2002. A variant of yellow fluorescent protein with fast and efficient maturation for cell-biological applications. Nat. Biotechnol. 20:87-90.

42. Purevdorj-Gage, B., W.J. Costerton, and P. Stoodley. 2005. Phenotypic differentiation and seeding dispersal in non-mucoid and mucoid *Pseudomonas aeruginosa* biofilms. Microbiology 151:1569-76.

43. Purevdorj, B., and P. S. J.W. Costerton. 2002. Influence of hydrodynamics and cell signaling on the structure and behavior of *Pseudomonas aeruginosa* biofilms. Appl. Environ. Microbiol. 68:4457-64.

44. Ramsey, M. M., and M. Whiteley. 2004. *Pseudomonas aeruginosa* attachment and biofilm development in dynamic environments. Mol. Microbiol. 53:1075-1087.

45. Reimmann, C., M. Beyeler, A. Latifi, H. Winteler, M. Foglino, A. Lazdunski, and D. Haas. 1997. The global activator GacA of *Pseudomonas aeruginosa* PAO1 positively controls the production of the autoinducer N-butyryl-homoserine lactone and the formation of the virulence factors pyocyanin, cyanide, and lipase. Mol. Microbiol. 24:309-19.

46. Sauer, K., A.K. Camper, G.D. Ehrlich, J.W. Costerton, and D. G. Davies. 2002. *Pseudomonas aeruginosa* displays multiple phenotypes during development as a biofilm. J. Bacteriol. 184:1140-1154.

47. Sauer, K., M.C. Cullen, A.H. Rickard, L.A. Zeef, D.G. Davies, and P. Gilbert. 2004. Characterization of nutrient-induced dispersion in *Pseudomonas aeruginosa* PAO1 biofilm. J. Bacteriol.

186:7312-26.

48. Schuster, M., C.P. Lostroh, T. Ogi, and E. P. Greenberg. 2003. Identification, timing, and signal specificity of *Pseudomonas aeruginosa* quorum-controlled genes: a transcriptome analysis. J. Bacteriol. 185:2066-2079.

49. Seed, P. C., L. Passador, and B. H. Iglewski. 1995. Activation of the *Pseudomonas aeruginosa* lasI gene by lasR and the Pseudomonas autoinducer PAI - an autoinduction regulatory hierarchy. J. Bacteriol. 177:654-659.

50. Sio, C. F., L.G. Otten, R.H. Cool, S.P. Diggle, P.G. Braun, R. Bos, M. Daykin, M. Cmara, P. Williams, and W. J. Quax. 2006. Quorum quenching by an N-acyl-homoserine lactone acylase from *Pseudomonas aeruginosa* PAO1. Infect. Immun. 74:1673-82.

51. Smith, R. S., and B. H. Iglewski. 2003. *P. aeruginosa* quorum-sensing systems and virulence. Curr. Opin. Microbiol. 6:56-60.

52. Stewart, P. S. 1993. A model of biofilm detachment. Biotechnol. Bioeng. 41:111-117.

53. Stoodley, P., K. Sauer, D.G. Davies, and J. W. Costerton. 2002. Biofilms as complex differentiated communities. Annu. Rev. Microbiol. 56:187-209.

54. Stoodley, P., Z. Lewandowski, J.D. Boyle, and H. M. Lappin-Scott. 1999. Structural deformation of bacterial biofilms caused by short-term fluctuations in fluid shear: an in situ investigation of biofilm rheology. Biotechnol. Bioeng. 65:83-92.

55. Teal, T. K., D.P. Lies, B.J. Wold, and D. K. Newman. 2006. Spatiometabolic stratification of Shewanella oneidensis biofilms. Appl. Environ. Microbiol. 72:7324-30.

56. Venturi, V. 2006. Regulation of quorum sensing in Pseudomonas. FEMS Microbiol. Rev. 30:274-91.

57. Wade, D. S., M.W. Calfee, E.R. Rocha, E.A. Ling, E. Engstrom, J.P. Coleman, and E. C. Pesci. 2005. Regulation of Pseudomonas quinolone signal synthesis in Pseudomonas aeruginosa. J. Bacteriol. 187:4372-80.

58. Wagner, V. E., D. Bushnell, L. Passador, A.I. Brooks, and B. H. Iglewski. 2003. Microarray analysis of *Pseudomonas aeruginosa* quorum-sensing regulons: Effects of growth phase and environment. J. Bacteriol. 185:2080-2095.

59. Waite, R. D., A. Papakonstantinopoulou, E. Littler, and M. A. Curtis. 2005. Transcriptome analysis of *Pseudomonas aeruginosa* growth: comparison of gene expression in planktonic cultures and developing and mature biofilms. J. Bacteriol. 187:6571-6.

60. Webb, J. S., L.S. Thompson, S. James, T. Charlton, T. Tolker-Nielsen, B. Koch, M. Givskov,

and S. Kjelleberg. 2003. Cell death in *Pseudomonas aeruginosa* biofilm development. J. Bacteriol. 185:4585-92.

61. Whitehead, N. A., A.M. Barnard, H. Slater, N.J. Simpson, and G. P. Salmond. 2001. Quorum-sensing in gram-negative bacteria. FEMS Microbiol. Rev. 25:365-404.

62. Whiteley, M., and E. P. Greenberg. 2001. Promoter specificity elements in *Pseudomonas aeruginosa* quorum- sensing-controlled genes. J. Bacteriol. 183:5529-5534.

63. Whiteley, M., K. M. Lee, and E. P. Greenberg. 1999. Identification of genes controlled by quorum sensing in Pseudomonas aeruginosa. Proc. Natl. Acad. Sci. USA 96:13904-13909.

64. Xiao, G., J. He, and L. G. Rahme. 2006. Mutation analysis of the *Pseudomonas aeruginosa* mvfR and pqsABCDE gene promoters demonstrates complex quorum-sensing circuitry. Microbiology 152:1679-86.

65. Yarwood, J. M., E.M. Volper, and E. P. Greenberg. 2005. Delays in *Pseudomonas aeruginosa* quorum-controlled gene expression are conditional. Proc. Natl. Acad. Sci. USA 102:9008-13.

5.8 Supplementary Methods

5.8.1 β-gal assays and promoter probing

The plasmid PQF50 containing a promoterless lacZ was used for reporter fusion experiments (18). Putative promoter fragment C, a total of 769 bp covering regions from 131 base pairs from the start of PA1033 and 638 base pairs upstream of PA1033, was made by amplifying the region from PAO1 genomic DNA with primers PQF50C_F and R, digested with HindIII and BamHI restriction enzymes and ligated into PQF50. Fragment B, which was 719 base pairs with 35 basepairs after the start of PA1032 and 684 base pairs upstream of PA1032, was amplified with primers PQF50B_F and R, digested with HindIII and BamHI restriction digests and ligated into the PQF50 plasmid. Fragment C was positive for activity and fragments G and R, which were smaller regions within C, were amplified and cloned into PQF50 to narrow down the section with promoter activity (primers provided in Supplemental Table 5.3). Fragment D, a region of DNA known not to have promoter activity, was cloned into PQF50 as a control. Constructs were confirmed by PCR and DNA sequencing. Putative promoter constructs were purified from *E. coli* and PQF50 plasmids transformed into PAO1 and PAO1$_{lagless}$ strains via electroporation. Beta galactosidase assays (40) were performed on cultures grown at 37°C in a shaker at 250rpm with minimal medium with 5 mM succinate, 1 mM C10HSL (Sigma) or 5mM succinate with 5, 10 or 20μM C4HSL, 3OC12HSL, or both signals.

5.8.2 Method for knock out mutants

Knock out mutants in the genes: PA1431 (*rsaL*), PA2591 (*vqsR*), PA1003 (*mvfR*), PA1430 (*lasR*), PA1898 (*qscR*), and a *lasR* and*qscR* double mutant were made in the background of wild type PAO1 and in PAO1$_{lagless}$ by homologous recombination. One kb flanking regions of the genes were amplified from PAO1 genomic DNA using primers listed in Supplemental Table 5.3 and cloned into the multi-cloning sites of the plasmid pCM351 (39). Three basepairs from the start codon and three basepairs from the stop codon remained in the PA1431, PA1003, PA1898 and PA1430 (*lasR*) mutants and six basepairs from the start and three basepairs from the stop codon remained of the gene in the PA2591 knock out mutant. The Gm resistance gene was removed from the lasR mutant using a cre-lox system (39). The plasmid pCM157 (39) was transformed into the lasR mutant strain and colonies that were gentamycin sensitive, which indicated successful cre-mediated excision of the gm resistance gene, were picked. The pCM157 plasmid was lost after two rounds of growth in LB without antibiotic selection. The *qscR* double mutant was made by transforming the lasR mutant

Table 5.3: Plasmids and primers for knock out mutations and promoter probing experiments

Plasmids	Characteristics	Source
pQF50	contains promoterless lacZ for promoter probing, AmpR	(18)
pCM351	GmR, AmprR TetR , allelic exchange plasmid	(39)
pCM157	AmpR, cre enzyme -containing plasmid	(39)

Primers used for knock out mutations:
QscR_MCS1_KpnI_F: AAAGGTACCACGAAGTAGGCGGCGAA
QscR_MCS1_NdeI_R: AAAAAAACATATGATGCATGCCAGCTTCACCAGT
QscR_MCS2_AgeI_F: AAAACCGGTAACTGAATCGACGCCTC
QscR_MCS2_SacI_R: AAAGAGCTCTATCTCCTCTTGAATTGGAATAGACATT
LasR_MCS1_KpnI_F: AAAGGTACCAGATCCTCTGGATCAACATGG TC
LasR_MCS1_NdeI_R: AAAAAAACATATGGCCATAGCGCTACGTTCTTCTTA
LasR_MCS2_AgeI_F: AAAACCGGTCTCTGATCTTGCCTCTCAGGTCG
LasR_MCS2_SacI_R: AAAGAGCTCCGACAGGTCCCCGTCATGAAAC
PA1431_MCS1_Kpn_F: AAAGGTACCCGAAGCGGTCTATCGCA
PA1431_MCS1_Nde_R: AAAAAACATATGAGCCATTGCTCTGATCTTTTCGGA
PA1431_MCS2_SacII_F: AAAAAACCGCGGGAGTAATAAGACCCAAATTAA
PA1431_MCS2_SacI_R: AAAGAGCTCTGCTTACCCTCTAGGA
PA2591_MCS1_KpnI_F: AAAGGTACCGCATCCTTGAGCAGC
PA2591_MCS1_NdeI_R: AAAAAAACATATGGATATCCACACAACTACTCC
PA2591_MCS2_AgeI_F: AAAACCGGTCGCTAGTGCGCCGC
PA2591_MCS2_SacI_R: AAAGAGCTCAAGCCGTCGCCGTCGCC
PA1003_MCS1_KpnI_F: AAAGGTACCAGTAGTAATGCGCCACCA
PA1003_MCS1_NdeI_R: AAAAAAACATATGCAGGTTATGAATAGGCATCCC
PA1003_MCS2_AgeI_F: AAAACCGGTGAGTAGAGCGTTCTCCAGCAGA
PA1003_MCS2_SacI_R: AAAGAGCTCGGTACGCGGCAGGTGCG

Primers used for promoter probing experiments:
PQF50C_F: AAAAAAGGATCCGTGCAACTGAACGACATCCA
PQF50C_R: AAAAAAAAGCTTAGGAAATCCGCCTGGAACT
PQF50B_F: AAAAAAGGATCCCATCCATCCGATCAACATCA
PQF50B_R: AAAAAAAAGCTTGGGGAAGAAAACGCATGAAG
PQF50D_F: AAAAAAGGATCCAACGAAGAGTTCTTCGCTCTG
PQF50D_R: AAAAAAAAGCTTAGGCGCGAATAGATGTCGTA
PQF50R_F: AAAAAAGGATCCCTTTTCGTTGGCGCG
PQF50R_R: AAAAAAAAGCTTGATCATCGGTGCGTCT
PQF50G_F: AAAAAAGGATCCTACACGGCCCGAACTGCAA
PQF50G_R: AAAAAAAAGCTTCGCGCCAACGAAAAG

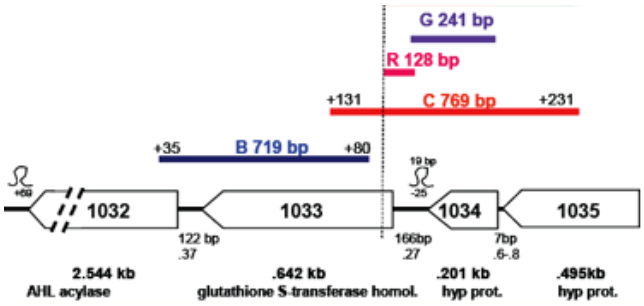

Figure 5.6: Map of putative promoter sequences for PA1032 used in promoter probe experiments.

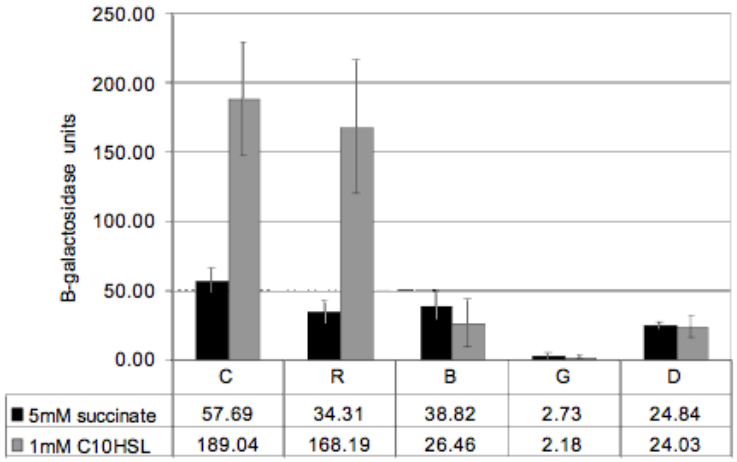

	C	R	B	G	D
5mM succinate	57.69	34.31	38.82	2.73	24.84
1mM C10HSL	189.04	168.19	26.46	2.18	24.03

Figure 5.7: Promoter probing experiment with PAO1$_{lagless}$. The PAO1$_{lagless}$ strain expressing either of several PQF50 plasmids that contained different regions of DNA sequence upstream of the PA1032 gene: regions B,C,D,G, or R (Supplemental Figure 5.8.2) cloned in front of a promoterless *lacZ* within the plasmid, were assayed for β-galactosidase activity during growth in succinate or 1mM C10HSL. Assays were performed at least in triplicate with averages shown under the bars.

strain with the plasmid pCM351_qscR and double recombinants were selected for by resistance to gentamycin and sensitivity to tetracycline.

Strains	Parent strain	Δ 1032::YFP	Δ 1032::YFP, attTn7::miniTn7T-Gm-PA1033-32 (single copy)	Δ *mvfR*::Gm	Δ *rsaL*::Gm	Δ *vqsR*::Gm	Δ *lasR*::Gm	Δ *qscR*::Gm	Δ *lasR* Δ *qscR*::Gm
$PAO1_{WT}$	+, 3 weeks	-	+, 3 weeks	+, several weeks, not blue	+, several weeks	+, several weeks	+, no lag not blue	+, several weeks	+, several weeks
$PAO1_{lagless1}$	+, no lag	-	+, 4 days	+, no lag, not blue	+, no lag	+, no lag	+, no lag not blue	+, no lag	+, no lag
$PAO1_{lagless2}$	+, no lag	-	+, 6 days	+, no lag, not blue	+, no lag	+, no lag	+, no lag, not blue	+, no lag	ND

Figure 5.8: Long chain AHL signal degradation and other phenotypes of $PAO1_{lagless}$ and $PAO1_{wt}$ mutants. The parent strains and mutants were tested for the AHL degradation and growth phenotype by providing cells with 1mM C10HSL as a sole carbon source in pH 5.5 minimal medium. Degradation of and growth on long chain AHL is indicated by a + followed by the amount of time before growth was observed; no growth is indicated by -; ND is not determined. Other phenotypes are noted. Blue coloring indicates the presence of pyocyanin.

Chapter 6

Diverse species of bacteria use SoxR to respond to endogenous redox-active compounds

6.1 Abstract

Under conditions of low-nutrients and high cell-density bacteria endogenously produce redox-active small molecules that act as antibiotics in other organisms. However it is not known how these small molecules are affecting the producing organisms or what role they might be playing in bacterial survival. A system that has previously been characterized in enteric bacteria as responding to superoxide radicals, the SoxR system, has been found to instead respond to redox active small molecules in *Pseudomonas aeruginosa*. To determine the ubiquity of this response mechanism and the types of genes regulated by SoxR in all organisms, we conducted bioinformatic analyses to discover all the genes regulated by SoxR. We confirm these predictions in a Gram-positive bacterium *Streptomyces coelicolor* and conclude that the majority of bacteria have a SoxR response mechanism more similar to that of *P. aeruginosa*. In these systems genes regulated by SoxR are transporters and oxidoreductases. These findings suggest that redox-active small molecules regulate systems in the bacteria that produce them and that they may have roles that are important in bacterial metabolism and maintenance.

6.2 Introduction

Bacteria are subjected to constant and sometimes rapid changes in environmental conditions and exposure to exogenous and endogenous compounds [31]. Bacteria in biofilms are able to survive

and thrive in these environments, but it is not known how they persist in communities that are inherently nutrient limiting. Under these biofilm conditions of high cell-density and low nutrients, bacteria are known to produce a variety of small molecules [21]. Some of these small molecules have been shown to be involved in activating community wide responses, such as in quorum sensing [4]. Others are known to be antibiotics and are thought to have primarily virulence effects. Yet many of these endogenously produced small molecules may play multiple roles in bacterial survival, and the purpose of others has remained largely unexplored. Antibiotics are of particular interest, because while they are virulent for other organisms, they are not toxic to the organisms that produce them and as redox-active molecules they may be involved in metabolism or maintenance in regions of the biofilm that are limited for an electron acceptor. However, it is not known how ubiquitous these endogenously produced redox-active compounds are or the types of systems that may be affected by them.

The biofilm forming organism, *Pseudomonas aeruginosa* produces the antibiotic compounds phenazines. One of these phenazines, pyocyanin, has been shown to affect the SoxR system normally associated with *E. coli* and *Salmonella enterica*'s response to the harmful radical superoxide [34]. The SoxR protein contains a redox-active [2Fe-2S] center [56] the oxidation state of which affects the conformation of the protein and allows the bacteria to sense the presence of oxidative agents such as superoxide radicals. In its reduced state SoxR binds DNA as a dimer [23], but when the [2Fe-2S] clusters of SoxR are oxidized, the dimer undergoes a conformational change allowing transcription of adjacent genes involved in the response pathway [58, 54, 57, 42]. Both SoxR itself and its binding site, a palindromic DNA sequence known as the soxbox [55, 96] are conserved across diverse species of bacteria [69, 93, 94].

The response of SoxR to exogenous factors has been well studied in the enteric bacteria *E. coli* and *Salmonella enterica* as model organisms [97, 96, 124, 152, 119]. In these organisms *soxR* is found next to the transcription factor *soxS* [57, 147, 97]. The regulatory region, the soxbox, lies in the intergenic region between the two genes that are transcribed in opposite directions. In *E. coli* and *S. enterica*, *soxR* is activated by oxidative stress imposed by external redox-cycling compounds such as paraquat, and induces transcription of its only known target *soxS* [136]. SoxS then activates a host of genes involved in dealing with oxidative stress (Figure 6.1) [152]. Mutants defective in SoxR are not able to respond to superoxide radicals and their viability is significantly compromised. Because the system has been so well-characterized in *E. coli* and *S. enterica*, the idea that SoxR regulates a response to oxidative stress is the prevailing view.

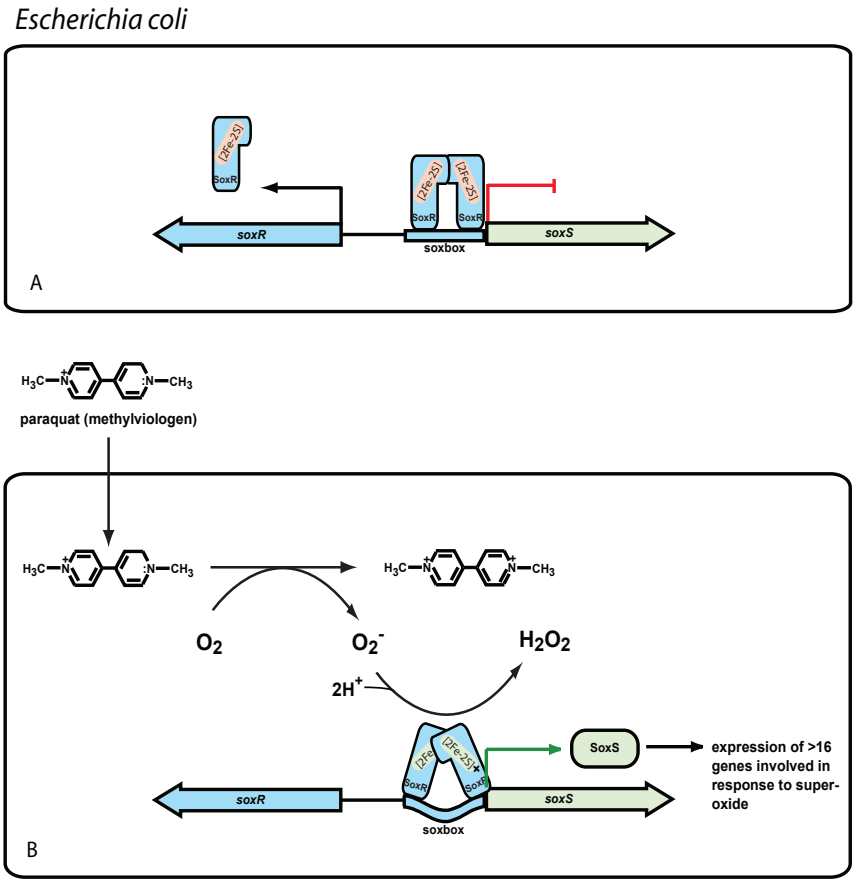

Figure 6.1: (a) In *E. coli* SoxR binds as a dimer to the soxbox when no superoxides are present, allowing for transcription of *soxR* but blocking transcription of *soxS*. (b) When activated by superoxides, the conformation of the SoxR dimer is changed enhancing transcription of the transcription factor *soxS*. SoxS activates more than 16 genes involved in the response of *E. coli* to oxidative stress.

However, in *P. aeruginosa*, *soxR* is upregulated in the presence of phenazines and instead of affecting genes involved in superoxide stress, it regulates two efflux pumps, PA4205-PA4208, or MexGHI-opmD, and PA3718 and one putative monooxygenase, PA2274 [34, 69, 93]. Its genome does not contain *soxS* and conditions of superoxide stress do not affect the viability of a SoxR mutant. Similarly, in the Demple lab, where much of the work on *E. coli* SoxR response and regulation has been done, they find that in *Pseudomonas putida* KT2440 the viability of *P. putida* SoxR mutants is not affected by oxidative stress conditions and that there is no homolog to SoxS [94].

These recent results suggest that endogenously produced small molecules may be ubiquitous and regulate a variety of systems. In particular, it appears that the *E. coli* SoxRS paradigm does not hold for microorganisms outside of the family of enterics and may instead act as a response regulator under conditions of low-nutrients and high cell-density, such as in biofilms. To gain insight into the functionality of SoxR across all types of bacterial species, we conducted bioinformatic analyses to determine the binding sites of SoxR and the genes that are potentially regulated by SoxR. Our binding site predictions matched with published data in *P. aeruginosa*, *P. putida*, *E. coli*, and *S. enterica* [34, 69, 93, 94], and we demonstrate that that the majority of genes regulated by SoxR do not match with the *E. coli* paradigm, but are similar to those found in *P. aeruginosa*. SoxS is not found outside of the enterics, and instead genes regulated by SoxR are transporters and oxidoreductases. Experiments with *Streptomyces coelicolor* confirm our binding site predictions and show that these genes are activated in the presence of the endogenously produced antibiotic, actinorhodin, suggesting that the more pervasive use of SoxR in the bacterial domain may be as a response regulator to endogenous redox-active compounds.

6.3 Materials and Methods

6.3.1 Finding Bacterial Genomes with SoxR

Bacterial genomes containg SoxR were found using `BLAST`. The *E. coli* K12 SoxR protein was blasted against the microbial genomes database. Proteins that did not encode a putative DNA binding domain (N-terminal) or Mer-type sensor domain (C-terminal) or were longer than the SoxR protein were removed. SoxR binds a [2Fe-2S] cluster that can be oxidized and allows cells to sense the presence of oxidative agents. The ligands responsible for binding the [2Fe-2S] cluster are encoded by four cysteine residues at the C-terminus end of the protein and are represented in the amino acid sequence GCIGCGCLSLRECP [15, 97]. These four cysteines specifically identify SoxR within the

Mer family. Therefore, the sequences were checked to determine if they had four cysteines in the C-terminal domain. Alignment of the SoxR proteins was made using ClustalW and displayed using CLC Protein Workbench 2.

6.3.2 Genomes

Bacterial genomes and protein table files were obtained for all completed genomes through April 29, 2007 - `ftp://ftp.ncbi.nlm.nih.gov/genomes/Bacteria/all.fna.tar.gz` and `ftp://ftp.ncbi.nlm.nih.gov/genomes/Bacteria/all.ptt.tar.gz` respectively. The genome for *Pseudomonas aeriginosa* PA01 was obtained from `http://www.pseudomonas.com/`, the updated *Pseudomonas aeruginosa* PA14 DNA Sequence (2005-Sept-27). Genomes searched were those containing SoxR. A list of these genomes is available at: `http://idyll.org/~tracyt/sox/list-genomes.txt`

6.3.3 Soxbox Matrix Construction

SoxR binds to a near-palindromic sequence known as the soxbox. Three 26bp soxbox sites from Kobayashi and Tagawa, 2004 [69] and three sites known to be regulated by SoxR in *Pseudomonas aeriginosa* PA01 were used as the initial sequences for creating a matrix: *E. coli* (from Kobayashi and Tagawa 2004) TTTACCTCAAGTTAACTTGAGGAATT, *Xanthomonas axonopodis* (from Kobayashi and Tagawa 2004) TTGACCTCAACTTAGGTTGAGGCAGG, *Chromobacterium axonopodis* (from Kobayashi and Tagawa 2004) TTGACTTCAAGTTAACTTGAACTTTG, *P. aeriginosa* upstream of PA2274 (from Pseudomonas.com) TTGACCTCAAGTTTGCTTGAGGTTTT, *P. aeriginosa* upstream of PA4205 (from Pseudomonas.com) TTGACCTCAACTTAACTTGAGGTTTT, and *P. aeriginosa* upstream of PA3718 (from Pseudomonas.com)TTTACCTCAAGTTAACTTGAGCTATC.

An energy matrix for this binding site was created as in Brown and Callan, 2003 [17], from which the total binding energy E could be calculated.

$$E = \sum_{i=1}^{L} \sigma_{b(i),j}$$

To calculate the position energy, $\sigma_{b(i),j}$ for each position, i, in a site, the number of occurrences $N_i(b)$ of each DNA base b in the list of sites is counted. Each matrix element is calculated using

$$\sigma_{bi} = \ln \frac{max_a N_i(a) + 1}{N_i(b) + 1}$$

The +1 in the calculation is used so that no divide by zero error is encountered in the case that there are zero bases at a particular position. The matrix is then normalized to assign zero to the most common base at a position, such that for the consensus sequence, $E = 0$ and all others have $E > 0$ [8, 9].

As an example:

Given a site Z with bases of C, C, C, T, C, and C.

$$A = \ln \frac{6+1}{0+1} = 1.946$$

$$G = \ln \frac{6+1}{0+1} = 1.946$$

$$C = \ln \frac{6+1}{5+1} = 0.154$$

$$T = \ln \frac{6+1}{1+1} = 1.253$$

Normalizing to zero, 0.154 is the lowest energy value, so this value is used for normalization and 0.154 is subtracted from each base pair, such that $A = 1.792$, $G = 1.792$, $C = 0$, and $T = 1.099$.

The program `openfill.py` [17] implements this algorithm and was used to create the matrix, `soxbox-sequences-long_PWM.open`, from the initial set of soxbox binding sites. `openfill.py` takes as input the list of known sites and generates an energy matrix as output.

6.3.4 Genomic Distribution of Sites.

A modified version of the program `pyscangen.py` [17] was used to find the energy distribution of all sites in all genomes containing SoxR. This program takes as input a genome, its protein table (the NCBI `ptt` file containing information on the bounding coordinates and the names of all coding regions, or open reading frames, in that genome), the energy matrix, the initial list of known sites

and a binding energy threshold value. `pyscangen.py` determines the number of sites that occur in genes and the number of sites that occur in intergenic regions. These statistics are of interest, because functional binding sites should be enriched in intergenic regions.

6.3.5 Binding-site Search.

A modified version of the program `pyscangenes.py` [17] was used to find the binding sites for SoxR and the genes up and downstream of the predicted binding sites in each genome containing SoxR. The program takes as input the energy matrix, a genome and a cutoff value. The output is a list of binding sites below the cutoff E value with their energy value and the predicted genes up and downstream of the binding site.

6.3.6 Determination of Background.

A background model was used to determine how many binding sites from a particular energy matrix would be predicted to occur at random in a given genome. Using the program, `background-intergenic.py`, the GC and AT content for the intergenic region of each genome was calculated. We used a theoretical genome model to calculate the number of predicted sites expected in a genome of that size and GC composition with the given matrix at that threshold. The input for this program is the energy matrix, a genome and a cutoff value. The output is the number of sites that were predicted to occur at random in that genome below a given cutoff (Brown, 2005, unpublished, http://cartwheel.idyll.org/).

6.3.7 Energy Matrix Refinement.

The energy values of predicted soxbox binding sites across all genomes containing SoxR were determined using the initial energy matrix, `soxbox-sequences-long_PWM.open` with a cutoff of 12. Regions with high energy values (> 8.0), upstream of *soxR*, confirmed as described above, were taken and used to create a refined energy matrix, `soxbox-sequences-long+sub-soxRs_PWM.open`. This energy matrix was used for all results presented.

6.3.8 Software and File Availability

All software and files, including programs, genomes, sequence lists, PWMs and output files are available at: http://idyll.org/∼tracyt/soxbox/

6.3.9 SoxR Tree Creation.

We constructed a phylogenetic tree based on SoxR protein sequences from 99 bacteria using the desktop software CLC protein workbench 2. The sequences were aligned with the ClustalW algorithm (gap open penalty = 35; gap extension penalty = 0.75; Scoring matrix = GONNET). Using this alignment we created neighbor joining tree and performed a bootstrap analysis with 100 replicates.

6.3.10 Bacterial strains and growth conditions

Streptomyces coelicolor A2(3) strains M145 (SCP1-, SCP2-, Pgl+) and M512 (M145 ΔredD ΔactII-ORF4) [38] were kindly provided by Andrew Hesketh (John Innes Institute, Norwich, UK). Streptomyces were grown at 30°C on R5- agar plates (103g/l sucrose, 0.25g/l K_2SO_4, 10.12g/l $MgCl_2$.6H2O, 10g/l H_2O, 0.1g/l Difco Casaminoacids, 2ml Trace element solutuion, 5g/l Difco yeast extract, 5.73g/l TES buffer, 22g/l Difco Bacto agar; after autoclaving 7ml 1N NaOH were added).

6.3.11 RNA isolation and Q-RT-PCR experiments

S. coelicolor strains M145 and M512 were grown on R5- plates that were overlaid with cellophane membranes. After one day (prodiginine production) or three days (actinorhodin production) cells from three plates were resuspended in 1ml H_2O and 2ml RNAProtect (Qiagen). The mixture was incubated for 5 min at room temperature, then centrifuged for 10 min at 5000xg. The pellet was frozen in liquid nitrogen, homogenized with mortar and pestle and total RNA was isolated and purified using the RNeasy Plant Kit (Qiagen), including the optional DNase treatment step. cDNA was generated in a random-primed reverse transcriptase reaction (iScript, BioRad) and subsequently used as template for quantitative PCR (Real Time 7300 PCR Machine, Applied Biosystems) using the Sybr Green detection system (Applied Biosystems). The signal was standardized to SCO4548 using the following equation: Relative expression = 2 ($CT_standard$ CT_sample),where CT (cycle time) was determined automatically by the Real Time 7300 PCR software (Applied Biosystems). Primers (Integrated DNA Technologies) for Q-RT-PCR were designed using Primer3 software [109]. Criteria for primer design were a melting temperature of 60°C, primer length of 20 nucleotides, and an amplified PCR fragment of 100 base pairs.

6.4 Results

6.4.1 Genomes containing SoxR.

99 SoxR proteins were found and a subset were aligned as described in *Methods*. Of the 99 SoxR's found, 56 were in genomes that are completed, meaning assembled and annotated, as determined by NCBI. We used these completed genomes for further analysis. A list of all genomes containing SoxR and those used in further analysis can be found at `http://web.mac.com/laahs/iWeb/Site/Organisms%20with%20SoxR.html`.

6.4.2 Matrix Construction.

SoxR has been shown to bind to a soxbox promoter region [55, 96]. To search for other soxbox binding sites across genomes, a representation of a consensus sequence is necessary. A standard representation of these sites is an energy matrix or Position Weight Matrix (PWM) that can be used to find other sites that match this consensus sites with varying degrees of orthology, represented as energy [9].

Employing this technique, we used six confirmed sites in *P. aeruginosa*, *E. coli*, *Xanthomonas axonopodis* and *Chromobacterium axonopodis* to create a PWM as described in *Methods*. We then used this PWM to search through all genomes containing SoxR and found all the predicted soxbox sites adjacent to *soxR* genes. Binding site energies for these sites ranged from 0.8 to 9.58. In order to capture the diversity of these sites, we added four sites with energies between 7.0 and 9.58 to our initial set of sequences and used this set of sites to create a refined PWM and consensus sequence, Figure 6.2. Using this new PWM, energies of soxbox sites adjacent to *soxR* ranged from 1.1 to 7.79. The refined PWM also found the known sites in *P. aeruginosa*, PA2273 and PA2274, PA3718, and PA4205 [34, 93].

6.4.3 Determination of Threshold

To determine the validity of this PWM for different thresholds, or energies, we looked at the distribution of found sites within a genome and compared the PWM to background models as well as closely related family members.

Using the refined PWM, we looked at the number of sites that are found and the distribution of these sites in intergenic regions versus within genes for different threshold values. Since SoxR is a transcription factor, we would expect real sites to occur primarily in intergenic regions leading to

(a)

Pseduomonas aeriginosa PAO1 PA2274 (from Pseudomonas.com)	TTGACCTCAAGTTTGCTTGAGGTTTT
Pseduomonas aeriginosa PAO1 PA4205 (from Pseudomonas.com)	TTGACCTCAACTTAACTTGAGGTTTT
Pseduomonas aeriginosa PAO1 PA3718 (from Pseudomonas.com)	TTTACCTCAAGTTAACTTGAGCTATC
Escherichi coli from Kobayashi_Tagawa2004)	TTTACCTCAAGTTAACTTGAGGAATT
Xanthomonas axonopodis from Kobayashi_Tagawa2004	TTGACCTCAACTTAGGTTGAGGCAGG
Chromobacterium axonopodis from Kobayashi_Tagawa2004	TTGACTTCAAGTTAACTTGAACTTTG
Hyphomonas neptunium ATCC 15444 found in initial run	TTGATCTAAAGTGAACTTGAGATTGT
Mycobacterium smegmatis str. MC2 155 found in initial run	TTCACCTGAAGTAAGGTTTAGGTGTC
*Saccharopolyspora erythrae*a NRRL 2338 found in initial run	TTGACCTCCAGCCAACTCGAAGTTTC
Silicibacter pomeroyi DSS-3 found in initial run	TTGACCTAAAGTTAGGTTTAGAAATT

(b)

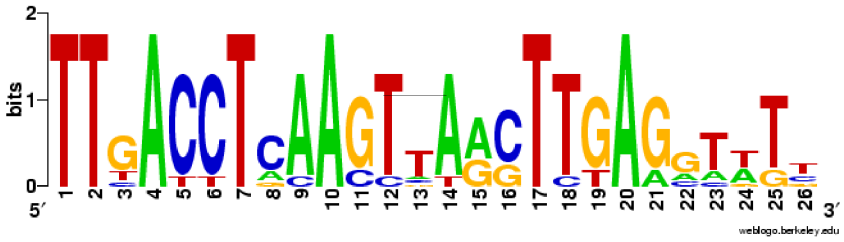

Figure 6.2: (a) Sequences used to create the position weight matrix (PWM) used in this study. Black bars indicate the palindromic region of the soxbox site. (b) Weblogo representation of the consensus sequence built from the sequences in (a). Larger letters are letters more highly represented at a particular position.

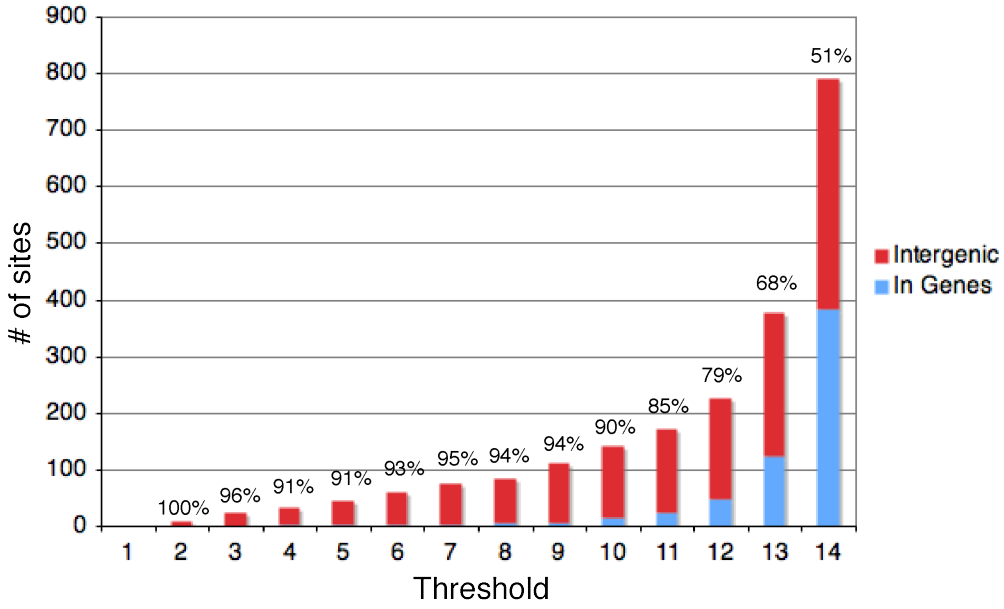

Figure 6.3: Number of sites found in genes and intergenic regions across all genomes containing SoxR for a given threshold. % indicates percent of sites found in intergenic regions. True transcriptional sites are expected to be over-represented in intergenic regions. As the threshold increases, the number of sites found also increases. However, the number of sites found in genes, and therefore likely false positives, also increases, indicating that higher thresholds, 11 and above, may be too lenient.

strong selection for sites in intergenic regions. The distribution of sites for various energy thresholds is presented in Figure 6.3. Complete results are in Appendix B.

Increasing the threshold increases the number of sites found, but the percentage of sites found in genes, and likely false positives, increases as well. At a threshold of 13.0 372 sites are found, but only 68% of them are intergenic, a significant drop off from 12.0 where 79% were intergenic.

To determine if we would expect sites to occur at random in intergenic regions for a given threshold, we ran the PWM against a background model of a random genome of a given GC-content. Results are presented in Table 6.1. The number of sites expected at random is very low for genomes across the range of GC-contents. At thresholds 10.0 and below with an average GC-content of 0.57, a maximum of only 0.011 sites would be expected to be found. While the number of sites found in each genome is low, usually one to four sites, these numbers are higher than the number of expected sites. Therefore the soxbox site, as described by our PWM, is not merely a site that would be expected to be found at random in intergenic regions.

When we looked for soxbox sites in genomes not containing SoxR, of the 402 completed genomes in the NCBI microbial resources database that are not predicted to have a SoxR, we found only 30 genomes that contained predicted soxbox binding sites with a threshold of less than 10. Of these,

	GC = 0.38		GC = 0.45		GC = 0.57	
cutoff	exp	found	exp	found	exp	found
1	1.04E-08	0.00 ± 0.0	8.26E-09	0.00 ± 0.0	1.36E-09	0.00 ± 0.0
2	1.32E-07	0.50 ± 0.5	1.05E-07	0.13 ± 0.4	1.81E-08	0.05 ± 0.2
3	1.25E-06	1.00 ± 0.9	9.66E-07	0.73 ± 0.5	1.70E-07	0.16 ± 0.4
4	8.73E-06	1.25 ± 1.3	6.63E-06	0.73 ± 0.5	1.19E-06	0.21 ± 0.4
5	5.20E-05	1.38 ± 1.2	3.87E-05	0.73 ± 0.5	7.14E-06	0.47 ± 0.7
6	2.75E-04	1.75 ± 1.5	2.02E-04	0.80 ± 0.6	3.85E-05	0.79 ± 0.7
7	0.001 ± 0.00	1.88 ± 1.4	9.00E-04	0.80 ± 0.6	1.79E-04	1.11 ± 0.7
8	0.005 ± 0.00	2.00 ± 1.6	0.004 ± 0.00	0.80 ± 0.6	7.72E-04	1.26 ± 0.7
9	0.019 ± 0.01	2.00 ± 1.6	0.014 ± 0.01	0.87 ± 0.6	0.003 ± 0.00	1.47 ± 1.0
10	0.067 ± 0.03	2.50 ± 1.9	0.049 ± 0.02	1.27 ± 1.0	0.011 ± 0.01	1.58 ± 1.1
11	0.219 ± 0.11	3.50 ± 2.2	0.162 ± 0.07	1.60 ± 0.8	0.038 ± 0.02	1.79 ± 1.1
12	0.669 ± 0.34	5.38 ± 2.9	0.498 ± 0.22	2.33 ± 1.4	0.124 ± 0.06	2.26 ± 1.7
13	1.900 ± 0.96	12.75 ± 8.7	1.428 ± 0.64	5.07 ± 1.8	0.372 ± 0.17	3.37 ± 2.2

	GC = 0.62		GC = 0.68	
cutoff	exp	found	exp	found
1	3.10E-10	0.00 ± 0.0	1.07E-10	0.00 ± 0.0
2	4.34E-09	0.08 ± 0.4	1.57E-09	0.00 ± 0.0
3	4.24E-08	0.12 ± 0.6	1.61E-08	0.00 ± 0.0
4	3.09E-07	0.31 ± 0.7	1.24E-07	0.00 ± 0.0
5	1.93E-06	0.46 ± 0.8	8.20E-07	0.13 ± 0.4
6	1.09E-05	0.58 ± 0.8	4.91E-06	0.50 ± 0.8
7	5.29E-05	0.77 ± 0.8	2.50E-05	0.88 ± 1.4
8	2.40E-04	0.88 ± 0.8	1.20E-04	1.38 ± 1.6
9	9.86E-04	1.50 ± 1.0	5.19E-04	2.13 ± 1.6
10	0.004 ± 0.00	2.08 ± 1.4	0.002 ± 0.00	2.50 ± 1.9
11	0.014 ± 0.01	2.35 ± 1.4	0.008 ± 0.00	3.25 ± 2.5
12	0.046 ± 0.02	2.62 ± 1.4	0.028 ± 0.01	4.63 ± 2.6
13	0.143 ± 0.07	3.46 ± 2.0	0.093 ± 0.03	5.63 ± 2.5

Table 6.1: Average expected versus found number of soxbox sites for different thresholds in genomes of differing GC content. Expected sites are the number of sites that would be expected to be found at random in a genome of a given GC content. GC content was grouped as follows. 30 - 39: 8 genomes, average GC content = 0.38; 40 - 49: 15 genomes, average GC content = 0.45; 50 - 59: 19 genomes, average GC content = 0.57; 60 - 64: 26 genomes, average GC content = 0.62; 65 - 70: 8 genomes, average GC content 0.68. For GC-content in all ranges, the number of sites expected to be found at random is very low for thresholds 12 and below, indicating that found soxbox sites are not just examples of random occurrences.

Promoter	Regulator	Sequence	Site Energy
Tn*501*/Tn*21 mer*	MerR	TTGACTCCGTACATGAGTACGGAAGT	27.18
Bacillus mer	MerR	TTTACCCTGTACTAAGGTACGTGGTT	26.77
Staphylococcus mer	MerR	TTGACCGTGTACTATGGTACAGGGTT	26.89
E. coli zntA	ZntR	TTGACTCTGGAGTCGACTCCAGAGTG	30.87
E. coli copA	CueR	TTGACCTTCCCCTTGCTGGAAGGTTT	16.22
E. coli cueO	CueR	TTGACCTTCCCGTAAGGGGAAGGACT	20.44
Snyechocystis coaT	CoaR	TTGACATTGACACTAATGTTAAGGTT	26.08
Ralstonia pbrA	PbrR	TTGACTCTATAGTAACTAGAGGGTGT	18.46
Pseudomonas cadA	CadR	TTGACCCTATAGTGGCTACAGGGTGT	21.69
S. lividans tipA	TipA_L	TTGCACCTCACGTCACGTGAGGAGGC	22.47
Bacillus bmr	BmrR	TTGACTCTCCCCTAGGAGGAGGTCTT	20.32
P. aeriginosa PAO1 PA2274	SoxR	TTGACCTCAAGTTTGCTTGAGGTTTT	1.94
P. aeriginosa PAO1 PA4205	SoxR	TTGACCTCAACTTAACTTGAGGTTTT	1.10
P. aeriginosa PAO1 PA3718	SoxR	TTTACCTCAAGTTAACTTGAGCTATC	2.42
E. coli soxS	SoxR	TTTACCTCAAGTTAACTTGAGGAATT	2.14
Xanthomonas axonopodis	SoxR	TTGACCTCAACTTAGGTTGAGGCAGG	5.49
Chromobacterium axonopodis	SoxR	TTGACTTCAAGTTAACTTGAACTTTG	4.25
Hyphomonas neptunium	SoxR	TTGATCTAAAGTGAACTTGAGATTGT	5.92
Mycobacterium smegmatis	SoxR	TTCACCTGAAGTAAGGTTTAGGTGTC	7.79
Saccharopolyspora erythraea	SoxR	TTGACCTCCAGCCAACTCGAAGTTTC	7.72
Silicibacter pomeroyi	SoxR	TTGACCTAAAGTTAGGTTTAGAAATT	5.12

Table 6.2: Site energy values of MerR-like promoter elements. The Mer-family is closely related to SoxR proteins, but the energy values for Mer-family binding sites is significantly higher than that of SoxR binding sites. The soxbox PWM is therefore specific to SoxR and can distinguish it from closely related family members.

only one genome had a site with energy value less than 5.0. This genome *Idiomarina loihiensis L2TR* has four predicted SoxRs, but the SoxRs do not contain the 4-cysteine residue required for us to identify the protein as a true SoxR. Nine species have sites with energies 5.0 - 9.0 and 23 with sites 9.0 - 10.0. Results for all sequences are available at

`http://idyll.org/~tracyt/sox/all_soxbox-sequences-12.html`

Finally to determine if soxbox sites could be discriminated from closely related family members, we checked the energy values of sites in the closely related MerR family [18]. As can be seen in Table 6.2 the energy values for MerR-family sites are significantly higher than for the initial soxR sites, demonstrating that this PWM is specific to SoxR regulated sites.

Analyzing the results of genomic distribution, background models and a comparison to closely related family members, a threshold of 10.0 minimizes excessive noise from likely false positives, but is not overly restrictive. Therefore a threshold of 10.0 will be used in our analyses of soxbox sites across genomes.

6.4.4 Soxbox sites across genomes

Using the refined PWM and a threshold of 10.0, we found soxbox sites across all genomes containing a SoxR. Complete results are available at `http://idyll.org/~tracyt/sox/soxbox-sequences-12.html` and in Appendix B. Our

site predictions match those in the literature for *P. aeruginosa*, *E. coli* species, *Salmonella* species [34, 69, 93, 97] and *Agrobacterium tumefaciens* [35]. In *Pseudomonas aeruginosa* however, we find one site that has not been found through experimental methods upstream of PA5115 and PA5116. This site is a weaker match than the other sites with an energy of 8.78 versus 1.10 to 2.42 for the other sites, but it is still a good match. It may be that this site is bound by another family member, even more closely related than other MerR-family proteins, or experimental conditions have not been such that this site has been affected. In *Pseudomonas putida*, Park et al predict that only the site adjacent to *soxR* has a soxbox, whereas we predict three binding sites [94]. To determine the location of putative binding sites, Park et al use the sequence motif CCTMAAGTTWRSTTGAGS, an eighteen base region of the binding site. We find that several of the specified sites, namely those at positions 4, 6, 14 and 15, while conserved in *E. coli* and *Salmonella*, are not conserved in species outside of the enterics, so that this site is likely an overspecification that does not allow all the sites in *P. putida* to be determined.

In Figure 6.4a it can be seen that the number of sites and the organization of the genes regulated by the soxbox is different in enterics than in non-enterics across significantly different genuses. In the enteric species only *soxR* and *soxS* are regulated by SoxR, as in *E. coli* and *Salmonella typhimurium* (Figure 6.4). In diverse non-enteric species, gram-negative *P. aeriginosa* and gram-positive *Streptomyces coelicolor*, multiple genes are regulated by SoxR, including genes involved in efflux and homeostasis (Figure 6.4b). Of genes regulated by SoxR across all genomes, only a small subset are the *soxS* that controls the superoxide stress response (Figure 6.5), suggesting that the purpose of SoxR in genomes outside of the enterics is different.

6.4.5 Pylogenetic tree of SoxR proteins

Using a neighbor-joining approach, we generated a tree of the SoxR proteins across these diverse taxa. As can be seen in Figure 6.6 the soxR proteins of the enterics are closely related with a bootstrap value of 100, while the SoxR proteins of other species are widely distributed and not grouped by genus. Bootstrap values for these connections are low as well, suggesting no strong grouping outside the enterics.

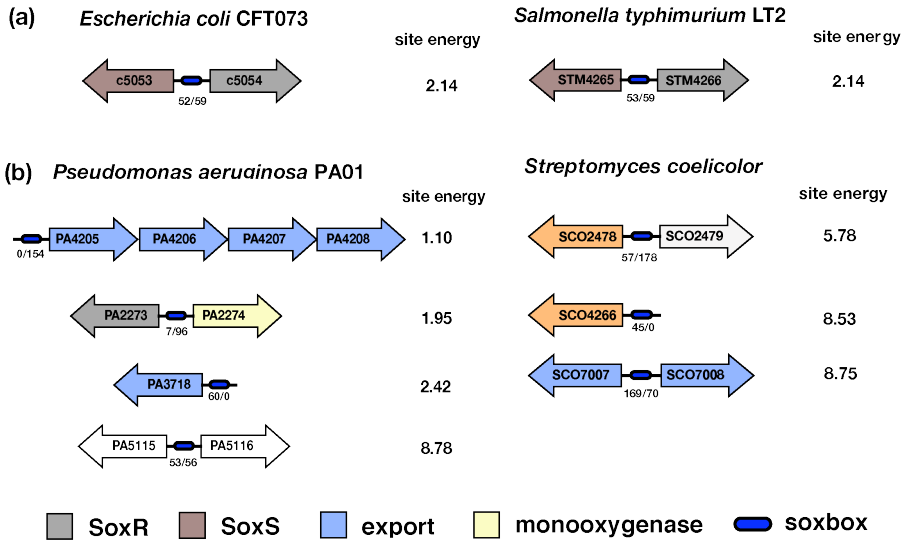

Figure 6.4: The arrangement of the regulated genes and site energy values for soxboxes in (a) enteric bacteria *E. coli* CFT073 and *Salmonella typhimurium* LT2 and (b) gram-negative *P. aeruginosa*PA01 and gram-positive *Streptomyces coelicolor*. In the enteric bacteria, only one soxbox is found and it regulates *soxR* and *soxS* in opposite directions. In bacteria outside the class of enterics, often multiple soxboxes are found, and genes regulated by the soxboxes are not confined to *soxR* and *soxS*.

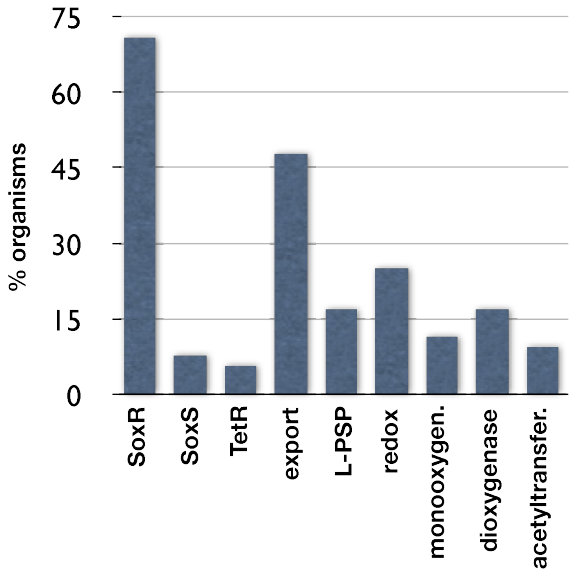

Figure 6.5: Distribution of the types of genes regulated by soxboxes. On the y-axis is the percentage of organisms that have a gene of that type located adjacent to a predicted soxbox. In organisms with soxbox binding sites, only a small percentage of those genomes have a *soxS* that is associated with the binding site. Most genes associated with soxboxes are transporters and oxidoreductases, and are not known to be a part of a superoxide stress response.

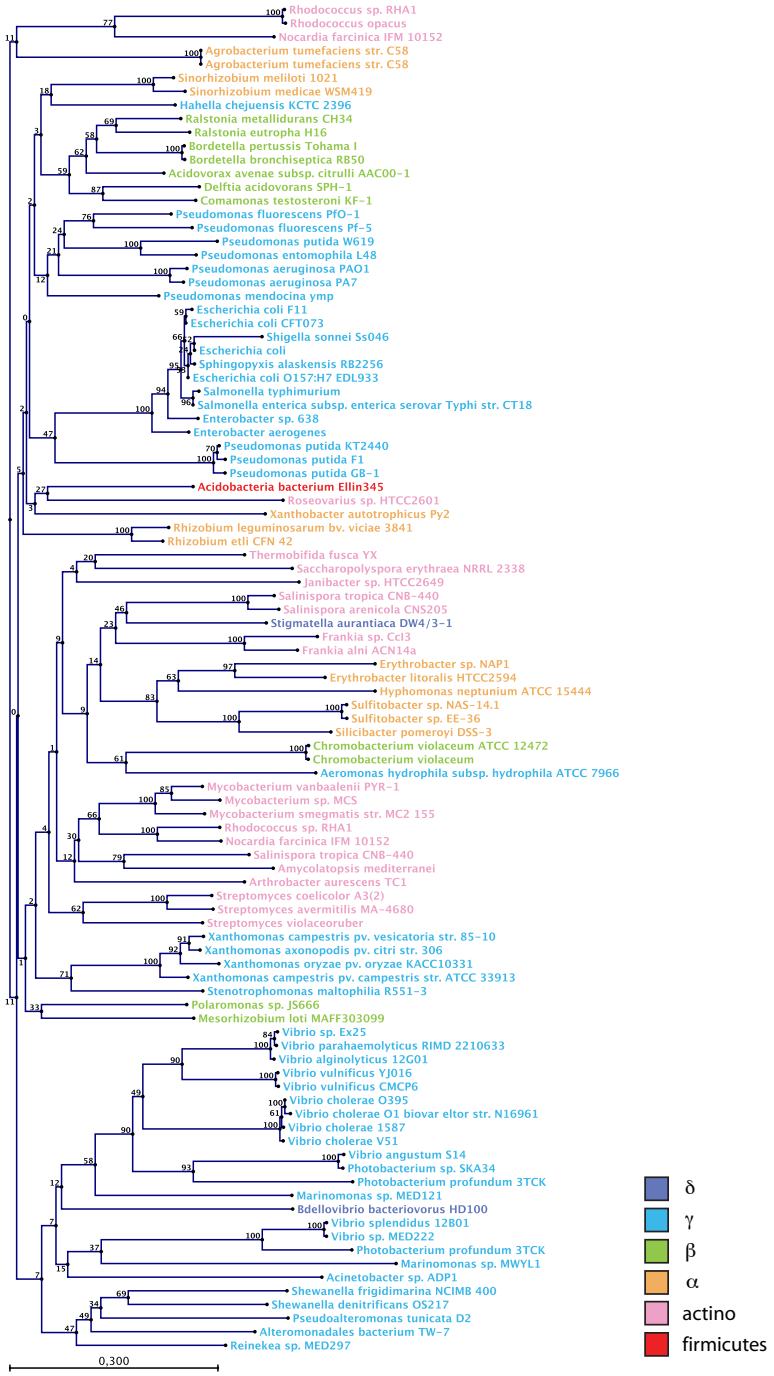

Figure 6.6: Phylogenetic tree of SoxR proteins created using a neighbor-joining algorithm. Enteric bacteria are highlighted in a red rectangle. The enteric SoxR proteins are closely related as indicated by the high bootstrap value, while there is no clear phylogeny among other SoxR proteins. The proteins of closely related species do not appear to be related and the bootstrap values among the relationships are weak.

6.4.6 Predicted *Streptomyces coelicolor* genes are regulated by actinorhodin

Three soxbox sites with thresholds less than 10 were found in *Streptomyces coelicolor* A3(2) potentially regulating genes SCO2478 and SCO2479, SCO4266, and SCO7007 and SCO7008 (Figure 6.4). We compared wild type to a δact mutant that does not produce actinorhodin, an antibiotic produced by *S. coelicolor* with a structure similar to that of phenazines produced by *P. aeruginosa*. In this experiment all five of these genes were affected in the wild type as compared to δact. SCO2478 was 18 times upregulated, SCO2479 was 1.7 times downregulated. SCO4266 was 53 times upregulated, and SCO7007 was 11 times upregulated, while the control gene SCO4548 [63] was not affected. This demonstrates that our predictions of soxbox regulatory sites is accurate and shows that a phenazine-like compound has similar effects on SoxR regulation as in *P. aeruginosa*.

6.5 Conclusion

In this study, we have shown that SoxR and the soxbox site it binds to are conserved across many diverse species. The types of genes adjacent to, and most likely regulated by SoxR, however are not constrained to SoxS-like proteins, as might be expected. Instead the types of genes regulated by SoxR appear to be redox enzymes as well as those involved in the processing of redox active compounds. These predictions match published data [34, 93, 94, 69] as well as our experiments in *Streptomyces coelicolor*.

It was initially hypothesized that SoxR might respond to antibiotics as well as oxidative stress [33, 45], and it is likely that in these organisms where SoxR does not seem to affect genes involved in oxidative stress, that the SoxR system is used to respond to the redox-active properties of compounds such as antibiotics or secondary metabolites. Many of these organisms are known to produce small molecules that can both aid in metabolism or community wide responses, as well as have detrimental effects on redox homeostasis. It seems reasonable that the bacteria must have a system in place to process the compounds that they produce and therefore remain in their local environment. Given the diversity and ubiquity of these small molecules, it is possible that this is an ancient bacterial strategy. Park et al state that "We cannot exclude the possibility that a completely new oxidative defense system may have evolved in *Pseudomonas* species, thus rendering the SoxR-dependent system obsolete and taking over the control of genes that were formerly SoxR regulated" [94]. We suggest that it might be the converse. The use of SoxR to respond to endogenous redox-active

compounds may have been the initial strategy.

It is not possible to root the SoxR phylogenetic tree, but the tight grouping of the enterics and the loose association of SoxR proteins throughout the rest of the tree suggest lateral gene transfer (Figure 6.6). One way of determining if a lateral gene transfer event occurred is to detect whether the GC content of the soxR gene is different than the GC content of the genome [19]. Here, the GC-content of the genes seems to match that of the genomes, suggesting an ancient event or no lateral gene transfer. However, it is interesting to note that SoxR is not conserved among all species of the same genus. For instance in *Shewanella*, several of the species, *Shewanella frigidimarina* and *Shewanella denitrificans* have SoxR proteins, while *Shewanella oneidensis* and *Shewanella* sp. ANA-3 do not. More work would be required to determine whether SoxR occurs in such diverse genomes due to lateral gene transfer, but it suggests a mechanism for the acquisition of a redox-sensing system that could be used in a diversity of pathways.

In *P. aeruginosa* SoxR responds to the endogenously produced phenazine pyocyanin. In *S. coelicolor*, actinorhodin, another endogenously produced antibiotic, affects the genes regulated by SoxR. *Agrobacterium tumefaciens* which also has multiple genes directly activated by SoxR, produces a diffusible acyl homoserine lactone [39, 151]. The widespread occurrence of SoxR as a potential regulator of genes thought to be involved in sensing endogenous compounds suggests that secondary metabolites or small molecules are important in many domains. Because these compounds are produced under conditions of low-nutrients and high cell-density, they may be involved in maintenance in biofilm communities. Secondary metabolites may be of primary importance in the energy generation and community response of bacteria to their environments.

6.6 Acknowledgements

We would like to thank Dr. C. Titus Brown for original programs and for helpful discussions. This work was supported by grants from the Packard Foundation and Howard Hughes Medical Institute to D.K.N and EMBO grant to L.E.P.D. Dr. Lars E. P. Dietrich created the tree of SoxR proteins and conducted all *Streptomyces coelicolor* experiments.

Chapter 7

Conclusion

7.1 Summary

In this thesis, I set out to explore the spatial organization and dynamics of metabolic states within bacterial biofilms and to further investigate what types of processes and compounds might be important for maintaining populations of cells in these environments. Molecular methods, *in vivo* gene expression analyses, confocal microscopy and quantitative image analysis were used to determine profiles of growth and gene expression in *Shewanella oneidensis* and *Pseudomonas aeruginosa* biofilms. Bioinformatic analyses were conducted to determine the ubiquity of an endogenous small molecule sensing mechanism and elucidate the types of systems that are affected. With the work presented here, the questions posed in Chapter 1 can now be revisited.

7.1.1 What is the spatial and temporal stratification of growth and metabolic states within a biofilm? In particular, can cells decouple metabolism from growth?

We demonstrated that remarkably reproducible spatiometabolic stratification occurs in *S. oneidensis* biofilms with growth activity localized to the outer regions of the biofilm in a pattern that correlates with oxygen availability. Within domains of growth-inactive cells, genes typically upregulated under anaerobic conditions are expressed well after growth has ceased, showing that cells in nutrient-limited regions, previously thought to be dead, are instead maintained in a a non-growing state, where they are capable of generating energy and synthesizing proteins. Regions of growth activity and anaerobically induced gene expression are inversely correlated, definitively demonstrating that cells within biofilms can decouple metabolism and energy generation from growth.

7.1.2 Does nutrient availability affect growth and metabolic stratification dynamically?

Since subpopulations of cells in a biofilm are growth-inactive but still alive, we investigated whether *S. oneidensis* biofilms are able to respond to changes in nutrient conditions and how those changes affect growth-activity patterns. Bacteria in growth-inactive regions are able to respond to nutrient changes and their growth activity profiles match that of predictions for nutrient diffusion into the biofilm. Electron acceptor availability appears to affect growth activity profiles more significantly than electron donor concentrations. Nutrient availability has predictable effects on metabolic organization in biofilms and the community is able to dynamically respond to nutrient changes in the environment.

7.1.3 How are small molecules used differently within different regions of a biofilm?

Given that biofilm populations are metabolically stratified and can activate metabolic programs appropriate to their local microenvironment and developmental stage, we wondered whether endogenously produced small molecules might be influencing local environments or be differentially produced or degraded within the community. *P. aeruginosa* enodenously produces several small molecules. We studied one such molecule, acyl-homoserine lacone (AHL), which is involved in quorum sensing. We observed and quantified the degradation patterns in *P. aeruginosa* biofilms and determined that AHL degradation occurs in the middle of biofilm communities. In this study we also established that AHLs can be used as a substrate for growth. Whether it is being used as a nutrient or to affect the AHL signaling pathway, AHL degradation does not appear to be important in the biofilm/bulk interface, but occurs preferentially in the middle of biofilm colonies demonstrating that the role of small molecules varies within different regions of the community.

7.1.4 Might redox-active small molecule production and sensing be a ubiquitous process that could be utilized for metabolism under biofilm conditions?

Finally, since small molecules have differential effects on subpopulations of the biofilms, it is possible that small molecules or secondary metabolites may be important in these nutrient-limited domains where maintenance energy generation is not well understood. It must first be determined if small

molecules can elicit maintenance type processes. We used a bioinformatics analysis to determine the regulation patterns of the SoxR system and discovered that in bacterial organisms outside of the enterics, SoxR regulates transport and oxidoreductase genes and not the superoxide stress response as the *E. coli* paradigm would suggest. Results from the literature and our experiments in *Streptomyces coelicolor* confirm these predictions. These results suggest that the response to endogenously produced small molecules is ubiquitous across many types of organisms, and that genes in the response regulon are those that may be important in bacterial energy maintenance. Since these endogenous small molecules are produced primarily under biofilm-like conditions, they may play a primary role in the maintenance of biofilm communities.

7.2 Future directions

The work presented here definitively demonstrates that biofilm communities are stratified in terms of growth activity, metabolism and their response to endogenously produced small molecules, and that this stratification is dynamic and can be modified in response to changes in environmental conditions. However these studies only begin to elucidate the true heterogeneity and diversity of metabolisms and energy generating processes that are fundamental to biofilm growth and maintenance.

Studies of biofilm communities are inherently community based. Any protein or genetic analysis of a biofilm encompasses many distinct populations in many different growth states. While single-cell *in vivo* microscope studies allow a researcher to tease apart individual contributions or responses within the community, conducting these studies on a large scale is not realistic. However, having established a reporter construct that is expressed preferentially in the middle of a biofilm community may be useful in other methods of analysis. One way of assaying broader gene expression profiles within a subset of the community, that we have often discussed, would be to use these single-cell reporters to define particular sub-populations and then to use these reporters in sorting criteria, and a given sub-population can be extracted, so that microarray or proteomic analyses can be conducted on this population alone. By understanding the genes and proteins that are up or down regulated within a given region of the biofilm, we may be able to determine what processes are important for their maintenance. This data could also provide a starting point for creating mutants that could be essential in this maintenance phase of biofilm development. Certain technical challenges exist, including finding and developing appropriate reporter constructs and maintaining the RNA and protein pools during the sorting and extraction processes, but these are issues that can be addressed. In particular the environmental microbiology community has begun to explore the use of

fluorescence in situ hybridization (FISH) in extracting subsets of communities and while the studies are typically more focused on DNA analysis, some of the same techniques might be employed. It is surprising with so much focus on biofilm development and detachment and the effects of antibiotics on biofilm viability that more research hasn't been done on the basic metabolic properties of cells within the community. Taking this sub-population level approach would produce significant insight into metabolic processes in unexplored sub-domains of the biofilm. Additionally, a data set such as this might provide a good starting point for further research and invigorate the study of metabolism and maintenance essential for the cells in biofilm communities.

Another interesting direction for future research is that of the role of redox-active small molecules in biofilm metabolism and maintenance. Many of these compounds do act as antibiotics, so they have been primarily studied for their role in virulence. However, this virulence effect is potentially not enough to explain why bacteria would use their limited energy resources to produce these molecules only to fend off some competitors or host response that often isn't present. In the Newman lab, we began to explore alternate roles for these compounds and have already shown that these redox-active small molecules have multiple and broad effects. Since these molecules are upregulated under biofilm type conditions, easily diffusible and redox-active, it seems an interesting route of investigation to assay their role in biofilms. Studies of the effects of phenazines on biofilms and colony morphology in *P. aeruginosa* have already begun in the lab in more detail. And previous studies have investigated the role of redox active compounds in iron reduction at a distance. Using the growth reporter assay it would be interesting to see how these compounds can affect growth-activity profiles. Also combining the approach described above with the introduction of different compounds or mutants in endogenous compound production could elucidate the differential regulation and sensing mechanisms for these compounds in different regions of the biofilm.

These studies focus on the elucidation of metabolism in single-species biofilm systems, but similar questions remain to be explored in multi-species systems where bacteria compete for resources or exist in a syntrophic relationship. In these systems it is possible to see a more apparent spatial stratification within the system and to determine the effects of small molecule production across species. As bacteria in environment mainly exist in multi-species communities, small molecules may have a different role in these interactions and it would be interesting to conduct various competition experiments with for instance *P. aeruginosa* phenazine mutant strains and wild type strains against other species of bacteria that may or may not produce their own redox compounds.

Obtaining a more complete understanding of the growth states and metabolism of bacterial

biofilms, composed of different species and under different conditions, will aid in our understanding the lifecycle of bacteria and help us to understand what effects these communities have on the environment and human health. It will be easier to combat or foster biofilm communities when we understand the mechanisms involved in maintaining them.

Appendix A

Development of *Shewanella oneidensis* biofilms

A.1 Abstract

A method for growing and imaging *Shewanella oneidensis* biofilms in a flow cell system is presented. This work is an elaboration of the previously published work in Teal et al, 2006 [128].

A.2 Introduction

Over the last decade it has been recognized that many bacteria grow preferentially as surface-attached microbial communities, or biofilms. Bacteria attach to a surface and go through a developmental-like pathway that leads to a structure composed of hundreds of cells and the extracellular matrix that the cells produce [31]. Because of this structural configuration, individual cells within a community experience their own microenvironment due to gradients established by diffusion of nutrients and metabolism. Biofilm communities are therefore heterogeneous and spatially stratified, so that each cell's growth state and metabolism is affected by its location in the biofilm and the structure's biomass [135].

To explore the spatiometabolic stratification of developing and mature biofilms, we selected *Shewanella oneidensis* strain MR-1, a biofilm-forming, facultative anaerobe with remarkable metabolic versatility. *S. oneidensis* can use oxygen and many other lower potential substrates, including metals, as electron acceptors in respiration, making it an attractive experimental system in which to explore domains of metabolism within a biofilm [139, 52, 131].

Here we present a method for growing *Shewanella oneidensis* biofilms in a flow cell system that can be used to track biofilm development under controlled conditions.

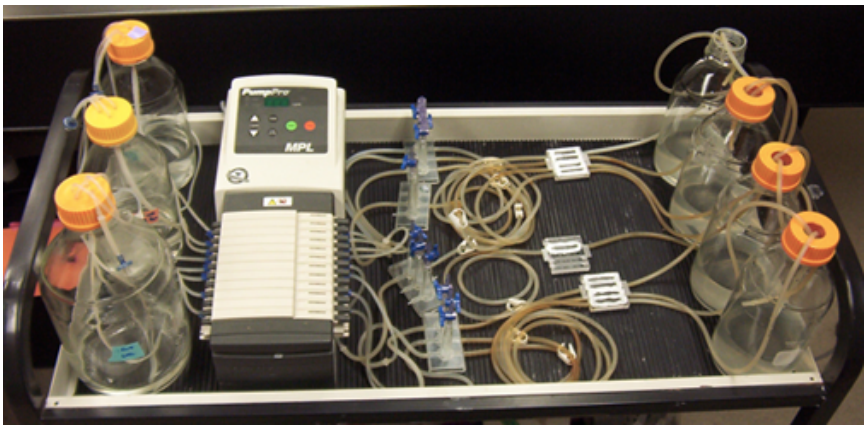

Figure A.1: Setup of biofilm once flow-through system on the biofilm cart.

A.3 Methods

A.3.1 Setup of flow cell system

To monitor biofilms over time, it is important to be able to image in a non-destructive way. For this purpose a once-through flow cell system was constructed as described [86]. A Watson-Marlow type pump, an MPL PumpPro, is used to flow media from a flask containing sterile media to a bubble trap to a flow cell device where biofilms are grown and can be imaged, to an effluent container as shown in Figure A.3.1.

To set up the system, Masterflex platinum cured silicone tubing, size 14 (Fisher Scientific #96410-14), is used to connect the media flask to the flow pump and between the bubble traps, flow cells and effluent. The tubing used through the flow pump is Cole Parmer 2-stop silicone tubing, 1.65mm (Cole-Parmer #07616-38). The bubble traps are PGC Scientific 3-cylinder bubble traps (PGC Scientific #82-106). Bubble traps are used to trap air bubbles that may have been introduced at the start of the system so they do not go through the flow cell. Flow cells were designed and manufactured at the California Institute of Technology. Flow cells have 4 channels machined from polyurethane with number 1 coverslips attached via epoxy. Each channel is 40.6 mm long, 11.4 mm wide and 0.203 mm deep. The coverslip is etched in a large grid pattern with a diamond pen, as a guide to localizing regions within the flow cell during microscopy.

Before starting the biofilm experiment, all tubing is autoclaved. Flow cells and bubble traps cannot be autoclaved, so they are bleached after each use as described below. Using sterile tubing and bleached flow cells and bubble traps, the setup is assembled. For each lane one line of tubing goes into the media and through the pump where it is connected to a bubble trap, then the flow cell

and finally into an effluent container. To rinse and sterilize the system, sterile water is run through the system for a minimum of one hour at at rate of 6.0 rpm on the MPL Pump Pro. The water is then emptied out of the system and the inflow is switched to media. The system, including the bubble traps are filled with media.

Media flow is stopped and 300 μL of culture is injected into the tubing just upstream of the flow cell chamber using a 1cc insulin syringe U-100 28G$\frac{1}{2}$ (Becton Dickinson #309309). The flow is kept off for 1 hour to allow the cells to attach to the surface. The flow is then started at a rate of 1.5 rpm (4.1 μL/sec). This flow rate is kept for the duration of the experiment.

When the experiment is finished 5% bleach is run through the system for a minimum of 2 hours. Initially a rate of 12.0 - 20.0 rpms is used to flush the biofilms from the system, but after approximately 30 minutes, a slower flow rate of 6.0 rpms is used. After bleaching, the system is rinsed with non-sterile water. The system is then disassembled and re-sterilized.

A.3.2 Media

For *Shewanella oneidensis* biofilms a .5mM lactate LML medium is used. The medium contains 0.2 g/L yeast extract, 0.1 g/L peptone, 2.5 g/L Na HEPES and 0.043 mL 60% lactate syrup and is at pH 8.0. If alternative electron acceptors are used, they are added to this medium base.

A.3.3 Cultures

Cultures of *S. oneidensis* MR-1 are in grown in LB to stationary phase. The cells are then subcultured 1:1000 into 5mM lactate LML media and grown shaking at 30°C for approximately 3 hours into early exponential phase at an OD_{600} of approximately 0.075. This early exponential phase culture is used to inoculate the flow cells.

A.3.4 Imaging

Biofilms in flow cells are imaged at the Caltech Beckman Institute Biological Imaging Center using a Zeiss LSM 510 inverted Confocal Laser Scanning Microscope with a 63x or 40x C-Apochromat 1.2W corr water immersion lens and an Argon laser line. Using the Zeiss LSM 510 software, Z-series images are acquired for multiple fields of view at multiple time points during the experiment.

For imaging EGFP or EYFP, the excitation is 488nm and the emission filter used is a BP500-550. For imaging ECFP the excitation is 420nm and the emission filter used is a BP465-485, consistent

with the EGFP, EYFP and ECFP excitation and emission spectra as seen in Figure A.2. Biofilms can be imaged in bright field using the ChD setting in the Zeiss LSM software.

A.3.5 Image processing

Images are processed using Zeiss LSM software or Imaris. Orthogonal views are obtained by using the orthogonal view setting in the LSM software and selecting an X, Y and Z plane of interest, usually through the middle of a biofilm colony. 3-D reconstructions were made using the Volume setting in the Imaris software. To visualize the middle of a colony, a cutting plane was used to virtually cut a colony in half, so that the inside of the colony could be viewed.

A.3.6 Quantitative image analysis

To determine a profile of fluorescence through a biofilm structure, quantitative measurements are made for biofilm images. For each image, the fluorescence intensity profile is mapped through the center x-axis of a biofilm structure using NIH ImageJ. These fluorescence values are exported as a text file of x-coordinates and fluorescence intensity for each pixel. An analysis program written in Python `image-recenter.py` is used to analyze and process this data. The program takes as input a text file with two columns - position and pixel - and a cutoff value that defines the low intensity cutoff. The brightest pixel is defined as 100% fluorescence and all fluorescence values are determined relative to that value. To automatically determine the edges of a structure, an edge detection algorithm is used where the region of greatest contrast between the empty space surrounding the biofilm structure and the fluorescence of the structure is defined to be the edge. Using the defined edges, the center is specified. Then, the intensity of each nine-pixel bin is determined in relationship to its distance from the center of the structure. The output is in two files. One file contains the colony size, calculated by the distance between the left and right edges, and the cutoff threshold used. Another file is the average position of the nine-pixel bin as a function of the distance from the center of the colony and the average intensity for that bin. Using this output, a plot of fluorescence intensity versus distance from the center of the structure can be constructed for each image. Biofilms of the same type are binned into representative sizes, and using the script `avg-error-files.py`, the average fluorescence profile and standard deviations across all the structures of that size are calculated. `avg-error-files.py` takes as input a list of files generated from `image-recenter.py` and generates as output: position, as a distance from the center of the colony, and the average and standard deviation of the fluorescence intensity at that position. This output is used to generate

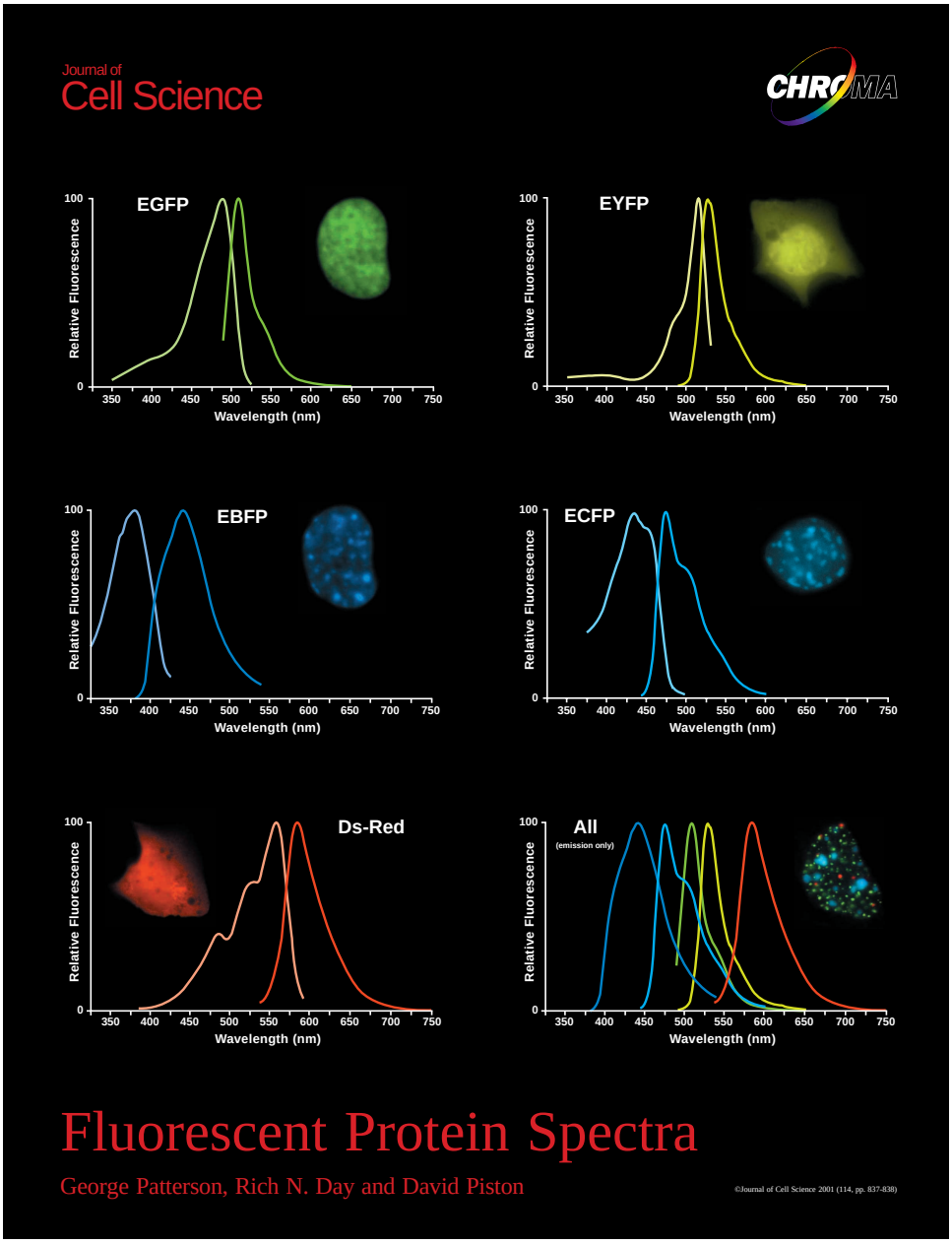

Figure A.2: Excitation and emission spectra for the enhanced fluorescent proteins. From Patterson, Day and Piston [95].

a plot of fluorescence intensity versus the distance from the center of the structure for all biofilm structures of a given size. Scripts are available at `http://idyll.org/~tracyt/qbiofilm/`.

Appendix B

Supplemental tables for Chapter 6

B.1 Pyscangen table

Table B.1 is the output of `pyscangen.py` for the soxbox position weight matrix (PWM) described in Chapter 6. For each genome containing a SoxR protein, the number of sites found at or below each threshold is shown along with the percentage of those sites found in intergenic regions versus the percentage found in genes. If the PWM is finding true binding sites, it is expected that there will be more sites found in intergenic regions than within genes.

Table B.2 is the output of `pyscangenes.py` for the soxbox PWM described in Chapter 6. For each genome containing a SoxR protein, the soxbox sites found and the operons adjacent to them are listed.

Table B.1: The number of sites found in intergenic regions and within genes for thresholds 1.0 - 13.0 in each genome containing SoxR.

Acidovorax avenae subsp. citrulli AAC00-1, complete genome			
Threshold	Total sites found	Percent in genes	Percent intergenic
1.00	0	0%	0%
2.00	0	0%	0%
3.00	0	0%	0%
4.00	0	0%	0%
5.00	1	0%	100%
6.00	1	0%	100%
7.00	1	0%	100%
8.00	1	0%	100%
9.00	2	0%	100%
10.00	3	0%	100%
11.00	3	0%	100%
12.00	3	0%	100%
13.00	4	0%	100%

Acidobacteria bacterium Ellin345, complete genome

Cutoff	Total sites found	Percent in genes	Percent intergenic
1.00	0	0%	0%
2.00	1	0%	100%
3.00	1	0%	100%
4.00	1	0%	100%
5.00	1	0%	100%
6.00	1	0%	100%
7.00	1	0%	100%
8.00	1	0%	100%
9.00	1	0%	100%
10.00	1	0%	100%
11.00	1	0%	100%
12.00	1	0%	100%
13.00	2	0%	100%

Acidovorax avenae subsp. citrulli AAC00-1, complete genome

Cutoff	Total sites found	Percent in genes	Percent intergenic
1.00	0	0%	0%
2.00	0	0%	0%
3.00	0	0%	0%
4.00	0	0%	0%
5.00	1	0%	100%
6.00	1	0%	100%
7.00	1	0%	100%
8.00	1	0%	100%
9.00	2	0%	100%
10.00	3	0%	100%
11.00	3	0%	100%
12.00	3	0%	100%
13.00	4	0%	100%

Acinetobacter sp. ADP1, complete genome

Cutoff	Total sites found	Percent in genes	Percent intergenic
1.00	0	0%	0%
2.00	1	0%	100%
3.00	1	0%	100%
4.00	1	0%	100%
5.00	1	0%	100%
6.00	1	0%	100%
7.00	1	0%	100%
8.00	1	0%	100%
9.00	1	0%	100%
10.00	1	0%	100%
11.00	2	50%	50%
12.00	7	57%	43%
13.00	18	72%	28%

Aeromonas hydrophila subsp. hydrophila ATCC 7966, complete genome

Cutoff	Total sites found	Percent in genes	Percent intergenic
1.00	0	0%	0%
2.00	0	0%	0%
3.00	0	0%	0%
4.00	0	0%	0%
5.00	1	0%	100%
6.00	1	0%	100%
7.00	1	0%	100%
8.00	1	0%	100%
9.00	1	0%	100%
10.00	1	0%	100%
11.00	1	0%	100%
12.00	1	0%	100%
13.00	3	33%	67%

Agrobacterium tumefaciens str. C58 chromosome circular, complete sequence

Cutoff	Total sites found	Percent in genes	Percent intergenic
1.00	0	0%	0%
2.00	0	0%	0%
3.00	0	0%	0%
4.00	0	0%	0%
5.00	0	0%	0%
6.00	0	0%	0%
7.00	1	0%	100%
8.00	1	0%	100%
9.00	1	0%	100%
10.00	1	0%	100%
11.00	2	50%	50%
12.00	2	50%	50%
13.00	2	50%	50%

Agrobacterium tumefaciens str. C58 chromosome linear, complete sequence

Cutoff	Total sites found	Percent in genes	Percent intergenic
1.00	0	0%	0%
2.00	0	0%	0%
3.00	0	0%	0%
4.00	0	0%	0%
5.00	0	0%	0%
6.00	1	0%	100%
7.00	2	0%	100%
8.00	2	0%	100%
9.00	2	0%	100%
10.00	2	0%	100%
11.00	3	0%	100%
12.00	5	0%	100%
13.00	8	13%	88%

Arthrobacter aurescens TC1, complete genome

Cutoff	Total sites found	Percent in genes	Percent intergenic
1.00	0	0%	0%
2.00	0	0%	0%
3.00	0	0%	0%
4.00	0	0%	0%
5.00	0	0%	0%
6.00	1	0%	100%
7.00	1	0%	100%
8.00	2	50%	50%
9.00	2	50%	50%
10.00	2	50%	50%
11.00	2	50%	50%
12.00	2	50%	50%
13.00	5	60%	40%

Bdellovibrio bacteriovorus HD100, complete genome

Cutoff	Total sites found	Percent in genes	Percent intergenic
1.00	0	0%	0%
2.00	1	0%	100%
3.00	1	0%	100%
4.00	1	0%	100%
5.00	1	0%	100%
6.00	1	0%	100%
7.00	1	0%	100%
8.00	1	0%	100%
9.00	2	0%	100%
10.00	2	0%	100%
11.00	2	0%	100%
12.00	5	40%	60%
13.00	9	56%	44%

Bordetella bronchiseptica RB50, complete genome

Cutoff	Total sites found	Percent in genes	Percent intergenic
1.00	0	0%	0%
2.00	0	0%	0%
3.00	0	0%	0%
4.00	0	0%	0%
5.00	0	0%	0%
6.00	0	0%	0%
7.00	1	0%	100%
8.00	1	0%	100%
9.00	1	0%	100%
10.00	1	0%	100%
11.00	1	0%	100%
12.00	2	0%	100%
13.00	3	33%	67%

Bordetella parapertussis 12822, complete genome

Cutoff	Total sites found	Percent in genes	Percent intergenic
1.00	0	0%	0%
2.00	0	0%	0%
3.00	0	0%	0%
4.00	0	0%	0%
5.00	0	0%	0%
6.00	0	0%	0%
7.00	0	0%	0%
8.00	0	0%	0%
9.00	1	0%	100%
10.00	1	0%	100%
11.00	1	0%	100%
12.00	2	0%	100%
13.00	3	33%	67%

Bordetella pertussis Tohama I, complete genome

Cutoff	Total sites found	Percent in genes	Percent intergenic
1.00	0	0%	0%
2.00	0	0%	0%
3.00	0	0%	0%
4.00	0	0%	0%
5.00	0	0%	0%
6.00	0	0%	0%
7.00	1	0%	100%
8.00	1	0%	100%
9.00	1	0%	100%
10.00	1	0%	100%
11.00	1	0%	100%
12.00	1	0%	100%
13.00	2	50%	50%

Burkholderia sp. 383 chromosome 3, complete sequence

Cutoff	Total sites found	Percent in genes	Percent intergenic
1.00	0	0%	0%
2.00	0	0%	0%
3.00	0	0%	0%
4.00	0	0%	0%
5.00	0	0%	0%
6.00	0	0%	0%
7.00	0	0%	0%
8.00	0	0%	0%
9.00	0	0%	0%
10.00	0	0%	0%
11.00	0	0%	0%
12.00	0	0%	0%
13.00	1	0%	100%

Burkholderia sp. 383 chromosome 1, complete sequence

Cutoff	Total sites found	Percent in genes	Percent intergenic
1.00	0	0%	0%
2.00	0	0%	0%
3.00	0	0%	0%
4.00	0	0%	0%
5.00	0	0%	0%
6.00	0	0%	0%
7.00	0	0%	0%
8.00	0	0%	0%
9.00	0	0%	0%
10.00	0	0%	0%
11.00	0	0%	0%
12.00	1	100%	0%
13.00	1	100%	0%

Burkholderia sp. 383 chromosome 2, complete sequence

Cutoff	Total sites found	Percent in genes	Percent intergenic
1.00	0	0%	0%
2.00	0	0%	0%
3.00	0	0%	0%
4.00	1	0%	100%
5.00	1	0%	100%
6.00	1	0%	100%
7.00	1	0%	100%
8.00	2	0%	100%
9.00	2	0%	100%
10.00	3	0%	100%
11.00	4	0%	100%
12.00	4	0%	100%
13.00	4	0%	100%

Chromobacterium violaceum ATCC 12472, complete genome

Cutoff	Total sites found	Percent in genes	Percent intergenic
1.00	0	0%	0%
2.00	0	0%	0%
3.00	0	0%	0%
4.00	0	0%	0%
5.00	1	0%	100%
6.00	2	0%	100%
7.00	2	0%	100%
8.00	2	0%	100%
9.00	2	0%	100%
10.00	2	0%	100%
11.00	2	0%	100%
12.00	3	0%	100%
13.00	3	0%	100%

Erythrobacter litoralis HTCC2594, complete genome

Cutoff	Total sites found	Percent in genes	Percent intergenic
1.00	0	0%	0%
2.00	0	0%	0%
3.00	0	0%	0%
4.00	1	100%	0%
5.00	1	100%	0%
6.00	1	100%	0%
7.00	1	100%	0%
8.00	1	100%	0%
9.00	1	100%	0%
10.00	1	100%	0%
11.00	1	100%	0%
12.00	1	100%	0%
13.00	1	100%	0%

Escherichia coli CFT073, complete genome

Cutoff	Total sites found	Percent in genes	Percent intergenic
1.00	0	0%	0%
2.00	0	0%	0%
3.00	1	0%	100%
4.00	1	0%	100%
5.00	1	0%	100%
6.00	1	0%	100%
7.00	1	0%	100%
8.00	1	0%	100%
9.00	1	0%	100%
10.00	1	0%	100%
11.00	3	67%	33%
12.00	4	75%	25%
13.00	6	67%	33%

Escherichia coli K12, complete genome

Cutoff	Total sites found	Percent in genes	Percent intergenic
1.00	0	0%	0%
2.00	0	0%	0%
3.00	1	0%	100%
4.00	1	0%	100%
5.00	1	0%	100%
6.00	1	0%	100%
7.00	1	0%	100%
8.00	1	0%	100%
9.00	1	0%	100%
10.00	1	0%	100%
11.00	2	50%	50%
12.00	2	50%	50%
13.00	4	50%	50%

Frankia alni ACN14a, complete genome

Cutoff	Total sites found	Percent in genes	Percent intergenic
1.00	0	0%	0%
2.00	0	0%	0%
3.00	0	0%	0%
4.00	0	0%	0%
5.00	0	0%	0%
6.00	0	0%	0%
7.00	0	0%	0%
8.00	0	0%	0%
9.00	0	0%	0%
10.00	0	0%	0%
11.00	0	0%	0%
12.00	3	67%	33%
13.00	4	50%	50%

Frankia sp. CcI3, complete genome

Cutoff	Total sites found	Percent in genes	Percent intergenic
1.00	0	0%	0%
2.00	0	0%	0%
3.00	0	0%	0%
4.00	0	0%	0%
5.00	0	0%	0%
6.00	0	0%	0%
7.00	0	0%	0%
8.00	1	0%	100%
9.00	1	0%	100%
10.00	2	0%	100%
11.00	3	0%	100%
12.00	4	0%	100%
13.00	5	0%	100%

Hahella chejuensis KCTC 2396, complete genome

Cutoff	Total sites found	Percent in genes	Percent intergenic
1.00	0	0%	0%
2.00	1	0%	100%
3.00	1	0%	100%
4.00	1	0%	100%
5.00	1	0%	100%
6.00	2	0%	100%
7.00	2	0%	100%
8.00	2	0%	100%
9.00	2	0%	100%
10.00	4	0%	100%
11.00	4	0%	100%
12.00	5	20%	80%
13.00	8	25%	75%

Hyphomonas neptunium ATCC 15444, complete genome

Cutoff	Total sites found	Percent in genes	Percent intergenic
1.00	0	0%	0%
2.00	0	0%	0%
3.00	0	0%	0%
4.00	0	0%	0%
5.00	0	0%	0%
6.00	1	0%	100%
7.00	1	0%	100%
8.00	1	0%	100%
9.00	1	0%	100%
10.00	1	0%	100%
11.00	1	0%	100%
12.00	1	0%	100%
13.00	1	0%	100%

Maricaulis maris MCS10, complete genome

Cutoff	Total sites found	Percent in genes	Percent intergenic
1.00	0	0%	0%
2.00	0	0%	0%
3.00	0	0%	0%
4.00	0	0%	0%
5.00	0	0%	0%
6.00	0	0%	0%
7.00	0	0%	0%
8.00	0	0%	0%
9.00	0	0%	0%
10.00	1	0%	100%
11.00	1	0%	100%
12.00	1	0%	100%
13.00	1	0%	100%

Mesorhizobium loti MAFF303099, complete genome

Cutoff	Total sites found	Percent in genes	Percent intergenic
1.00	0	0%	0%
2.00	0	0%	0%
3.00	0	0%	0%
4.00	1	0%	100%
5.00	2	0%	100%
6.00	2	0%	100%
7.00	2	0%	100%
8.00	2	0%	100%
9.00	3	0%	100%
10.00	3	0%	100%
11.00	3	0%	100%
12.00	3	0%	100%
13.00	3	0%	100%

Mycobacterium vanbaalenii PYR-1, complete genome

Cutoff	Total sites found	Percent in genes	Percent intergenic
1.00	0	0%	0%
2.00	0	0%	0%
3.00	0	0%	0%
4.00	0	0%	0%
5.00	0	0%	0%
6.00	0	0%	0%
7.00	0	0%	0%
8.00	0	0%	0%
9.00	0	0%	0%
10.00	2	0%	100%
11.00	4	0%	100%
12.00	4	0%	100%
13.00	6	0%	100%

Mycobacterium sp. JLS, complete genome

Cutoff	Total sites found	Percent in genes	Percent intergenic
1.00	0	0%	0%
2.00	0	0%	0%
3.00	0	0%	0%
4.00	0	0%	0%
5.00	0	0%	0%
6.00	0	0%	0%
7.00	1	0%	100%
8.00	1	0%	100%
9.00	2	0%	100%
10.00	4	0%	100%
11.00	4	0%	100%
12.00	4	0%	100%
13.00	4	0%	100%

Mycobacterium sp. KMS, complete genome

Cutoff	Total sites found	Percent in genes	Percent intergenic
1.00	0	0%	0%
2.00	0	0%	0%
3.00	0	0%	0%
4.00	0	0%	0%
5.00	0	0%	0%
6.00	0	0%	0%
7.00	1	0%	100%
8.00	1	0%	100%
9.00	2	0%	100%
10.00	4	0%	100%
11.00	4	0%	100%
12.00	5	0%	100%
13.00	5	0%	100%

Mycobacterium sp. MCS, complete genome

Cutoff	Total sites found	Percent in genes	Percent intergenic
1.00	0	0%	0%
2.00	0	0%	0%
3.00	0	0%	0%
4.00	0	0%	0%
5.00	0	0%	0%
6.00	0	0%	0%
7.00	1	0%	100%
8.00	1	0%	100%
9.00	2	0%	100%
10.00	4	0%	100%
11.00	4	0%	100%
12.00	5	0%	100%
13.00	5	0%	100%

Mycobacterium smegmatis str. MC2 155, complete genome

Cutoff	Total sites found	Percent in genes	Percent intergenic
1.00	0	0%	0%
2.00	0	0%	0%
3.00	0	0%	0%
4.00	0	0%	0%
5.00	0	0%	0%
6.00	0	0%	0%
7.00	0	0%	0%
8.00	1	0%	100%
9.00	3	0%	100%
10.00	4	0%	100%
11.00	4	0%	100%
12.00	4	0%	100%
13.00	9	0%	100%

Nocardia farcinica IFM 10152, complete genome

Cutoff	Total sites found	Percent in genes	Percent intergenic
1.00	0	0%	0%
2.00	0	0%	0%
3.00	0	0%	0%
4.00	0	0%	0%
5.00	1	0%	100%
6.00	1	0%	100%
7.00	1	0%	100%
8.00	1	0%	100%
9.00	3	0%	100%
10.00	5	0%	100%
11.00	7	0%	100%
12.00	9	0%	100%
13.00	9	0%	100%

Novosphingobium aromaticivorans DSM 12444, complete genome

Cutoff	Total sites found	Percent in genes	Percent intergenic
1.00	0	0%	0%
2.00	0	0%	0%
3.00	0	0%	0%
4.00	0	0%	0%
5.00	1	0%	100%
6.00	1	0%	100%
7.00	1	0%	100%
8.00	1	0%	100%
9.00	1	0%	100%
10.00	1	0%	100%
11.00	1	0%	100%
12.00	2	50%	50%
13.00	3	67%	33%

Photobacterium profundum SS9 chromosome 1, complete sequence

Cutoff	Total sites found	Percent in genes	Percent intergenic
1.00	0	0%	0%
2.00	0	0%	0%
3.00	0	0%	0%
4.00	0	0%	0%
5.00	0	0%	0%
6.00	0	0%	0%
7.00	0	0%	0%
8.00	0	0%	0%
9.00	0	0%	0%
10.00	0	0%	0%
11.00	1	0%	100%
12.00	3	67%	33%
13.00	4	75%	25%

Photobacterium profundum SS9 chromosome 2, complete sequence

Cutoff	Total sites found	Percent in genes	Percent intergenic
1.00	0	0%	0%
2.00	0	0%	0%
3.00	0	0%	0%
4.00	0	0%	0%
5.00	0	0%	0%
6.00	0	0%	0%
7.00	1	0%	100%
8.00	1	0%	100%
9.00	1	0%	100%
10.00	1	0%	100%
11.00	2	0%	100%
12.00	3	0%	100%
13.00	9	33%	67%

Polaromonas sp. JS666, complete genome

Cutoff	Total sites found	Percent in genes	Percent intergenic
1.00	0	0%	0%
2.00	0	0%	0%
3.00	1	0%	100%
4.00	1	0%	100%
5.00	1	0%	100%
6.00	1	0%	100%
7.00	1	0%	100%
8.00	1	0%	100%
9.00	1	0%	100%
10.00	1	0%	100%
11.00	1	0%	100%
12.00	1	0%	100%
13.00	2	50%	50%

Pseudomonas aeruginosa PAO1, complete genome

Cutoff	Total sites found	Percent in genes	Percent intergenic
1.00	0	0%	0%
2.00	2	0%	100%
3.00	3	0%	100%
4.00	3	0%	100%
5.00	3	0%	100%
6.00	3	0%	100%
7.00	3	0%	100%
8.00	3	0%	100%
9.00	4	0%	100%
10.00	4	0%	100%
11.00	4	0%	100%
12.00	4	0%	100%
13.00	5	0%	100%

Pseudomonas entomophila L48, complete genome

Cutoff	Total sites found	Percent in genes	Percent intergenic
1.00	0	0%	0%
2.00	0	0%	0%
3.00	0	0%	0%
4.00	0	0%	0%
5.00	0	0%	0%
6.00	0	0%	0%
7.00	1	0%	100%
8.00	1	0%	100%
9.00	1	0%	100%
10.00	1	0%	100%
11.00	3	0%	100%
12.00	3	0%	100%
13.00	4	0%	100%

Pseudomonas fluorescens Pf-5, complete genome

Cutoff	Total sites found	Percent in genes	Percent intergenic
1.00	0	0%	0%
2.00	0	0%	0%
3.00	0	0%	0%
4.00	0	0%	0%
5.00	0	0%	0%
6.00	0	0%	0%
7.00	0	0%	0%
8.00	1	0%	100%
9.00	1	0%	100%
10.00	1	0%	100%
11.00	1	0%	100%
12.00	1	0%	100%
13.00	3	33%	67%

Pseudomonas fluorescens PfO-1, complete genome

Cutoff	Total sites found	Percent in genes	Percent intergenic
1.00	0	0%	0%
2.00	0	0%	0%
3.00	0	0%	0%
4.00	0	0%	0%
5.00	1	0%	100%
6.00	1	0%	100%
7.00	1	0%	100%
8.00	1	0%	100%
9.00	1	0%	100%
10.00	1	0%	100%
11.00	1	0%	100%
12.00	3	67%	33%
13.00	7	57%	43%

Pseudomonas putida KT2440, complete genome

Cutoff	Total sites found	Percent in genes	Percent intergenic
1.00	0	0%	0%
2.00	0	0%	0%
3.00	1	100%	0%
4.00	1	100%	0%
5.00	2	50%	50%
6.00	2	50%	50%
7.00	3	33%	67%
8.00	3	33%	67%
9.00	4	25%	75%
10.00	5	20%	80%
11.00	5	20%	80%
12.00	7	14%	86%
13.00	7	14%	86%

Ralstonia eutropha H16 chromosome 1, complete sequence

Cutoff	Total sites found	Percent in genes	Percent intergenic
1.00	0	0%	0%
2.00	0	0%	0%
3.00	0	0%	0%
4.00	0	0%	0%
5.00	0	0%	0%
6.00	0	0%	0%
7.00	0	0%	0%
8.00	0	0%	0%
9.00	1	0%	100%
10.00	1	0%	100%
11.00	1	0%	100%
12.00	1	0%	100%
13.00	1	0%	100%

Ralstonia eutropha H16 chromosome 2, complete sequence

Cutoff	Total sites found	Percent in genes	Percent intergenic
1.00	0	0%	0%
2.00	0	0%	0%
3.00	0	0%	0%
4.00	1	0%	100%
5.00	1	0%	100%
6.00	1	0%	100%
7.00	1	0%	100%
8.00	1	0%	100%
9.00	1	0%	100%
10.00	1	0%	100%
11.00	1	0%	100%
12.00	1	0%	100%
13.00	1	0%	100%

Ralstonia metallidurans CH34 chromosome 1, complete sequence

Cutoff	Total sites found	Percent in genes	Percent intergenic
1.00	0	0%	0%
2.00	0	0%	0%
3.00	0	0%	0%
4.00	0	0%	0%
5.00	0	0%	0%
6.00	0	0%	0%
7.00	0	0%	0%
8.00	0	0%	0%
9.00	0	0%	0%
10.00	0	0%	0%
11.00	0	0%	0%
12.00	0	0%	0%
13.00	0	0%	0%

Ralstonia metallidurans CH34 chromosome 2, complete sequence

Cutoff	Total sites found	Percent in genes	Percent intergenic
1.00	0	0%	0%
2.00	0	0%	0%
3.00	0	0%	0%
4.00	0	0%	0%
5.00	0	0%	0%
6.00	1	0%	100%
7.00	1	0%	100%
8.00	1	0%	100%
9.00	1	0%	100%
10.00	1	0%	100%
11.00	1	0%	100%
12.00	1	0%	100%
13.00	2	50%	50%

Rhizobium etli CFN 42, complete genome

Cutoff	Total sites found	Percent in genes	Percent intergenic
1.00	0	0%	0%
2.00	0	0%	0%
3.00	0	0%	0%
4.00	0	0%	0%
5.00	0	0%	0%
6.00	0	0%	0%
7.00	1	0%	100%
8.00	2	0%	100%
9.00	2	0%	100%
10.00	2	0%	100%
11.00	2	0%	100%
12.00	3	0%	100%
13.00	5	0%	100%

Rhizobium leguminosarum bv. viciae 3841, complete genome

Cutoff	Total sites found	Percent in genes	Percent intergenic
1.00	0	0%	0%
2.00	0	0%	0%
3.00	0	0%	0%
4.00	1	100%	0%
5.00	2	100%	0%
6.00	2	100%	0%
7.00	2	100%	0%
8.00	2	100%	0%
9.00	3	100%	0%
10.00	3	100%	0%
11.00	4	100%	0%
12.00	4	100%	0%
13.00	4	100%	0%

Rhodococcus sp. RHA1, complete genome

Cutoff	Total sites found	Percent in genes	Percent intergenic
1.00	0	0%	0%
2.00	0	0%	0%
3.00	0	0%	0%
4.00	0	0%	0%
5.00	0	0%	0%
6.00	0	0%	0%
7.00	0	0%	0%
8.00	0	0%	0%
9.00	2	50%	50%
10.00	4	25%	75%
11.00	4	25%	75%
12.00	4	25%	75%
13.00	6	17%	83%

Rhodopseudomonas palustris BisB5, complete genome

Cutoff	Total sites found	Percent in genes	Percent intergenic
1.00	0	0%	0%
2.00	0	0%	0%
3.00	0	0%	0%
4.00	0	0%	0%
5.00	0	0%	0%
6.00	1	0%	100%
7.00	1	0%	100%
8.00	1	0%	100%
9.00	1	0%	100%
10.00	1	0%	100%
11.00	1	0%	100%
12.00	1	0%	100%
13.00	1	0%	100%

Saccharopolyspora erythraea NRRL 2338, complete genome

Cutoff	Total sites found	Percent in genes	Percent intergenic
1.00	0	0%	0%
2.00	0	0%	0%
3.00	0	0%	0%
4.00	0	0%	0%
5.00	0	0%	0%
6.00	0	0%	0%
7.00	0	0%	0%
8.00	2	0%	100%
9.00	3	0%	100%
10.00	3	0%	100%
11.00	3	0%	100%
12.00	6	0%	100%
13.00	7	0%	100%

Salmonella enterica subsp. enterica serovar Typhi str. CT18, complete genome

Cutoff	Total sites found	Percent in genes	Percent intergenic
1.00	0	0%	0%
2.00	0	0%	0%
3.00	1	0%	100%
4.00	1	0%	100%
5.00	1	0%	100%
6.00	1	0%	100%
7.00	1	0%	100%
8.00	1	0%	100%
9.00	1	0%	100%
10.00	1	0%	100%
11.00	1	0%	100%
12.00	1	0%	100%
13.00	5	20%	80%

Salmonella typhimurium LT2, complete genome

Cutoff	Total sites found	Percent in genes	Percent intergenic
1.00	0	0%	0%
2.00	0	0%	0%
3.00	1	0%	100%
4.00	1	0%	100%
5.00	1	0%	100%
6.00	1	0%	100%
7.00	1	0%	100%
8.00	1	0%	100%
9.00	1	0%	100%
10.00	1	0%	100%
11.00	1	0%	100%
12.00	1	0%	100%
13.00	6	17%	83%

Shewanella frigidimarina NCIMB 400, complete genome

Cutoff	Total sites found	Percent in genes	Percent intergenic
1.00	0	0%	0%
2.00	0	0%	0%
3.00	1	0%	100%
4.00	1	0%	100%
5.00	1	0%	100%
6.00	1	0%	100%
7.00	1	0%	100%
8.00	1	0%	100%
9.00	1	0%	100%
10.00	2	50%	50%
11.00	4	50%	50%
12.00	6	50%	50%
13.00	25	68%	32%

Shewanella denitrificans OS217, complete genome

Cutoff	Total sites found	Percent in genes	Percent intergenic
1.00	0	0%	0%
2.00	1	0%	100%
3.00	2	0%	100%
4.00	2	0%	100%
5.00	2	0%	100%
6.00	2	0%	100%
7.00	2	0%	100%
8.00	2	0%	100%
9.00	2	0%	100%
10.00	5	40%	60%
11.00	8	38%	63%
12.00	11	45%	55%
13.00	23	65%	35%

Shigella flexneri 2a str. 2457T, complete genome

Cutoff	Total sites found	Percent in genes	Percent intergenic
1.00	0	0%	0%
2.00	0	0%	0%
3.00	1	0%	100%
4.00	1	0%	100%
5.00	1	0%	100%
6.00	1	0%	100%
7.00	1	0%	100%
8.00	1	0%	100%
9.00	1	0%	100%
10.00	2	50%	50%
11.00	2	50%	50%
12.00	2	50%	50%
13.00	4	50%	50%

Shigella flexneri 2a str. 301, complete genome

Cutoff	Total sites found	Percent in genes	Percent intergenic
1.00	0	0%	0%
2.00	0	0%	0%
3.00	1	0%	100%
4.00	1	0%	100%
5.00	1	0%	100%
6.00	1	0%	100%
7.00	1	0%	100%
8.00	1	0%	100%
9.00	1	0%	100%
10.00	2	50%	50%
11.00	2	50%	50%
12.00	2	50%	50%
13.00	4	50%	50%

Shigella flexneri 5 str. 8401, complete genome

Cutoff	Total sites found	Percent in genes	Percent intergenic
1.00	0	0%	0%
2.00	0	0%	0%
3.00	1	0%	100%
4.00	1	0%	100%
5.00	1	0%	100%
6.00	1	0%	100%
7.00	1	0%	100%
8.00	1	0%	100%
9.00	1	0%	100%
10.00	2	50%	50%
11.00	2	50%	50%
12.00	2	50%	50%
13.00	4	50%	50%

Shigella sonnei Ss046, complete genome

Cutoff	Total sites found	Percent in genes	Percent intergenic
1.00	0	0%	0%
2.00	0	0%	0%
3.00	1	0%	100%
4.00	1	0%	100%
5.00	1	0%	100%
6.00	1	0%	100%
7.00	1	0%	100%
8.00	1	0%	100%
9.00	1	0%	100%
10.00	1	0%	100%
11.00	2	50%	50%
12.00	2	50%	50%
13.00	4	50%	50%

Silicibacter pomeroyi DSS-3, complete genome

Cutoff	Total sites found	Percent in genes	Percent intergenic
1.00	0	0%	0%
2.00	0	0%	0%
3.00	0	0%	0%
4.00	0	0%	0%
5.00	0	0%	0%
6.00	1	0%	100%
7.00	1	0%	100%
8.00	1	0%	100%
9.00	2	0%	100%
10.00	2	0%	100%
11.00	2	0%	100%
12.00	3	0%	100%
13.00	3	0%	100%

Sinorhizobium meliloti 1021, complete genome

Cutoff	Total sites found	Percent in genes	Percent intergenic
1.00	0	0%	0%
2.00	0	0%	0%
3.00	0	0%	0%
4.00	0	0%	0%
5.00	0	0%	0%
6.00	0	0%	0%
7.00	1	0%	100%
8.00	1	0%	100%
9.00	2	0%	100%
10.00	2	0%	100%
11.00	2	0%	100%
12.00	2	0%	100%
13.00	3	0%	100%

Sphingopyxis alaskensis RB2256, complete genome

Cutoff	Total sites found	Percent in genes	Percent intergenic
1.00	0	0%	0%
2.00	0	0%	0%
3.00	0	0%	0%
4.00	0	0%	0%
5.00	0	0%	0%
6.00	0	0%	0%
7.00	0	0%	0%
8.00	1	0%	100%
9.00	1	0%	100%
10.00	1	0%	100%
11.00	1	0%	100%
12.00	1	0%	100%
13.00	2	0%	100%

Streptomyces avermitilis MA-4680, complete genome

Cutoff	Total sites found	Percent in genes	Percent intergenic
1.00	0	0%	0%
2.00	0	0%	0%
3.00	0	0%	0%
4.00	0	0%	0%
5.00	0	0%	0%
6.00	2	0%	100%
7.00	4	0%	100%
8.00	5	0%	100%
9.00	5	0%	100%
10.00	5	0%	100%
11.00	6	0%	100%
12.00	6	0%	100%
13.00	8	0%	100%

Streptomyces coelicolor A3(2), complete genome

Cutoff	Total sites found	Percent in genes	Percent intergenic
1.00	0	0%	0%
2.00	0	0%	0%
3.00	0	0%	0%
4.00	0	0%	0%
5.00	0	0%	0%
6.00	1	0%	100%
7.00	1	0%	100%
8.00	1	0%	100%
9.00	3	0%	100%
10.00	3	0%	100%
11.00	5	20%	80%
12.00	6	17%	83%
13.00	7	14%	86%

Thermobifida fusca YX, complete genome

Cutoff	Total sites found	Percent in genes	Percent intergenic
1.00	0	0%	0%
2.00	0	0%	0%
3.00	0	0%	0%
4.00	1	0%	100%
5.00	1	0%	100%
6.00	1	0%	100%
7.00	2	0%	100%
8.00	2	0%	100%
9.00	3	0%	100%
10.00	3	0%	100%
11.00	3	0%	100%
12.00	3	0%	100%
13.00	5	0%	100%

Thermococcus kodakarensis KOD1, complete genome

Cutoff	Total sites found	Percent in genes	Percent intergenic
1.00	0	0%	0%
2.00	0	0%	0%
3.00	0	0%	0%
4.00	0	0%	0%
5.00	0	0%	0%
6.00	0	0%	0%
7.00	0	0%	0%
8.00	0	0%	0%
9.00	0	0%	0%
10.00	0	0%	0%
11.00	0	0%	0%
12.00	0	0%	0%
13.00	3	100%	0%

Vibrio cholerae O1 biovar eltor str. N16961 chromosome I, complete sequence

Cutoff	Total sites found	Percent in genes	Percent intergenic
1.00	0	0%	0%
2.00	0	0%	0%
3.00	0	0%	0%
4.00	0	0%	0%
5.00	0	0%	0%
6.00	0	0%	0%
7.00	0	0%	0%
8.00	0	0%	0%
9.00	0	0%	0%
10.00	1	100%	0%
11.00	1	100%	0%
12.00	2	100%	0%
13.00	3	67%	33%

Vibrio cholerae O1 biovar eltor str. N16961 chromosome II, complete sequence

Cutoff	Total sites found	Percent in genes	Percent intergenic
1.00	0	0%	0%
2.00	0	0%	0%
3.00	1	0%	100%
4.00	1	0%	100%
5.00	1	0%	100%
6.00	1	0%	100%
7.00	1	0%	100%
8.00	1	0%	100%
9.00	1	0%	100%
10.00	1	0%	100%
11.00	1	0%	100%
12.00	2	0%	100%
13.00	6	67%	33%

Vibrio parahaemolyticus RIMD 2210633 chromosome II, complete sequence

Cutoff	Total sites found	Percent in genes	Percent intergenic
1.00	0	0%	0%
2.00	0	0%	0%
3.00	0	0%	0%
4.00	0	0%	0%
5.00	1	0%	100%
6.00	4	0%	100%
7.00	4	0%	100%
8.00	5	0%	100%
9.00	5	0%	100%
10.00	5	0%	100%
11.00	5	0%	100%
12.00	7	14%	86%
13.00	15	13%	87%

Vibrio vulnificus CMCP6 chromosome I, complete sequence

Cutoff	Total sites found	Percent in genes	Percent intergenic
1.00	0	0%	0%
2.00	0	0%	0%
3.00	0	0%	0%
4.00	0	0%	0%
5.00	0	0%	0%
6.00	0	0%	0%
7.00	0	0%	0%
8.00	0	0%	0%
9.00	0	0%	0%
10.00	0	0%	0%
11.00	1	0%	100%
12.00	3	33%	67%
13.00	6	50%	50%

Vibrio vulnificus CMCP6 chromosome II, complete sequence

Cutoff	Total sites found	Percent in genes	Percent intergenic
1.00	0	0%	0%
2.00	1	0%	100%
3.00	2	0%	100%
4.00	3	0%	100%
5.00	3	0%	100%
6.00	3	0%	100%
7.00	3	0%	100%
8.00	3	0%	100%
9.00	3	0%	100%
10.00	3	0%	100%
11.00	3	0%	100%
12.00	3	0%	100%
13.00	4	25%	75%

Vibrio vulnificus YJ016 chromosome I, complete sequence

Cutoff	Total sites found	Percent in genes	Percent intergenic
1.00	0	0%	0%
2.00	0	0%	0%
3.00	0	0%	0%
4.00	0	0%	0%
5.00	0	0%	0%
6.00	0	0%	0%
7.00	0	0%	0%
8.00	0	0%	0%
9.00	0	0%	0%
10.00	0	0%	0%
11.00	0	0%	0%
12.00	2	50%	50%
13.00	4	75%	25%

Vibrio vulnificus YJ016 chromosome II, complete sequence

Cutoff	Total sites found	Percent in genes	Percent intergenic
1.00	0	0%	0%
2.00	1	0%	100%
3.00	2	0%	100%
4.00	3	0%	100%
5.00	3	0%	100%
6.00	3	0%	100%
7.00	3	0%	100%
8.00	3	0%	100%
9.00	3	0%	100%
10.00	3	0%	100%
11.00	3	0%	100%
12.00	3	0%	100%
13.00	4	25%	75%

Xanthomonas campestris pv. campestris str. 8004, complete genome

Cutoff	Total sites found	Percent in genes	Percent intergenic
1.00	0	0%	0%
2.00	0	0%	0%
3.00	0	0%	0%
4.00	0	0%	0%
5.00	0	0%	0%
6.00	0	0%	0%
7.00	0	0%	0%
8.00	0	0%	0%
9.00	1	0%	100%
10.00	1	0%	100%
11.00	2	0%	100%
12.00	2	0%	100%
13.00	3	0%	100%

Xanthomonas campestris pv. campestris str. ATCC 33913, complete genome

Cutoff	Total sites found	Percent in genes	Percent intergenic
1.00	0	0%	0%
2.00	0	0%	0%
3.00	0	0%	0%
4.00	0	0%	0%
5.00	0	0%	0%
6.00	0	0%	0%
7.00	0	0%	0%
8.00	0	0%	0%
9.00	1	0%	100%
10.00	1	0%	100%
11.00	2	0%	100%
12.00	2	0%	100%
13.00	3	0%	100%

Xanthomonas campestris pv. vesicatoria str. 85-10, complete genome

Cutoff	Total sites found	Percent in genes	Percent intergenic
1.00	0	0%	0%
2.00	0	0%	0%
3.00	0	0%	0%
4.00	0	0%	0%
5.00	0	0%	0%
6.00	1	0%	100%
7.00	1	0%	100%
8.00	1	0%	100%
9.00	1	0%	100%
10.00	1	0%	100%
11.00	2	50%	50%
12.00	3	67%	33%
13.00	5	40%	60%

Xanthomonas axonopodis pv. citri str. 306, complete genome

Cutoff	Total sites found	Percent in genes	Percent intergenic
1.00	0	0%	0%
2.00	0	0%	0%
3.00	0	0%	0%
4.00	0	0%	0%
5.00	0	0%	0%
6.00	1	0%	100%
7.00	1	0%	100%
8.00	1	0%	100%
9.00	2	0%	100%
10.00	2	0%	100%
11.00	2	0%	100%
12.00	2	0%	100%
13.00	2	0%	100%

Xanthomonas oryzae pv. oryzae MAFF 311018, complete genome

Cutoff	Total sites found	Percent in genes	Percent intergenic
1.00	0	0%	0%
2.00	0	0%	0%
3.00	0	0%	0%
4.00	0	0%	0%
5.00	0	0%	0%
6.00	0	0%	0%
7.00	0	0%	0%
8.00	0	0%	0%
9.00	0	0%	0%
10.00	1	0%	100%
11.00	1	0%	100%
12.00	2	0%	100%
13.00	2	0%	100%

B.2 Pyscangenes table

Table B.2: The soxbox sites found in genomes containing SoxR. Column 1 is the site energy of the site. Column 2 is the sequence of the site. Column 3 is the operon position, whether the named operon is to the left or the right of the soxbox site. Column 4 is the distance from the soxbox site to the start of the operon. Column 5 are the genes contained in the adjacent operon.

Acidovorax avenae subsp. citrulli AAC00-1, complete genome

Site Energy	Sequence	Operon pos	Distance to start	Genes in operon
4.90	TTGACCTCAAGTTTAGTTGAGGTTCC	left right	-62 -90	Aave_2275 Aave_2276
8.12	TTGACCTCAACAATGGTTGAGGTTTG	left	-214	Aave_1362
9.29	TTGACTTCAAGTGGACTTGAAGTCGT	left right	-71 -62	Aave_2578 Aave_2579

Acidobacteria bacterium Ellin345, complete genome

Site Energy	Sequence	Operon pos	Distance to start	Genes in operon
1.61	TTGACCTCAAGTTTACTTGAGGTTTT	left right	-14 -97	Acid345_3972 Acid345_3973- Acid345_3974

Acidovorax avenae subsp. citrulli AAC00-1, complete genome

Site Energy	Sequence	Operon pos	Distance to start	Genes in operon
4.90	TTGACCTCAAGTTTAGTTGAGGTTCC	left right	-62 -90	Aave_2275 Aave_2276
8.12	TTGACCTCAACAATGGTTGAGGTTTG	left	-214	Aave_1362
9.29	TTGACTTCAAGTGGACTTGAAGTCGT	left right	-71 -62	Aave_2578 Aave_2579

Acinetobacter sp. ADP1, complete genome

Site Energy	Sequence	Operon pos	Distance to start	Genes in operon
1.54	TTGACCTCAAGTTAACTTGAGCTTTG	left right	-4 -42	soxR (ACIAD3082) ACIAD3083- ACIAD3084

Aeromonas hydrophila subsp. hydrophila ATCC 7966, complete genome

Site Energy	Sequence	Operon pos	Distance to start	Genes in operon
4.88	TTGACCTCAAGTTAGCTTTAACTTGC	left right	-8 -90	soxR (AHA_2710) AHA_2711

Agrobacterium tumefaciens str. C58 chromosome circular, complete sequence

Site Energy	Sequence	Operon pos	Distance to start	Genes in operon
6.29	TTGACCTCAACTATGGTTGAGGAATT	left	-33	Atu2361

Agrobacterium tumefaciens str. C58 chromosome linear, complete sequence

Site Energy	Sequence	Operon pos	Distance to start	Genes in operon
5.95	TTGACCTCAACTATAGTTGAGGAATT	left	-68	soxR (Atu3915)
6.67	TCGACCTCAACTCAAGTTGAGGTTGT	left	-108	Atu4895

Agrobacterium tumefaciens str. C58 chromosome linear, complete sequence

Site Energy	Sequence	Operon pos	Distance to start	Genes in operon
5.95	TTGACCTCAACTATAGTTGAGGAATT	left	-68	soxR (Atu3915)
6.67	TCGACCTCAACTCAAGTTGAGGTTGT	left	-108	Atu4895

Arthrobacter aurescens TC1, complete genome

Site Energy	Sequence	Operon pos	Distance to start	Genes in operon
5.78	TTGACCTCAACTTAAGTTGAGGTCCT	left right	-64 -160	AAur_0213 ureA (AAur_0214)- ureB (AAur_0215)- ureC (AAur_0216)- ureE (AAur_0217)

Bdellovibrio bacteriovorus HD100, complete genome

Site Energy	Sequence	Operon pos	Distance to start	Genes in operon
1.10	TTGACCTCAAGTTAACTTGAGGTTGT	left right	-7 -113	soxR (Bd1002) Bd1003
8.34	TTTACATCAACTTAACTCGAGTTTTC	left right	-67 -98	Bd1662 Bd1663

Bordetella bronchiseptica RB50, complete genome

Site Energy	Sequence	Operon pos	Distance to start	Genes in operon
6.63	TTGACCTCAAGCTAGCTTGAGGGTCC	left	-90	BB4154

Bordetella parapertussis 12822, complete genome

Site Energy	Sequence	Operon pos	Distance to start	Genes in operon
8.93	TTGACCTCAAGCTCGCTTGAGGGTCC	left	-89	BPP3708

Bordetella pertussis Tohama I, complete genome

Site Energy	Sequence	Operon pos	Distance to start	Genes in operon
6.63	TTGACCTCAAGCTAGCTTGAGGGTCC	left	-141	BP2837

Burkholderia sp. 383 chromosome 3, complete sequence

Site Energy	Sequence	Operon pos	Distance to start	Genes in operon

Burkholderia sp. 383 chromosome 1, complete sequence

Site Energy	Sequence	Operon pos	Distance to start	Genes in operon

Burkholderia sp. 383 chromosome 2, complete sequence

Site Energy	Sequence	Operon pos	Distance to start	Genes in operon
3.99	TTGACCTCAAGTGAACTTGAAGTTGC	left	-2	Bcep18194_B1905
		right	-164	Bcep18194_B1906
7.14	TTGACTTGAAGTTAACTTCAACTTTT	left	-19	Bcep18194_B1003
		right	-87	Bcep18194_B1004-Bcep18194_B1005-Bcep18194_B1006
9.80	TTGACCTCAAGCCGGCTTGAAGCAGC	left	-42	Bcep18194_B1876
		right	-185	Bcep18194_B1877-Bcep18194_B1878

Burkholderia cenocepacia AU 1054 chromosome 1, complete sequence

Site Energy	Sequence	Operon pos	Distance to start	Genes in operon

Burkholderia cenocepacia AU 1054 chromosome 2, complete sequence

Site Energy	Sequence	Operon pos	Distance to start	Genes in operon
3.99	TTGACCTCAAGTGAACTTGAAGTTGC	left	-2	Bcen_4236
		right	-164	Bcen_4237
7.14	TTGACTTGAAGTTAACTTCAACTTTT	left	-18	Bcen_3620
		right	-87	Bcen_3621

Burkholderia cenocepacia AU 1054 chromosome 3, complete sequence

Site Energy	Sequence	Operon pos	Distance to start	Genes in operon

Burkholderia cenocepacia HI2424 chromosome 1, complete sequence

Site Energy	Sequence	Operon pos	Distance to start	Genes in operon

Burkholderia cenocepacia HI2424 chromosome 2, complete sequence

Site Energy	Sequence	Operon pos	Distance to start	Genes in operon
3.99	TTGACCTCAAGTGAACTTGAAGTTGC	left	-112	Bcen2424_4129
		right	-54	Bcen2424_4130
7.14	TTGACTTGAAGTTAACTTCAACTTTT	left	-35	Bcen2424_4746- Bcen2424_4745- Bcen2424_4744
		right	-70	Bcen2424_4747

Burkholderia cenocepacia HI2424 chromosome 3, complete sequence

Site Energy	Sequence	Operon pos	Distance to start	Genes in operon

Burkholderia cenocepacia HI2424 plasmid 1, complete sequence

Site Energy	Sequence	Operon pos	Distance to start	Genes in operon

Chromobacterium violaceum ATCC 12472, complete genome

Site Energy	Sequence	Operon pos	Distance to start	Genes in operon
4.25	TTGACTTCAAGTTAACTTGAACTTTG	left	-7	soxR (CV2793)
		right	-87	CV2794- CV2795
5.06	TTGACTTCAAGTTAACTTTAACTTTC	left	-87	ebrB (CV3243)

Erythrobacter litoralis HTCC2594, complete genome

Site Energy	Sequence	Operon pos	Distance to start	Genes in operon
3.23	TTGACCTCAAGTCAGCTTGAGGTTGC	left	-27	ELI_02950
		right	-142	ELI_02955

Escherichia coli CFT073, complete genome

Site Energy	Sequence	Operon pos	Distance to start	Genes in operon
2.14	TTTACCTCAAGTTAACTTGAGGAATT	left	-52	soxS (c5053)
		right	-59	soxR (c5054)

Escherichia coli K12, complete genome

Site Energy	Sequence	Operon pos	Distance to start	Genes in operon
2.14	TTTACCTCAAGTTAACTTGAGGAATT	left	-52	soxS (b4062)
		right	-59	soxR (b4063)

Frankia alni ACN14a, complete genome

Site Energy	Sequence	Operon pos	Distance to start	Genes in operon

Frankia sp. CcI3, complete genome

Site Energy	Sequence	Operon pos	Distance to start	Genes in operon
9.44	TTGACTTCAATCATGGTTGAGGTTTT	left	-113	Francci3_1887

Hahella chejuensis KCTC 2396, complete genome

Site Energy	Sequence	Operon pos	Distance to start	Genes in operon
1.67	TTGACCTAAAGTTAAGTTGAGGTTTT	left	-10	soxR (HCH_01441)
		right	-96	HCH_01442
5.63	TTGACCTCAAGTCGACTTGAGCTTGT	left	-6	HCH_01327
		right	-140	HCH_01328
9.44	TTGACCTAAAGCTGACTTTAACTTGC	left	-7	HCH_01117
		right	-98	HCH_01118

Hyphomonas neptunium ATCC 15444, complete genome

Site Energy	Sequence	Operon pos	Distance to start	Genes in operon
5.92	TTGATCTAAAGTGAACTTGAGATTGT	left	-43	HNE_3425
		right	-64	soxR (HNE_3426)

Maricaulis maris MCS10, complete genome

Site Energy	Sequence	Operon pos	Distance to start	Genes in operon
9.33	TTGACCTCAACCAAGGTTAAGCAATT	left	-3	Mmar10_0144
		right	-103	Mmar10_0145

Mesorhizobium loti MAFF303099, complete genome

Site Energy	Sequence	Operon pos	Distance to start	Genes in operon
3.74	TTGACCTCAACTTAAGTTGAGATTGT	left	-104	mlr7819
4.58	TTGACCTCAAGTTATGTTGAGCTTGT	left	-66	mlr2720
8.86	TTGACCTCAAGTCGGCTTGAACTCGT	left	-9	mll5378
		right	-100	mlr5379

Mycobacterium vanbaalenii PYR-1, complete genome

Site Energy	Sequence	Operon pos	Distance to start	Genes in operon
9.98	TTGACCTGAACAATAGTTGAGGTTGC	left	-125	Mvan_5552
		right	-64	Mvan_5553

Mycobacterium sp. JLS, complete genome

Site Energy	Sequence	Operon pos	Distance to start	Genes in operon
6.91	TTGACCTGAACTTTGGTTGAGGTCTT	left	-13	Mjls_1491
		right	-108	Mjls_1492
8.71	TTGACCTGAACTTTGGTTGAGGTCGG	left	-32	Mjls_2737
		right	-64	Mjls_2738
9.40	TTGACCTGAAGTTCTGTTGAGGTACG	left	-15	Mjls_1552
		right	-63	Mjls_1553
9.94	TTGACCTCACCTTTTGTTGAGGTTCT	left	-11	Mjls_4828
		right	-89	Mjls_4829

Mycobacterium sp. KMS, complete genome

Site Energy	Sequence	Operon pos	Distance to start	Genes in operon
6.91	TTGACCTGAACTTTGGTTGAGGTCTT	left	-13	Mkms_1515
		right	-180	Mkms_1516
8.71	TTGACCTGAACTTTGGTTGAGGTCGG	left	-32	Mkms_2751
		right	-64	Mkms_2752
9.40	TTGACCTGAAGTTCTGTTGAGGTACG	left	-15	Mkms_1606
		right	-63	Mkms_1607
9.94	TTGACCTCACCTTTTGTTGAGGTTCT	left	-11	Mkms_4533
		right	-90	Mkms_4534

Mycobacterium sp. MCS, complete genome

Site Energy	Sequence	Operon pos	Distance to start	Genes in operon
6.91	TTGACCTGAACTTTGGTTGAGGTCTT	left	-13	Mmcs_1493
		right	-180	Mmcs_1494
8.71	TTGACCTGAACTTTGGTTGAGGTCGG	left	-32	Mmcs_2707
		right	-64	Mmcs_2708
9.40	TTGACCTGAAGTTCTGTTGAGGTACG	left	-15	Mmcs_1582
		right	-102	Mmcs_1583
9.94	TTGACCTCACCTTTTGTTGAGGTTCT	left	-11	Mmcs_4446
		right	-90	Mmcs_4447

Mycobacterium smegmatis str. MC2 155, complete genome

Site Energy	Sequence	Operon pos	Distance to start	Genes in operon
7.79	TTCACCTGAAGTAAGGTTTAGGTGTC	left	-20	arcA (MSMEG_5448)
		right	-58	soxR (MSMEG_5450)
8.44	TTGACCTCATCATTGGTTGAGGTTTT	left	-11	MSMEG_5661
		right	-130	prrA (MSMEG_5662)-MSMEG_5663
8.71	TTGACCTCAACCTCACTTGAGGTGCC	left	-171	MSMEG_0572-MSMEG_0571-MSMEG_0570-MSMEG_0569-MSMEG_0568-MSMEG_0567-MSMEG_0566-MSMEG_0565-MSMEG_0564
		right	-170	MSMEG_0574
9.34	TTGACCTCAACTTTCGTTGAGGTCCT	left	-63	MSMEG_5819-MSMEG_5820

Nocardia farcinica IFM 10152, complete genome

Site Energy	Sequence	Operon pos	Distance to start	Genes in operon
4.94	TTGACTTCAAGTGAACTTGAAATTTT	left	-66	nfa33330
		right	-76	nfa33340
8.71	TTGACCTCAACATTGGTTGAGGAAGC	left	-54	nfa29630-nfa29620
9.04	TTGACCTCGAGCGAGGTCGAGGTTGT	left	-117	nfa21820
		right	-58	nfa21830
9.31	TTGCCCTGAACTTTGGTTGAGGTCTT	left	-29	nfa56070
		right	-100	nfa56080

Novosphingobium aromaticivorans DSM 12444, complete genome

Site Energy	Sequence	Operon pos	Distance to start	Genes in operon
4.72	TTGATCTCAAGCTAACTTGAGGTTGC	left	-49	Saro_0953-Saro_0952
		right	-128	Saro_0954

Photobacterium profundum SS9 chromosome 1, complete sequence

Site Energy	Sequence	Operon pos	Distance to start	Genes in operon

Photobacterium profundum SS9 chromosome 2, complete sequence

Site Energy	Sequence	Operon pos	Distance to start	Genes in operon
6.16	TTGACCTCAAGTTAACCTGAGGCACT	left right	-23 -91	PBPRB1505 PBPRB1506

Polaromonas sp. JS666, complete genome

Site Energy	Sequence	Operon pos	Distance to start	Genes in operon
2.71	TTGACCTCAACTTTACTTGAGGTTTT	left right	-10 -112	Bpro_1373 Bpro_1374

Pseudomonas aeruginosa PAO1, complete genome

Site Energy	Sequence	Operon pos	Distance to start	Genes in operon
1.10	TTGACCTCAACTTAACTTGAGGTTTT	left	-154	mexG (PA4205)-mexH (PA4206)-mexI (PA4207)-opmD (PA4208)
1.95	TTGACCTCAAGTTTGCTTGAGGTTTT	left right	-7 -96	PA2273 PA2274
2.42	TTTACCTCAAGTTAACTTGAGCTATC	left	-60	PA3718
8.78	TTGACCTCAAGTCGACTTGAAGTGGA	left right	-53 -56	PA5115 PA5116

Pseudomonas entomophila L48, complete genome

Site Energy	Sequence	Operon pos	Distance to start	Genes in operon
6.68	TTGACCTTGAGTTAACTGGAGGTTTT	left right	-48 -63	PSEEN3529 soxR (PSEEN3530)

Pseudomonas fluorescens Pf-5, complete genome

Site Energy	Sequence	Operon pos	Distance to start	Genes in operon
7.78	TTGACCTTGACTTAACTAGAGGTTTT	left right	-55 -79	PFL_4159 soxR (PFL_4160)

Pseudomonas fluorescens PfO-1, complete genome

Site Energy	Sequence	Operon pos	Distance to start	Genes in operon
4.89	TTTACCTCTAGTTAACTCGAGGTTTT	left right	-50 -66	Pfl_3919 Pfl_3920

Pseudomonas putida KT2440, complete genome

Site Energy	Sequence	Operon pos	Distance to start	Genes in operon
4.92	TCGACCTAAAGTTAAGTTGAGCTTTT	left	-6	soxR (PP_2060)
6.80	TTGACCTCGAGTTAAGTCAAGGTTTT	left	-288	PP_2505
		right	-55	PP_2506
8.88	TTGACCTTGACTTTACTTGAGGTCTT	left	-100	PP_2235
9.18	TTGACCTCGAGTTAACTTAAGGTCCG	left	-37	PP_3522
		right	-147	PP_3523

Ralstonia eutropha H16 chromosome 1, complete sequence

Site Energy	Sequence	Operon pos	Distance to start	Genes in operon
8.24	TTGACCTCAAGTCGACTTGAACTGGC	left	-45	h16_A0054 (H16_A0054)-h16_A0053 (H16_A0053)
		right	-55	h16_A0055 (H16_A0055)

Ralstonia eutropha H16 chromosome 2, complete sequence

Site Energy	Sequence	Operon pos	Distance to start	Genes in operon
3.92	TTGACCTCAATTTAGGTTGAGGTTTG	left	-50	h16_B2318 (H16_B2318)
		right	-71	h16_B2319 (H16_B2319)

Ralstonia metallidurans CH34 chromosome 1, complete sequence

Site Energy	Sequence	Operon pos	Distance to start	Genes in operon

Ralstonia metallidurans CH34 chromosome 2, complete sequence

Site Energy	Sequence	Operon pos	Distance to start	Genes in operon
5.63	TTGACCTCAAGCGTGCTTGAGGTTTG	left	-63	Rmet_4538
		right	-85	Rmet_4539

Rhizobium etli CFN 42, complete genome

Site Energy	Sequence	Operon pos	Distance to start	Genes in operon
6.80	TTGACCTCAATATTAGTTGAGGTTTT	left	-6	soxR (RHE_CH03863)
		right	-606	RHE_CH03864-RHE_CH03865
7.56	TTGACCTCAACCATAGTTGAGGAATT	left	-399	RHE_CH02960
		right	-89	RHE_CH02961

Rhizobium leguminosarum bv. viciae 3841, complete genome

Site Energy	Sequence	Operon pos	Distance to start	Genes in operon
3.56	TTGACCTCAGGTTAACTTGAGGAATT	left	-92	RL3412
4.60	TTGACCTCAAGATTAGTTGAGGTTTT	left	-6	RL4397
		right	-103	RL4398
8.62	TTGACCTCAAGTGGGGTTGGGGTTGC	left	-24	arcB (RL3003)

Rhodococcus sp. RHA1, complete genome

Site Energy	Sequence	Operon pos	Distance to start	Genes in operon
8.52	TTGACCTCGAGTAACGTTGAGGTTCT	left	-57	RHA1_ro06043
9.39	TTGACATGAAGTGGACTCGAGGTTTC	left	-3	RHA1_ro00215-RHA1_ro00214
		right	-171	RHA1_ro00216
9.98	TTGACCTGAACGCAACTCGACGTTTT	left	-11	RHA1_ro04736

Rhodopseudomonas palustris BisB5, complete genome

Site Energy	Sequence	Operon pos	Distance to start	Genes in operon
5.71	TTGACCTCAACTAAGGTTGAGGTTCT	left	-73	RPD_3140-RPD_3139
		right	-58	RPD_3141

Saccharopolyspora erythraea NRRL 2338, complete genome

Site Energy	Sequence	Operon pos	Distance to start	Genes in operon
7.72	TTGACCTCCAGCCAACTCGAAGTTTC	left	-11	SACE_5763-SACE_5762
		right	-98	soxR (SACE_5764)
7.80	TTGACCTCGACCTTGCTTGAGCTTTT	left	-44	SACE_4991
		right	-95	SACE_4992
8.19	TTGACCTGGAGTCAACTCGAAGTTTC	left	-206	SACE_1156
		right	-146	SACE_1157

Salmonella enterica subsp. enterica serovar Typhi str. CT18, complete genome

Site Energy	Sequence	Operon pos	Distance to start	Genes in operon
2.14	TTTACCTCAAGTTAACTTGAGGAATT	left	-53	soxS (STY4463)
		right	-59	soxR (STY4464)

Salmonella typhimurium LT2, complete genome

Site Energy	Sequence	Operon pos	Distance to start	Genes in operon
2.14	TTTACCTCAAGTTAACTTGAGGAATT	left right	-53 -59	soxS (STM4265) soxR (STM4266)

Shewanella frigidimarina NCIMB 400, complete genome

Site Energy	Sequence	Operon pos	Distance to start	Genes in operon
2.60	TTTACCTCAAGTTAGCTTTAGGTATT	left right	-41 -86	Sfri_1565 Sfri_1566

Shewanella denitrificans OS217, complete genome

Site Energy	Sequence	Operon pos	Distance to start	Genes in operon
1.18	TTGACCTCAAGTTAGCTTGAGCTTTT	left right	-38 -271	Sden_0647 Sden_0648
2.59	TTTACCTCAAGCTAACTTGAGGTTTT	left right	-33 -145	Sden_2124 Sden_2125
9.31	TGAACCTCAACTTAACTTTAGCTTTA	left	-89	Sden_0935

Shigella dysenteriae Sd197, complete genome

Site Energy	Sequence	Operon pos	Distance to start	Genes in operon
2.14	TTTACCTCAAGTTAACTTGAGGAATT	left right	-7 -104	soxR (SDY_4504) soxS (SDY_4505)

Shigella flexneri 2a str. 2457T, complete genome

Site Energy	Sequence	Operon pos	Distance to start	Genes in operon
2.14	TTTACCTCAAGTTAACTTGAGGAATT	left right	-52 -59	soxS (S3589) soxR (S3590)

Shigella flexneri 2a str. 301, complete genome

Site Energy	Sequence	Operon pos	Distance to start	Genes in operon
2.14	TTTACCTCAAGTTAACTTGAGGAATT	left right	-52 -59	soxS (SF4122) soxR (SF4123)

Shigella flexneri 5 str. 8401, complete genome

Site Energy	Sequence	Operon pos	Distance to start	Genes in operon
2.14	TTTACCTCAAGTTAACTTGAGGAATT	left	-7	soxR (SFV_4149)
		right	-104	soxS (SFV_4150)

Shigella sonnei Ss046, complete genome

Site Energy	Sequence	Operon pos	Distance to start	Genes in operon
2.14	TTTACCTCAAGTTAACTTGAGGAATT	left	-52	soxS (SSON_4242)
		right	-349	SSON_4243

Silicibacter sp. TM1040, complete genome

Site Energy	Sequence	Operon pos	Distance to start	Genes in operon
5.48	TTGATCTAAAGTGAGCTTGAGGAATT	left	-96	TM1040_1862-TM1040_1861-TM1040_1860-TM1040_1859
		right	-122	TM1040_1863
8.24	TTGACCTCAAGTTGACTTGAATTCGT	left	-2	TM1040_2614
		right	-91	TM1040_2615

Silicibacter pomeroyi DSS-3, complete genome

Site Energy	Sequence	Operon pos	Distance to start	Genes in operon
5.12	TTGACCTAAAGTTAGGTTTAGAAATT	left	-38	SPO0313
		right	-72	soxR (SPO0314)
8.64	TTGACCTCAAGTTGACTTGAATTCGC	left	-2	SPO3734
		right	-91	SPO3735

Sinorhizobium meliloti 1021, complete genome

Site Energy	Sequence	Operon pos	Distance to start	Genes in operon
6.98	TTGACCTCAACTATAGTTGAGGTTCT	left	-44	SMc00183
		right	-60	SMc00182
8.01	TTGACCTCAAGTACGGTTGAGGTCGC	left	-88	SMc03095

Sphingopyxis alaskensis RB2256, complete genome

Site Energy	Sequence	Operon pos	Distance to start	Genes in operon
7.65	TTGACCTCCACTGCACTTGAGCTTTC	left	-37	Sala_2373

Streptomyces avermitilis MA-4680, complete genome

Site Energy	Sequence	Operon pos	Distance to start	Genes in operon
5.53	TTGACCTGAAGTTTGGTTGAGGTTGC	left	-637	gbsA1 (SAV1622)
		right	-64	SAV1623
6.45	TTGACCTCAAGATTGCTTGAGGTTCT	left	-253	SAV7217
		right	-64	SAV7218
7.73	TTGACCTCAAGATTGGTTGAGGTACC	left	-328	SAV5664
		right	-82	SAV5665

Streptomyces coelicolor A3(2), complete genome

Site Energy	Sequence	Operon pos	Distance to start	Genes in operon
5.78	TTGACCTCAAGCAAACTTGAGGTACC	left	-57	SCO2478
		right	-178	SCO2479
8.53	TTGACCTCAAGCAGGCTTGAGGTCGT	left	-45	SCO4266
8.75	TTGACCTCAAGGTTGGTCGAGGTTCT	left	-169	SCO7007
		right	-70	SCO7008

Thermobifida fusca YX, complete genome

Site Energy	Sequence	Operon pos	Distance to start	Genes in operon
3.74	TTGACCTCAACTTTGGTTGAGGTTTT	left	-278	Tfu_1696-Tfu_1695
		right	-133	Tfu_1697
6.65	TTGACCTCAACCTAACCTGAGATTTG	left	-27	Tfu_0408
		right	-141	Tfu_0409
8.94	TGGATCTCACCTTAGGTTGAGGTTTC	left	-431	Tfu_1567

Thermococcus kodakarensis KOD1, complete genome

Site Energy	Sequence	Operon pos	Distance to start	Genes in operon

Vibrio cholerae O1 biovar eltor str. N16961 chromosome I, complete sequence

Site Energy	Sequence	Operon pos	Distance to start	Genes in operon

Vibrio cholerae O1 biovar eltor str. N16961 chromosome II, complete sequence

Site Energy	Sequence	Operon pos	Distance to start	Genes in operon
2.14	TTTACCTAAAGTTAACTTGAGGTATT	left	-115	VCA0084
		right	-89	VCA0085

Vibrio parahaemolyticus RIMD 2210633 chromosome II, complete sequence

Site Energy	Sequence	Operon pos	Distance to start	Genes in operon
4.79	TTTACCTCAAGTTTACTTGAGGTTCT	left	-89	VPA0335
5.08	TTGACCTAAACCAAACTTGAGGTTTT	left	-99	VPA1738
5.48	TTTACCTCGATTTAACTTGAGGTTTT	left	-96	VPA1685
5.59	TTTACCTAAACTTAGCTTGAGGTTCT	left right	-163 -98	VPA0390 VPA0391

Vibrio vulnificus CMCP6 chromosome I, complete sequence

Site Energy	Sequence	Operon pos	Distance to start	Genes in operon

Vibrio vulnificus CMCP6 chromosome II, complete sequence

Site Energy	Sequence	Operon pos	Distance to start	Genes in operon
1.16	TTGACCTCAAGTTAACTTGAGGAATT	left	-109	VV2_1129
2.52	TTTACCTCAAGTTAAGTTGAGCTTTT	left right	-57 -97	VV2_0936 VV2_0937
3.18	TTTACCTCAATTTAACTTGAGGTTTT	left right	-35 -230	VV2_0607 VV2_0608

Vibrio vulnificus YJ016 chromosome I, complete sequence

Site Energy	Sequence	Operon pos	Distance to start	Genes in operon

Vibrio vulnificus YJ016 chromosome II, complete sequence

Site Energy	Sequence	Operon pos	Distance to start	Genes in operon
1.16	TTGACCTCAAGTTAACTTGAGGAATT	left	-110	VVA1655- VVA1656
2.52	TTTACCTCAAGTTAAGTTGAGCTTTT	left right	-57 -79	VVA1425 VVA1426
3.18	TTTACCTCAATTTAACTTGAGGTTTT	left right	-35 -230	VVA1158 VVA1159

Xanthomonas campestris pv. campestris str. 8004, complete genome

Site Energy	Sequence	Operon pos	Distance to start	Genes in operon
8.71	TTGACCTCAACCTTGGTTGAGGCAGG	left right	-166 -56	XC_1279 XC_1280

Xanthomonas campestris pv. campestris str. ATCC 33913, complete genome

Site Energy	Sequence	Operon pos	Distance to start	Genes in operon
8.71	TTGACCTCAACCTTGGTTGAGGCAGG	left	-4	soxR (XCC2831)
		right	-729	XCC2832

Xanthomonas campestris pv. vesicatoria str. 85-10, complete genome

Site Energy	Sequence	Operon pos	Distance to start	Genes in operon
5.49	TTGACCTCAACTTAGGTTGAGGCAGG	left	-4	soxR (XCV3149)
		right	-121	XCV3150

Xanthomonas axonopodis pv. citri str. 306, complete genome

Site Energy	Sequence	Operon pos	Distance to start	Genes in operon
5.49	TTGACCTCAACTTAGGTTGAGGCAGG	left	-4	soxR (XAC3000)
		right	-121	ptr (XAC3001)
8.02	TTGACCTCAACTGCGCTTGAGGTCGT	left	-31	XAC0314
		right	-278	XAC0315

Xanthomonas oryzae pv. oryzae MAFF 311018, complete genome

Site Energy	Sequence	Operon pos	Distance to start	Genes in operon
9.07	TTGACCTCAACTCAGGTTAAGGCAGG	left	-70	XOO1154 (XOO_1154)
		right	-56	XOO1155 (XOO_1155)

Bibliography

[1] J. B. Andersen, C. Sternberg, L. K. Poulsen, S. P. Bjorn, M. Givskov, and S. Molin. New unstable variants of green fluorescent protein for studies of transient gene expression in bacteria. *Appl Environ Microbiol*, 64(6):2240–6, Jun 1998.

[2] Y. Bao, D. P. Lies, H. Fu, and G. P. Roberts. An improved Tn7-based system for the single-copy insertion of cloned genes into chromosomes of gram-negative bacteria. *Gene*, 109(1):167–8, Dec 1991.

[3] M. S. Bartlett and R. L. Gourse. Growth rate-dependent control of the rrnB P1 core promoter in *Escherichia coli*. *J Bacteriol*, 176(17):5560–4, Sep 1994. (eng) (hard copy only).

[4] B. L. Bassler. How bacteria talk to each other: regulation of gene expression by quorum sensing. *Curr Opin Microbiol*, 2(6):582–7, Dec 1999.

[5] A. S. Beliaev, D. M. Klingeman, J. A. Klappenbach, L. Wu, M. F. Romine, J. M. Tiedje, K. H. Nealson, J. K. Fredrickson, and J. Zhou. Global transcriptome analysis of *Shewanella oneidensis* MR-1 exposed to different terminal electron acceptors. *J Bacteriol*, 187(20):7138–45, Oct 2005.

[6] A. S. Beliaev, D. K. Thompson, T. Khare, H. Lim, C. C. Brandt, G. Li, A. E. Murray, J. F. Heidelberg, C. S. Giometti, 3. r. d. Yates J, K. H. Nealson, J. M. Tiedje, and J. Zhoui. Gene and protein expression profiles of *Shewanella oneidensis* during anaerobic growth with different electron acceptors. *OMICS*, 6(1):39–60, 2002.

[7] R. Bencheikh-Latmani, S. M. Williams, L. Haucke, C. S. Criddle, L. Wu, J. Zhou, and B. M. Tebo. Global transcriptional profiling of *Shewanella oneidensis* MR-1 during Cr(VI) and U(VI) reduction. *Appl Environ Microbiol*, 71(11):7453–60, Nov 2005.

[8] O. G. Berg and P. H. von Hippel. Selection of DNA binding sites by regulatory proteins. Statistical-mechanical theory and application to operators and promoters. *J Mol Biol*, 193(4):723–50, Feb 1987.

[9] O. G. Berg and P. H. von Hippel. Selection of DNA binding sites by regulatory proteins. II. The binding specificity of cyclic AMP receptor protein to recognition sites. *J Mol Biol*, 200(4):709–23, Apr 1988.

[10] M. Berney, F. Hammes, F. Bosshard, H. U. Weilenmann, and T. Egli. Assessment and Interpretation of Bacterial Viability by Using the LIVE/DEAD BacLight Kit in Combination with Flow Cytometry. *Appl Environ Microbiol*, 73(10):3283–90, May 2007.

[11] J. C. Biffinger, J. Pietron, R. Ray, B. Little, and B. R. Ringeisen. A biofilm enhanced miniature microbial fuel cell using Shewanella oneidensis DSP10 and oxygen reduction cathodes. *Biosens Bioelectron*, 22(8):1672–9, Mar 2007.

[12] G. V. Bloemberg, A. H. Wijfjes, G. E. Lamers, N. Stuurman, and B. J. Lugtenberg. Simultaneous imaging of *Pseudomonas fluorescens* WCS365 populations expressing three different autofluorescent proteins in the rhizosphere: new perspectives for studying microbial communities. *Mol Plant Microbe Interact*, 13(11):1170–6, Nov 2000.

[13] B. R. Boles, M. Thoendel, and P. K. Singh. Self-generated diversity produces ïnsurance effectsïn biofilm communities. *Proc Natl Acad Sci U S A*, Nov 2004.

[14] R. C. Boucher. Airway surface dehydration in cystic fibrosis: pathogenesis and therapy. *Annu Rev Med*, 58:157–70, 2007.

[15] T. M. Bradley, E. Hidalgo, V. Leautaud, H. Ding, and B. Demple. Cysteine-to-alanine replacements in the *Escherichia coli* SoxR protein and the role of the [2Fe-2S] centers in transcriptional activation. *Nucleic Acids Res*, 25(8):1469–75, Apr 1997.

[16] F. Bredenbruch, R. Geffers, M. Nimtz, J. Buer, and S. Haussler. The *Pseudomonas aeruginosa* quinolone signal (PQS) has an iron-chelating activity. *Environ Microbiol*, 8(8):1318–29, Aug 2006.

[17] C. T. Brown and J. r. Callan CG. Evolutionary comparisons suggest many novel cAMP response protein binding sites in *Escherichia coli*. *Proc Natl Acad Sci U S A*, 101(8):2404–9, Feb 2004.

[18] N. L. Brown, J. V. Stoyanov, S. P. Kidd, and J. L. Hobman. The MerR family of transcriptional regulators. *FEMS Microbiol Rev*, 27(2-3):145–63, Jun 2003.

[19] F. Bushman. *Lateral DNA Transfer, Mechanisms and Consquences*. Cold Spring Harbor Laboratory Press, 2002.

[20] N. C. Caiazza and G. A. O'Toole. SadB is required for the transition from reversible to irreversible attachment during biofilm formation by *Pseudomonas aeruginosa* PA14. *J Bacteriol*, 186(14):4476–85, Jul 2004.

[21] A. Camilli and B. L. Bassler. Bacterial small-molecule signaling pathways. *Science*, 311(5764):1113–6, Feb 2006.

[22] W. Carpentier, K. Sandra, I. De Smet, A. Brige, L. De Smet, and J. Van Beeumen. Microbial reduction and precipitation of vanadium by Shewanella oneidensis. *Appl Environ Microbiol*, 69(6):3636–9, Jun 2003.

[23] M. Chander and B. Demple. Functional analysis of SoxR residues affecting transduction of oxidative stress signals into gene expression. *J Biol Chem*, 279(40):41603–10, Oct 2004.

[24] E. J. Cho and A. D. Ellington. Optimization of the biological component of a bioelectrochemical cell. *Bioelectrochemistry*, 70(1):165–72, Jan 2007.

[25] K. H. Choi, J. B. Gaynor, K. G. White, C. Lopez, C. M. Bosio, R. R. Karkhoff-Schweizer, and H. P. Schweizer. A Tn7-based broad-range bacterial cloning and expression system. *Nat Methods*, 2(6):443–8, Jun 2005.

[26] A. C. Cole, M. J. Semmens, and T. M. LaPara. Stratification of activity and bacterial community structure in biofilms grown on membranes transferring oxygen. *Appl Environ Microbiol*, 70(4):1982–9, Apr 2004.

[27] J. W. Costerton. Cystic fibrosis pathogenesis and the role of biofilms in persistent infection. *Trends Microbiol*, 9(2):50–2, Feb 2001.

[28] J. W. Costerton, L. Montanaro, and C. R. Arciola. Biofilm in implant infections: its production and regulation. *Int J Artif Organs*, 28(11):1062–8, Nov 2005.

[29] N. L. Craig. Tn7: a target site-specific transposon. *Mol Microbiol*, 5(11):2569–73, Nov 1991.

[30] M. E. Davey, N. C. Caiazza, and G. A. O'Toole. Rhamnolipid surfactant production affects biofilm architecture in *Pseudomonas aeruginosa* PAO1. *J Bacteriol*, 185(3):1027–36, Feb 2003.

[31] M. E. Davey and G. A. O'toole. Microbial biofilms: from ecology to molecular genetics. *Microbiol Mol Biol Rev*, 64(4):847–67, Dec 2000.

[32] D. G. Davies and G. G. Geesey. Regulation of the alginate biosynthesis gene algC in Pseudomonas aeruginosa during biofilm development in continuous culture. *Appl Environ Microbiol*, 61(3):860–7, Mar 1995.

[33] B. Demple. Study of redox-regulated transcription factors in prokaryotes. *Methods*, 11(3):267–78, Mar 1997.

[34] L. E. Dietrich, A. Price-Whelan, A. Petersen, M. Whiteley, and D. K. Newman. The phenazine pyocyanin is a terminal signalling factor in the quorum sensing network of *Pseudomonas aeruginosa*. *Mol Microbiol*, 61(5):1308–21, Sep 2006.

[35] W. Eiamphungporn, N. Charoenlap, P. Vattanaviboon, and S. Mongkolsuk. *Agrobacterium tumefaciens* soxR is involved in superoxide stress protection and also directly regulates superoxide-inducible expression of itself and a target gene. *J Bacteriol*, 188(24):8669–73, Dec 2006.

[36] A. S. Engel, M. L. Porter, L. A. Stern, S. Quinlan, and P. C. Bennett. Bacterial diversity and ecosystem function of filamentous microbial mats from aphotic (cave) sulfidic springs dominated by chemolithoautotrophic *Epsilonproteobacteria*. *FEMS Microbiol Ecol*, 51(1):31–53, Dec 2004.

[37] A. Finelli, C. V. Gallant, K. Jarvi, and L. L. Burrows. Use of In-Biofilm Expression Technology To Identify Genes Involved in *Pseudomonas aeruginosa* Biofilm Development. *J Bacteriol*, 185(9):2700–10, May 2003.

[38] B. Floriano and M. Bibb. afsR is a pleiotropic but conditionally required regulatory gene for antibiotic production in *Streptomyces coelicolor* A3(2). *Mol Microbiol*, 21(2):385–96, Jul 1996.

[39] W. C. Fuqua and S. C. Winans. A LuxR-LuxI type regulatory system activates Agrobacterium Ti plasmid conjugal transfer in the presence of a plant tumor metabolite. *J Bacteriol*, 176(10):2796–806, May 1994.

[40] W. C. Fuqua, S. C. Winans, and E. P. Greenberg. Quorum sensing in bacteria: the LuxR-LuxI family of cell density-responsive transcriptional regulators. *J Bacteriol*, 176(2):269–75, Jan 1994.

[41] W. Gao, Y. Liu, J. Zhou, and H. Pan. Effects of a strong static magnetic field on bacterium Shewanella oneidensis: an assessment by using whole genome microarray. *Bioelectromagnetics*, 26(7):558–63, Oct 2005.

[42] P. Gaudu and B. Weiss. SoxR, a [2Fe-2S] transcription factor, is active only in its oxidized form. *Proc Natl Acad Sci U S A*, 93(19):10094–8, Sep 1996.

[43] J. M. Ghigo. Are there biofilm-specific physiological pathways beyond a reasonable doubt? *Res Microbiol*, 154(1):1–8, Jan 2003.

[44] C. S. Giometti, T. Khare, S. L. Tollaksen, A. Tsapin, W. Zhu, 3. r. d. Yates JR, and K. H. Nealson. Analysis of the *Shewanella oneidensis* proteome by two-dimensional gel electrophoresis under nondenaturing conditions. *Proteomics*, 3(5):777–85, May 2003.

[45] J. T. Greenberg, P. Monach, J. H. Chou, P. D. Josephy, and B. Demple. Positive control of a global antioxidant defense regulon activated by superoxide-generating agents in *Escherichia coli*. *Proc Natl Acad Sci U S A*, 87(16):6181–5, Aug 1990.

[46] J. L. Groh, Q. Luo, J. D. Ballard, and L. R. Krumholz. A method adapting microarray technology for signature-tagged mutagenesis of Desulfovibrio desulfuricans G20 and *Shewanella oneidensis* MR-1 in anaerobic sediment survival experiments. *Appl Environ Microbiol*, 71(11):7064–74, Nov 2005.

[47] J. P. Grotzinger and A. H. Knoll. Stromatolites in Precambrian carbonates: evolutionary mileposts or environmental dipsticks? *Annu Rev Earth Planet Sci*, 27:313–58, 1999.

[48] L. Hall-Stoodley and P. Stoodley. Developmental regulation of microbial biofilms. *Curr Opin Biotechnol*, 13(3):228–33, Jun 2002.

[49] M. C. Hansen, J. r. Palmer RJ, C. Udsen, D. C. White, and S. Molin. Assessment of GFP fluorescence in cells of Streptococcus gordonii under conditions of low pH and low oxygen concentration. *Microbiology*, 147(Pt 5):1383–91, May 2001.

[50] H. J. Harmsen, H. M. Kengen, A. D. Akkermans, A. J. Stams, and W. M. de Vos. Detection and localization of syntrophic propionate-oxidizing bacteria in granular sludge by in situ hybridiza-

tion using 16S rRNA-based oligonucleotide probes. *Appl Environ Microbiol*, 62(5):1656–63, May 1996.

[51] S. Heeb, Y. Itoh, T. Nishijyo, U. Schnider, C. Keel, J. Wade, U. Walsh, F. O'Gara, and D. Haas. Small, stable shuttle vectors based on the minimal pVS1 replicon for use in gram-negative, plant-associated bacteria. *Mol Plant Microbe Interact*, 13(2):232–7, Feb 2000.

[52] J. F. Heidelberg, I. T. Paulsen, K. E. Nelson, E. J. Gaidos, W. C. Nelson, T. D. Read, J. A. Eisen, R. Seshadri, N. Ward, B. Methe, R. A. Clayton, T. Meyer, A. Tsapin, J. Scott, M. Beanan, L. Brinkac, S. Daugherty, R. T. DeBoy, R. J. Dodson, A. S. Durkin, D. H. Haft, J. F. Kolonay, R. Madupu, J. D. Peterson, L. A. Umayam, O. White, A. M. Wolf, J. Vamathevan, J. Weidman, M. Impraim, K. Lee, K. Berry, C. Lee, J. Mueller, H. Khouri, J. Gill, T. R. Utterback, L. A. McDonald, T. V. Feldblyum, H. O. Smith, J. C. Venter, K. H. Nealson, and C. M. Fraser. Genome sequence of the dissimilatory metal ion-reducing bacterium *Shewanella oneidensis*. *Nat Biotechnol*, Oct 2002.

[53] M. E. Hernandez, A. Kappler, and D. K. Newman. Phenazines and Other Redox-Active Antibiotics Promote Microbial Mineral Reduction. *Appl Environ Microbiol*, 70(2):921–928, Feb 2004.

[54] E. Hidalgo and B. Demple. An iron-sulfur center essential for transcriptional activation by the redox-sensing SoxR protein. *EMBO J*, 13(1):138–46, Jan 1994.

[55] E. Hidalgo and B. Demple. Spacing of promoter elements regulates the basal expression of the soxS gene and converts SoxR from a transcriptional activator into a repressor. *EMBO J*, 16(5):1056–65, Mar 1997.

[56] E. Hidalgo, H. Ding, and B. Demple. Redox signal transduction via iron-sulfur clusters in the SoxR transcription activator. *Trends Biochem Sci*, 22(6):207–10, Jun 1997.

[57] E. Hidalgo, V. Leautaud, and B. Demple. The redox-regulated SoxR protein acts from a single DNA site as a repressor and an allosteric activator. *EMBO J*, 17(9):2629–36, May 1998.

[58] E. Hidalgo, J. r. Bollinger JM, T. M. Bradley, C. T. Walsh, and B. Demple. Binuclear [2Fe-2S] clusters in the *Escherichia coli* SoxR protein and role of the metal centers in transcription. *J Biol Chem*, 270(36):20908–14, Sep 1995.

[59] D. E. Holmes, D. R. Bond, R. A. O'Neil, C. E. Reimers, L. R. Tender, and D. R. Lovley. Microbial communities associated with electrodes harvesting electricity from a variety of aquatic sediments. *Microb Ecol*, 48(2):178–90, Aug 2004.

[60] C. K. Hope, D. Clements, and M. Wilson. Determining the spatial distribution of viable and nonviable bacteria in hydrated microcosm dental plaques by viability profiling. *J Appl Microbiol*, 93(3):448–55, 2002.

[61] C. T. Huang, K. D. Xu, G. A. McFeters, and P. S. Stewart. Spatial patterns of alkaline phosphatase expression within bacterial colonies and biofilms in response to phosphate starvation. *Appl Environ Microbiol*, 64(4):1526–31, Apr 1998.

[62] C. T. Huang, F. P. Yu, G. A. McFeters, and P. S. Stewart. Nonuniform spatial patterns of respiratory activity within biofilms during disinfection. *Appl Environ Microbiol*, 61(6):2252–6, Jun 1995.

[63] J. Huang, J. Shi, V. Molle, B. Sohlberg, D. Weaver, M. J. Bibb, N. Karoonuthaisiri, C. J. Lih, C. M. Kao, M. J. Buttner, and S. N. Cohen. Cross-regulation among disparate antibiotic biosynthetic pathways of *Streptomyces coelicolor*. *Mol Microbiol*, 58(5):1276–87, Dec 2005.

[64] S. M. Hunt, E. M. Werner, B. Huang, M. A. Hamilton, and P. S. Stewart. Hypothesis for the role of nutrient starvation in biofilm detachment. *Appl Environ Microbiol*, 70(12):7418–25, Dec 2004.

[65] M. Juhas, L. Eberl, and B. Tummler. Quorum sensing: the power of cooperation in the world of Pseudomonas. *Environ Microbiol*, 7(4):459–71, Apr 2005.

[66] S. T. Kelley, U. Theisen, L. T. Angenent, A. St Amand, and N. R. Pace. Molecular analysis of shower curtain biofilm microbes. *Appl Environ Microbiol*, 70(7):4187–92, Jul 2004.

[67] T. R. De Kievit, M. D. Parkins, R. J. Gillis, R. Srikumar, H. Ceri, K. Poole, B. H. Iglewski, and D. G. Storey. Multidrug efflux pumps: expression patterns and contribution to antibiotic resistance in *Pseudomonas aeruginosa* biofilms. *Antimicrob Agents Chemother*, 45(6):1761–70, Jun 2001.

[68] M. Klausen, A. Aaes-Jorgensen, S. Molin, and T. Tolker-Nielsen. Involvement of bacterial migration in the development of complex multicellular structures in *Pseudomonas aeruginosa* biofilms. *Mol Microbiol*, 50(1):61–8, Oct 2003.

[69] K. Kobayashi and S. Tagawa. Activation of SoxR-dependent transcription in Pseudomonas aeruginosa. *J Biochem (Tokyo)*, 136(5):607–15, Nov 2004.

[70] B. Koch, L. E. Jensen, and O. Nybroe. A panel of Tn7-based vectors for insertion of the gfp marker gene or for delivery of cloned DNA into Gram-negative bacteria at a neutral chromosomal site. *J Microbiol Methods*, 45(3):187–95, Jul 2001. (eng) (hard copy only).

[71] P. E. Kolenbrander. Oral microbial communities: biofilms, interactions, and genetic systems. *Annu Rev Microbiol*, 54:413–37, 2000.

[72] L. Lambertsen, C. Sternberg, and S. Molin. Mini-Tn7 transposons for site-specific tagging of bacteria with fluorescent proteins. *Environ Microbiol*, 6(7):726–32, Jul 2004.

[73] J. B. Laursen and J. Nielsen. Phenazine natural products: biosynthesis, synthetic analogues, and biological activity. *Chem Rev*, 104(3):1663–86, Mar 2004.

[74] A. B. Leaphart, D. K. Thompson, K. Huang, E. Alm, X. F. Wan, A. Arkin, S. D. Brown, L. Wu, T. Yan, X. Liu, G. S. Wickham, and J. Zhou. Transcriptome profiling of *Shewanella oneidensis* gene expression following exposure to acidic and alkaline pH. *J Bacteriol*, 188(4):1633–42, Feb 2006.

[75] Y. Lequette and E. P. Greenberg. Timing and Localization of Rhamnolipid Synthesis Gene Expression in *Pseudomonas aeruginosa* Biofilms. *J Bacteriol*, 187(1):37–44, Jan 2005.

[76] K. Lewis. Persister cells, dormancy and infectious disease. *Nat Rev Microbiol*, 5(1):48–56, Jan 2007.

[77] D. P. Lies, M. E. Hernandez, A. Kappler, R. E. Mielke, J. A. Gralnick, and D. K. Newman. *Shewanella oneidensis* MR-1 Uses Overlapping Pathways for Iron Reduction at a Distance and by Direct Contact under Conditions Relevant for Biofilms. *Appl Environ Microbiol*, 71(8):4414–26, Aug 2005.

[78] J. Liu. . PhD thesis, University of Wisconsin, 2003.

[79] Y. Liu, W. Gao, Y. Wang, L. Wu, X. Liu, T. Yan, E. Alm, A. Arkin, D. K. Thompson, M. W. Fields, and J. Zhou. Transcriptome Analysis of *Shewanella oneidensis* MR-1 in Response to Elevated Salt Conditions. *J Bacteriol*, 187(7):2501–7, Apr 2005.

[80] T. F. Mah, B. Pitts, B. Pellock, G. C. Walker, P. S. Stewart, and G. A. O'Toole. A genetic basis for *Pseudomonas aeruginosa* biofilm antibiotic resistance. *Nature*, 426(6964):306–10, Nov 2003.

[81] T. M. Maier, J. M. Myers, and C. R. Myers. Identification of the gene encoding the sole physiological fumarate reductase in *Shewanella oneidensis* MR-1. *J Basic Microbiol*, 43(4):312–27, 2003.

[82] P. D. Majors, J. S. McLean, G. E. Pinchuk, J. K. Fredrickson, Y. A. Gorby, K. R. Minard, and R. A. Wind. NMR methods for in situ biofilm metabolism studies. *J Microbiol Methods*, Jun 2005.

[83] S. L. McKnight, B. H. Iglewski, and E. C. Pesci. The Pseudomonas quinolone signal regulates rhl quorum sensing in *Pseudomonas aeruginosa*. *J Bacteriol*, 182(10):2702–8, May 2000.

[84] G. Meshulam-Simon, S. Behrens, A. D. Choo, and A. M. Spormann. Hydrogen metabolism in *Shewanella oneidensis* MR-1. *Appl Environ Microbiol*, 73(4):1153–65, Feb 2007.

[85] D. Minz, J. L. Flax, S. J. Green, G. Muyzer, Y. Cohen, M. Wagner, B. E. Rittmann, and D. A. Stahl. Diversity of sulfate-reducing bacteria in oxic and anoxic regions of a microbial mat characterized by comparative analysis of dissimilatory sulfite reductase genes. *Appl Environ Microbiol*, 65(10):4666–71, Oct 1999.

[86] S. Moller, C. Sternberg, J. B. Andersen, B. B. Christensen, J. L. Ramos, M. Givskov, and S. Molin. In situ gene expression in mixed-culture biofilms: evidence of metabolic interactions between community members. *Appl Environ Microbiol*, 64(2):721–32, Feb 1998.

[87] T. S. Murray, M. Egan, and B. I. Kazmierczak. *Pseudomonas aeruginosa* chronic colonization in cystic fibrosis patients. *Curr Opin Pediatr*, 19(1):83–8, Feb 2007.

[88] C. R. Myers and J. M. Myers. Replication of plasmids with the p15A origin in *Shewanella putrefaciens* MR-1. *Lett Appl Microbiol*, 24(3):221–5, Mar 1997.

[89] Y. V. Nancharaiah, V. P. Venugopalan, S. Wuertz, P. A. Wilderer, and M. Hausner. Compatibility of the green fluorescent protein and a general nucleic acid stain for quantitative description of a *Pseudomonas putida* biofilm. *J Microbiol Methods*, 60(2):179–87, Feb 2005.

[90] A. T. Nielsen, T. Tolker-Nielsen, K. B. Barken, and S. Molin. Role of commensal relationships on the spatial structure of a surface-attached microbial consortium. *Environ Microbiol*, 2(1):59–68, Feb 2000.

[91] S. Okabe, T. Itoh, H. Satoh, and Y. Watanabe. Analyses of spatial distributions of sulfate-reducing bacteria and their activity in aerobic wastewater biofilms. *Appl Environ Microbiol*, 65(11):5107–16, Nov 1999.

[92] G. A. O'Toole. To build a biofilm. *J Bacteriol*, 185(9):2687–9, May 2003.

[93] M. Palma, J. Zurita, J. A. Ferreras, S. Worgall, D. H. Larone, L. Shi, F. Campagne, and L. E. Quadri. *Pseudomonas aeruginosa* SoxR does not conform to the archetypal paradigm for SoxR-dependent regulation of the bacterial oxidative stress adaptive response. *Infect Immun*, 73(5):2958–66, May 2005.

[94] W. Park, S. Pena-Llopis, Y. Lee, and B. Demple. Regulation of superoxide stress in *Pseudomonas putida* KT2440 is different from the SoxR paradigm in *Escherichia coli*. *Biochem Biophys Res Commun*, 341(1):51–6, Mar 2006.

[95] G. Patterson, R. N. Day, and D. Piston. Fluorescent protein spectra. *J Cell Sci*, 114(Pt 5):837–8, Mar 2001.

[96] P. J. Pomposiello and B. Demple. Identification of SoxS-regulated genes in *Salmonella enterica* serovar typhimurium. *J Bacteriol*, 182(1):23–9, Jan 2000.

[97] P. J. Pomposiello and B. Demple. Redox-operated genetic switches: the SoxR and OxyR transcription factors. *Trends Biotechnol*, 19(3):109–14, Mar 2001.

[98] L. K. Poulsen, G. Ballard, and D. A. Stahl. Use of rRNA fluorescence in situ hybridization for measuring the activity of single cells in young and established biofilms. *Appl Environ Microbiol*, 59(5):1354–60, May 1993.

[99] L. A. Pratt and R. Kolter. Genetic analyses of bacterial biofilm formation. *Curr Opin Microbiol*, 2(6):598–603, Dec 1999.

[100] B. M. Pruss, C. Besemann, A. Denton, and A. J. Wolfe. A complex transcription network controls the early stages of biofilm development by *Escherichia coli*. *J Bacteriol*, 188(11):3731–9, Jun 2006.

[101] X. Qiu, M. J. Daly, A. Vasilenko, M. V. Omelchenko, E. K. Gaidamakova, L. Wu, J. Zhou, G. W. Sundin, and J. M. Tiedje. Transcriptome analysis applied to survival of *Shewanella oneidensis* MR-1 exposed to ionizing radiation. *J Bacteriol*, 188(3):1199–204, Feb 2006.

[102] X. Qiu, G. W. Sundin, B. Chai, and J. M. Tiedje. Survival of *Shewanella oneidensis* MR-1 after UV Radiation Exposure. *Appl Environ Microbiol*, 70(11):6435–6443, 11 2004.

[103] J. r. Renye JA, P. J. Piggot, L. Daneo-Moore, and B. A. Buttaro. Persistence of *Streptococcus mutans* in stationary-phase batch cultures and biofilms. *Appl Environ Microbiol*, 70(10):6181–7, Oct 2004.

[104] K. Rabaey, N. Boon, S. D. Siciliano, M. Verhaege, and W. Verstraete. Biofuel cells select for microbial consortia that self-mediate electron transfer. *Appl Environ Microbiol*, 70(9):5373–82, Sep 2004.

[105] R. J. Ram, N. C. Verberkmoes, M. P. Thelen, G. W. Tyson, B. J. Baker, R. C. Blake Ii, M. Shah, R. L. Hettich, and J. F. Banfield. Community Proteomics of a Natural Microbial Biofilm. *Science*, May 2005.

[106] S. A. Rani, B. Pitts, H. Beyenal, R. A. Veluchamy, Z. Lewandowski, W. M. Davison, K. Buckingham-Meyer, and P. S. Stewart. Spatial Patterns of DNA Replication, Protein Synthesis and Oxygen Concentration within Bacterial Biofilms Reveal Diverse Physiological States. *J Bacteriol*, Mar 2007.

[107] K. Rasmussen and Z. Lewandowski. Microelectrode measurements of local mass transport rates in heterogeneous biofilms. *Biotechnol Bioeng*, 59(3):302–9, Aug 1998.

[108] B. R. Ringeisen, E. Henderson, P. K. Wu, J. Pietron, R. Ray, B. Little, J. C. Biffinger, and J. M. Jones-Meehan. High power density from a miniature microbial fuel cell using *Shewanella oneidensis* DSP10. *Environ Sci Technol*, 40(8):2629–34, Apr 2006.

[109] S. Rozen and H. Skaletsky. Primer3 on the WWW for general users and for biologist programmers. *Methods Mol Biol*, 132:365–86, 2000.

[110] C. W. Saltikov, A. Cifuentes, K. Venkateswaran, and D. K. Newman. The ars Detoxification System Is Advantageous but Not Required for As(V) Respiration by the Genetically Tractable *Shewanella* Species Strain ANA-3. *Appl Environ Microbiol*, 69(5):2800–9, May 2003.

[111] B. Sampathkumar, S. Napper, C. D. Carrillo, P. Willson, E. Taboada, J. H. Nash, A. A. Potter, L. A. Babiuk, and B. J. Allan. Transcriptional and translational expression patterns associated with immobilized growth of *Campylobacter jejuni*. *Microbiology*, 152(Pt 2):567–77, Feb 2006.

[112] K. Y. San, G. N. Bennett, S. J. Berrios-Rivera, R. V. Vadali, Y. T. Yang, E. Horton, F. B. Rudolph, B. Sariyar, and K. Blackwood. Metabolic engineering through cofactor manipulation and its effects on metabolic flux redistribution in *Escherichia coli*. *Metab Eng*, 4(2):182–92, Apr 2002.

[113] K. Sauer. The genomics and proteomics of biofilm formation. *Genome Biol*, 4(6):219, 2003.

[114] K. Sauer and A. K. Camper. Characterization of Phenotypic Changes in *Pseudomonas putida* in Response to Surface-Associated Growth. *J Bacteriol*, 183(22):6579–89, Nov 2001.

[115] K. Sauer, A. K. Camper, G. D. Ehrlich, J. W. Costerton, and D. G. Davies. *Pseudomonas aeruginosa* displays multiple phenotypes during development as a biofilm. *J Bacteriol*, 184(4):1140–54, Feb 2002.

[116] J. H. Scott and K. H. Nealson. A biochemical study of the intermediary carbon metabolism of *Shewanella putrefaciens*. *J Bacteriol*, 176(11):3408–11, Jun 1994.

[117] Christopher J Southey-Pillig, David G Davies, and Karin Sauer. Characterization of Temporal Protein Production in Pseudomonas aeruginosa Biofilms. *J Bacteriol*, 187(23):8114–8126, Dec 2005.

[118] C. M. Southward and M. G. Surette. The dynamic microbe: green fluorescent protein brings bacteria to light. *Mol Microbiol*, 45(5):1191–6, Sep 2002.

[119] S. Spiro. Regulators of bacterial responses to nitric oxide. *FEMS Microbiol Rev*, 31(2):193–211, Mar 2007.

[120] N. R. Stanley and B. A. Lazazzera. Environmental signals and regulatory pathways that influence biofilm formation. *Mol Microbiol*, 52(4):917–24, May 2004.

[121] C. Sternberg, B. B. Christensen, T. Johansen, A. Toftgaard Nielsen, J. B. Andersen, M. Givskov, and S. Molin. Distribution of bacterial growth activity in flow-chamber biofilms. *Appl Environ Microbiol*, 65(9):4108–17, Sep 1999.

[122] P. S. Stewart. Diffusion in biofilms. *J Bacteriol*, 185(5):1485–91, Mar 2003.

[123] P. Stoodley, D. G. Davies, and J. W. Costerton. Biofilms as Complex Differentiated Communities. *Annu Rev Microbiol*, Apr 2002.

[124] G. Storz and J. A. Imlay. Oxidative stress. *Curr Opin Microbiol*, 2(2):188–94, Apr 1999.

[125] Y. J. Tang, J. S. Hwang, D. E. Wemmer, and J. D. Keasling. *Shewanella oneidensis* MR-1 fluxome under various oxygen conditions. *Appl Environ Microbiol*, 73(3):718–29, Feb 2007.

[126] Y. J. Tang, A. L. Meadows, and J. D. Keasling. A kinetic model describing *Shewanella oneidensis* MR-1 growth, substrate consumption, and product secretion. *Biotechnol Bioeng*, 96(1):125–33, Jan 2007.

[127] Y. J. Tang, A. L. Meadows, J. Kirby, and J. D. Keasling. Anaerobic central metabolic pathways in *Shewanella oneidensis* MR-1 reinterpreted in the light of isotopic metabolite labeling. *J Bacteriol*, 189(3):894–901, Feb 2007.

[128] T. K. Teal, D. P. Lies, B. J. Wold, and D. K. Newman. Spatiometabolic stratification of *Shewanella oneidensis* biofilms. *Appl Environ Microbiol*, 72(11):7324–30, Nov 2006.

[129] D. K. Thompson, A. S. Beliaev, C. S. Giometti, S. L. Tollaksen, T. Khare, D. P. Lies, K. H. Nealson, H. Lim, 3. r. d. Yates J, C. C. Brandt, J. M. Tiedje, and J. Zhou. Transcriptional and Proteomic Analysis of a Ferric Uptake Regulator (Fur) Mutant of *Shewanella oneidensis*: Possible Involvement of Fur in Energy Metabolism, Transcriptional Regulation, and Oxidative Stress. *Appl Environ Microbiol*, 68(2):881–892, Feb 2002.

[130] K. M. Thormann, S. Duttler, R. M. Saville, M. Hyodo, S. Shukla, Y. Hayakawa, and A. M. Spormann. Control of formation and cellular detachment from Shewanella oneidensis MR-1 biofilms by cyclic di-GMP. *J Bacteriol*, 188(7):2681–91, Apr 2006.

[131] K. M. Thormann, R. M. Saville, S. Shukla, D. A. Pelletier, and A. M. Spormann. Initial Phases of Biofilm Formation in *Shewanella oneidensis* MR-1. *J Bacteriol*, 186(23):8096–8104, Dec 2004.

[132] K. M. Thormann, R. M. Saville, S. Shukla, and A. M. Spormann. Induction of Rapid Detachment in *Shewanella oneidensis* MR-1 Biofilms. *J Bacteriol*, 187(3):1014–1021, Feb 2005.

[133] J. M. Tiedje. Shewanella–the environmentally versatile genome. *Nat Biotechnol*, 20(11):1093–4, Nov 2002.

[134] T. Tolker-Nielsen, U. C. Brinch, P. C. Ragas, J. B. Andersen, C. S. Jacobsen, and S. Molin. Development and dynamics of Pseudomonas sp. biofilms. *J Bacteriol*, 182(22):6482–9, Nov 2000.

[135] T. Tolker-Nielsen and S. Molin. Spatial Organization of Microbial Biofilm Communities. *Microb Ecol*, 40(2):75–84, Aug 2000.

[136] I. R. Tsaneva and B. Weiss. soxR, a locus governing a superoxide response regulon in Escherichia coli K-12. *J Bacteriol*, 172(8):4197–205, Aug 1990.

[137] A. I. Tsapin, I. Vandenberghe, K. H. Nealson, J. H. Scott, T. E. Meyer, M. A. Cusanovich, E. Harada, T. Kaizu, H. Akutsu, D. Leys, and J. J. Van Beeumen. Identification of a small tetraheme cytochrome c and a flavocytochrome c as two of the principal soluble cytochromes c in *Shewanella oneidensis* strain MR1. *Appl Environ Microbiol*, 67(7):3236–44, Jul 2001.

[138] H. C. van der Mei, D. J. White, J. Atema-Smit, E. van de Belt-Gritter, and H. J. Busscher. A method to study sustained antimicrobial activity of rinse and dentifrice components on biofilm viability in vivo. *J Clin Periodontol*, 33(1):14–20, Jan 2006.

[139] K. Venkateswaran, D. P. Moser, M. E. Dollhopf, D. P. Lies, D. A. Saffarini, B. J. MacGregor, D. B. Ringelberg, D. C. White, M. Nishijima, H. Sano, J. Burghardt, E. Stackebrandt, and K. H. Nealson. Polyphasic taxonomy of the genus Shewanella and description of Shewanella oneidensis sp. nov. *Int J Syst Bacteriol*, 49 Pt 2:705–24, Apr 1999.

[140] J. Vieira and J. Messing. New pUC-derived cloning vectors with different selectable markers and DNA replication origins. *Gene*, 100:189–94, Apr 1991.

[141] R. T. Villavicencio. The history of blue pus. *J Am Coll Surg*, 187(2):212–6, Aug 1998.

[142] N. S. Webster and A. P. Negri. Site-specific variation in Antarctic marine biofilms established on artificial surfaces. *Environ Microbiol*, 8(7):1177–90, Jul 2006.

[143] E. J. Wentland, P. S. Stewart, C. T. Huang, and G. A. McFeters. Spatial variations in growth rate within *Klebsiella pneumoniae* colonies and biofilm. *Biotechnol Prog*, 12(3):316–21, May 1996.

[144] E. Werner, F. Roe, A. Bugnicourt, M. J. Franklin, A. Heydorn, S. Molin, B. Pitts, and P. S. Stewart. Stratified Growth in *Pseudomonas aeruginosa* Biofilms. *Appl Environ Microbiol*, 70(10):6188–6196, 10 2004.

[145] C. B. Whitchurch, T. Tolker-Nielsen, P. C. Ragas, and J. S. Mattick. Extracellular DNA required for bacterial biofilm formation. *Science*, 295(5559):1487, Feb 2002.

[146] M. Whiteley, M. G. Bangera, R. E. Bumgarner, M. R. Parsek, G. M. Teitzel, S. Lory, and E. P. Greenberg. Gene expression in *Pseudomonas aeruginosa* biofilms. *Nature*, 413(6858):860–4, Oct 2001.

[147] J. Wu and B. Weiss. Two divergently transcribed genes, soxR and soxS, control a superoxide response regulon of *Escherichia coli*. *J Bacteriol*, 173(9):2864–71, May 1991.

[148] K. D. Xu, P. S. Stewart, F. Xia, C. T. Huang, and G. A. McFeters. Spatial physiological heterogeneity in *Pseudomonas aeruginosa* biofilm is determined by oxygen availability. *Appl Environ Microbiol*, 64(10):4035–9, Oct 1998.

[149] J. M. Yarwood, E. M. Volper, and E. P. Greenberg. Delays in *Pseudomonas aeruginosa* quorum-controlled gene expression are conditional. *Proc Natl Acad Sci U S A*, 102(25):9008–13, Jun 2005.

[150] A. Yoshida and H. K. Kuramitsu. *Streptococcus mutans* biofilm formation: utilization of a gtfB promoter-green fluorescent protein (PgtfB::gfp) construct to monitor development. *Microbiology*, 148(Pt 11):3385–94, Nov 2002.

[151] L. Zhang, P. J. Murphy, A. Kerr, and M. E. Tate. Agrobacterium conjugation and gene regulation by N-acyl-L-homoserine lactones. *Nature*, 362(6419):446–8, Apr 1993.

[152] M. Zheng, X. Wang, L. J. Templeton, D. R. Smulski, R. A. LaRossa, and G. Storz. DNA microarray-mediated transcriptional profiling of the *Escherichia coli* response to hydrogen peroxide. *J Bacteriol*, 183(15):4562–70, Aug 2001.